

REPUBLIC OF CAMEROON
REPUBLIQUE DU CAMEROUN



DEPARTMENT OF CIVIL ENGINEERING
DEPARTEMENT DE GENIE CIVIL

MINISTRY OF HIGHER EDUCATION
MINISTERE DE L'ENSEIGNEMENT SUPERIEUR



UNIVERSITÀ
DEGLI STUDI
DI PADOVA

DEPARTMENT OF CIVIL, ARCHITECTURAL
AND ENVIRONMENTAL ENGINEERING

PROGRESSIVE COLLAPSE OF STEEL BUILDING
SUBJECTED TO BLAST LOADS
CASE STUDY: METALLIC HANGAR IN EDEA-
CAMEROON

Thesis submitted in partial fulfilment of the requirement for the degree of Masters in Engineering
Curriculum: Civil Engineering

Presented by:

KAMGUEP TANKEU Stephane Angela

Student Matricula number: **15TP20947**

Supervised by:

Prof. Carlo Pellegrino

Co-supervised by:

Dr. Paolo ZAMPIERI

Dr. Cyrille TETOUGUENI

Academic year: 2019/2020

REPUBLIC OF CAMEROON

REPUBLIQUE DU CAMEROUN



DEPARTMENT OF CIVIL ENGINEERING

DEPARTEMENT DE GENIE CIVIL

MINISTRY OF HIGHER EDUCATION

MINISTERE DE L'ENSEIGNEMENT SUPERIEUR



UNIVERSITÀ
DEGLI STUDI
DI PADOVA

DEPARTMENT OF CIVIL, ARCHITECTURAL

AND ENVIRONMENTAL ENGINEERING

PROGRESSIVE COLLAPSE OF STEEL BUILDING
SUBJECTED TO BLAST LOADS
CASE STUDY: METALLIC HANGAR IN EDEA-
CAMEROON

Thesis submitted in partial fulfilment of the requirement for the degree of Masters in Engineering

Curriculum: Civil Engineering

Presented by:

KAMGUEP TANKEU Stephane Angela

Student Matricula number: **15TP20947**

Supervised by:

Prof. Carlo Pellegrino

Co-supervised by:

Dr. Paolo ZAMPIERI

Dr. Cyrille TETOUGUENI

Academic year: 2019/2020

DEDICATION

To my family
Especially to my beloved parents

ACKNOWLEDGEMENTS

This work would not have been completed without the combined efforts of individuals who contributed directly and/or indirectly to its realization. I wish to express my sincere thanks and gratitude to :

- The President of the jury ;
- The Examiner of this jury for accepting to bring his criticisms and observations to ameliorate this work ;
- My supervisors Prof. Carlo PELLEGRINO, Dr. Paolo ZAMPIERI and Dr. Cyrille TETOUGUENI for all the guidance and advices they provide me with, during this thesis work ;
- Professors George NKENG and Carmelo MAJORANA for all their academic and administrative support during these five years spent at ENSTP in the MEng program in partnership with University of Padua in Italy ;
- The vice-director of ENSTP, Dr M. BWEMBA Charles Loic for his perpetual help and advices during our sojourn in this school ;
- Prof. Michel MBESSA, the head of department of Civil Engineering for his tutoring and valuable advices ;
- All the teaching staff of ENSTP and University of Padua for their good quality teaching and the motivation they developed in us to continue our studies ;
- My family and more specially my father KAMGUEP Theophile and my mother NGNEZE KOUTEU Laura, for the education and financial support during all these years;
- Eng. Guillaume DJIODJIO for his advises and help which helped me during this work;
- All my classmates and all my friends who were a source of motivation and tenacity. As a team, together we have been able to achieve more.

LIST OF ABBREVIATIONS AND SYMBOLS

ABBREVIATIONS

EC, Eurocode

EN, European Norm

FEA, Finite Element Analysis

RC, Reinforce concrete

SCI, Steel Construction Institute

SLS, Serviceability Limit State

SAP, Structural Analysis Program

ULS, Ultimate Limit State

SYMBOLS

A, area of cross-section of the members

A_b , effective area of bolt

E, Young's modulus of elasticity

D, rigidity of the equivalent plate

d, diameter of bolt

C_{dir} , direction factor

C_{season} , Season factor

C_r , roughness factor

C_o , Orography factor

C_r , roughness factor

C_p , Pressure coefficient

C_e , Exposure coefficient

$C_{e(z)}$, exposure factor

DCR, Demand-to-capacity ratios

K_r , terrain factor

K_i , Turbulence factor

I_v , Turbulence intensity

PI, Pressure Impulse

P_o , Ambient pressure

P_r , Maximum reflected pressure

$P_{r\alpha}$, Peak reflected pressure

$P_{residual}$, Residual load carrying capacity

P_{so} , Peak side-on positive overpressure

P_{so}^- , Peak side-on negative pressure

P_{so} , Peak incident overpressure

q , Uniformly distributed load

q_0 , Dynamic pressure

R , Standoff distance

q_b , basic velocity pressure

q_p , peak velocity pressure

TNT, Trinitrotoluene

ULS, Ultimate limit states

w , Natural frequency

$x(t)$, Displacement at time t

$\dot{x}(t)$, Velocity at time t

Z , Scaled distance

$V_{b,0}$, the fundamental wind speeds

V_b , Basic wind speed

W_e , wind pressure

z_0 , roughness length

z_{min} , minimum height

ABSTRACT

The main objective of this work was to evaluate the progressive collapse of a steel structure caused by the removal of one column under blast loads. The case study for this thesis was a 20m wide by 50m long and 7m high metallic hangar, to be constructed in the Edea, Cameroon. To achieve our objective, the literature review was done firstly to understand the concept of progressive collapse and blast loads. Then, the modelling of the structure was done, and the static and blast analysis was performed in the computer program, SAP2000 version 22. RC blast software was used in order to obtain the pressure-time function of the blast loads. It is worth noting that in the blast analysis, different blast loads scenario was considered, one with a 50kg equivalent mass of TNT applied on a braced column and a column without a bracing system. Another 100kg equivalent mass of TNT was applied on the column without bracing considering two different steel cross-sections of similar area. Finally, for all these scenario, the Demand-to-capacity ratios was used as acceptance criteria for the progressive collapse and the impact of column removal due to blast loads on the surrounding columns was investigated to have an insight on the order of the progressive collapse. The results obtained from the blast analysis revealed that, as the charge weight is increased from 50kg to 100kg equivalent mass of TNT for a fixed standoff distance, the level of damage of the column increases at an increasing rate but the progressive collapse of the surrounding column will not occur in the case of a charge weight of 50kg. In addition, the bracing system plays an important role in the redistribution of lateral forces, which reduces the solicitations of columns to which it is linked during the blast. Finally, a progressive collapse after the column removal is observed when a blast load of charge weight 100kg is subjected to a column with an IPE330 as section, whereas the same blast loads force applied on the same column with a section of HE200B which is similar to the IPE in terms of cross section area will not lead to progressive collapse.

Keywords: Blast explosions, standoff distance, charge weight, demand-to-capacity ratios, structural analysis, progressive collapse.

RESUME

L'objectif principal de ce travail était d'évaluer l'effondrement progressif d'une structure en acier provoqué par l'enlèvement d'un poteau soumis à des charges d'explosion. Le cas d'étude pour ce mémoire était un hangar métallique de 20 m de large sur 50 m de long et 7 m de hauteur, qui doit être construit à Edéa, au Cameroun. Pour atteindre notre objectif, la revue de la littérature a été réalisée dans un premier temps pour comprendre le concept d'effondrement progressif et des charges d'explosion. Ensuite, la modélisation de la structure a été réalisée et l'analyse statique et celle de la structure soumise à des charges d'explosion a été réalisée dans le programme informatique SAP2000 version 22. Le logiciel RC blast a été utilisé afin d'obtenir la fonction de la pression avec le temps des charges d'explosion. Il convient de noter que dans l'analyse de l'explosion, différents scénarios de charges d'explosions ont été considérés, l'un avec une masse équivalente de 50 kg de TNT appliquée sur un poteau contreventé et un poteau sans système de contreventement. Une autre masse équivalente de 100 kg de TNT a été appliquée sur un poteau sans contreventement en considérant deux sections transversales en acier différentes de surface similaire. Enfin, pour tous ces scénarios, le rapport demande / capacité a été utilisé comme critère d'acceptation pour l'effondrement progressif et l'impact du retrait du poteau dû aux charges d'explosions sur les poteaux environnants a été étudié pour avoir un aperçu de l'ordre de l'effondrement progressif. Les résultats obtenus à partir de l'analyse des charges d'explosions ont révélé que, à mesure que le poids de charge passe de 50 kg à 100 kg de masse équivalente de TNT pour une distance d'écartement fixe, le niveau d'endommagement du poteau augmente à une vitesse croissante mais l'effondrement progressif des poteaux environnants se produira pas dans le cas d'un poids de charge de 50 kg. De plus, le système de contreventement joue un rôle important dans la redistribution des efforts latéraux, ce qui réduit les sollicitations des poteaux auxquelles il est lié lors de l'explosion. Enfin, un effondrement progressif après le retrait du poteau est observé lorsqu'une charge d'explosion de poids de charge 100kg est soumise à un poteau de section IPE330, alors que la charge d'explosion appliquée sur le même poteau avec une section de HE200B qui est similaire à l'IPE en termes de section transversale ne conduira pas à un effondrement progressif

Mots clés : explosion, distance de séparation, poids de la charge, rapport demande-capacité, analyse structurelle, effondrement progressif.

LIST OF FIGURES

Figure 1.1. Typology of progressive collapse (Starossek, 2007).	11
Figure 1.2. Visual sketches of the propagation types (Smith JW,2006).	11
Figure 1.3. Ideal blast wave’s pressure time history (Shirbhate & Goel, 2020).	14
Figure 1.4. Influence of distance on the blast positive pressure phase (Karlos & Solomos, 2013).	16
Figure 1.5. Simplified blast wave overpressure profile (Yandzio et al.,1999).	18
Figure 1.6. Reflected overpressure (Remennikov,2003).	20
Figure 1.7. Face-on reflection (Yandzio et al.,1999).	20
Figure 1.8. Last overpressure-time profile for a face-on reflected wave (Yandzio et al.,1999).	21
Figure 1.9. Regular reflection (Yandzio et al.,1999).	21
Figure 1.10. Reflection coefficients vs. angle of incidence. (Yandzio et al.,1999).	22
Figure 1.11. Mach reflection (Yandzio et al. 1999).	22
Figure 1.12. Standoff distance of the explosion from the structure. (Shirbhate & Goel, 2020).	25
Figure 1.13. Free-air bursts loads (Army, Navy, 1990).	26
Figure 1.14. Air Burst Loads (Army, Navy, 1990).	27
Figure 1.15. Surface Burst Loads (Army, Navy, 1990).	27
Figure 1.16. Types of confined explosions (Yandzio et al.,1999).	27
Figure 1.17. (a) SDOF system and (b) blast loading (Ngo et al., 2007).	29
Figure 1.18. Simplified elasto-plastic SDOF model for blast load (Ngo et al., 2007).	30
Figure 1.19. Maximum response of elasto-plastic SDOF systems under triangular load pulse with zero rise time (Ngo et al., 2007).	31
Figure 2.1. Wind pressure on external surfaces (source: BS-EN1991 E_2002).	37
Figure 2.2. Hemispherical blast wave propagation (Remennikov,2003).	38
Figure 2.3. Simple diagram for blast load determination (Karlos & Solomos, 2013).	38
Figure 2.4. Positive phase parameters of shock hemispherical wave of TNT charges from surface bursts (TM5-1300 1990).	39
Figure 2.5. Reflected pressure coefficients versus angle of incidence (a) for larger and (b) for smaller values of incident overpressure (TM5-1300 1990).	40
Figure 2.6. Buckling curves (source: EC3 1-1 , 2005).	47
Figure 2.7. Tangent lines on the base plate which determine uplift (Morel, 2005).	53
Figure 2.8. Spacing of the holes on the plate (Morel, 2005).	55

Figure 3.1. 3D-view of the steel hangar.	61
Figure 3.2. Wind pressure on external surfaces (source: BS-EN1991 E_2002).....	64
Figure 3.3. Columns on the front face of the building.	65
Figure 3.4. Pressure-Time graph for a charge weight of 50 kg of TNT.....	66
Figure 3.5. Element in tension to be designed on the reticular steel roof.....	70
Figure 3.6. Element in compression to be designed on the reticular steel roof.	71
Figure 3.7. Results of the push-over analysis.	74
Figure 3.8. moment-rotation curve in pushover analysis of one hinge.	75
Figure 3.9. The pressure-time graph of the 11 columns.	75
Figure 3.10. Application of blast loads on column 1.	77
Figure 3.11. Deformation of structural elements due to the application of blast loads on column 1.....	77
Figure 3.12. Displacement-time curve due to the application of blast loads of charge weight 50kg on column 1.....	78
Figure 3.13. Moment-time curve due to the application of blast loads of charge weight 50kg on column 1.	78
Figure 3.14. Moment results due to the application of blast loads of charge weight 50kg on column 1.	79
Figure 3.15. DCR values results due to the application of blast loads of charge weight 50kg on column 1.	80
Figure 3.16. Application of blast loads on column 4.	80
Figure 3.17. Deformation of structural elements due to the application of blast loads on column 4.....	81
Figure 3.18. Displacement-time curve due to the application of blast loads of charge weight 50kg on column 4.....	81
Figure 3.19. Moment-time curve due to the application of blast loads of charge weight 50kg on column 4.	82
Figure 3.20. Moment results due to the application of blast loads of charge weight 50kg on column 4.	83
Figure 3.21. DCR values results due to the application of blast loads of charge weight 50kg on column 4.	83
Figure 3.22. Column 4 removal.	84
Figure 3.23. Rampth function for the column removal.	84
Figure 3.24. Moments results due to the application of blast loads of charge weight 50kg after column 4 removal.....	85

Figure 3.25. DCR values results due to the application of blast loads of charge weight 50kg after column 4 removal.....	85
Figure 3.26. Deformation of structural elements due to the application of blast loads on column 4.....	86
Figure 3.27. Moments results due to the application of blast loads of charge weight 100kg on column 4.	87
Figure 3.28. DCR values results due to the application of blast loads of charge weight 100kg on column 4.....	88
Figure 3.29. Moments results due to the application of blast loads of charge weight 100kg after column 4 removal.....	89
Figure 3.30. DCR values results due to the application of blast loads of charge weight 100kg after column 4 removal.....	89
Figure 3.31. Results of the push-over analysis after column removal	90
Figure 3.32. moment-rotation curve in pushover analysis of one hinge.	91
Figure 3.33. Deformation of structural elements due to the application of blast loads on column 4 of section HE 200B.	92
Figure 3.34. Displacement-time curve due to the application of blast loads of charge weight 100kg on column 4 for the IPE 330 and HE 200B sections.	93
Figure 3.35. Moment-time curve due to the application of blast loads of charge weight 100kg on column 4 for the IPE 330 and HE 200B sections.....	94
Figure 3.36. Moments results due to the application of blast loads of charge weight 100kg on column.	95
Figure 3.37. DCR values results due to the application of blast loads of charge weight 100kg on column.	95
Figure 3.38. (a) Single diagonal (b) cross (c) chevron (d) V-bracing (e) K-bracing	97
Figure 3.39. Pressure-time history graph for a charge weight of 50kg TNT with different standoff distance.....	98

LIST OF TABLES

Table 1.1. Physical properties of steel.	4
Table 1.2. Mechanical properties of steel.	4
Table 1.3. Type of explosives and TNT equivalent.....	23
Table 1.4. Explosion load categories (Army, Navy, 1990).....	26
Table 2.1. Maximum width-to-thickness ratios for internal compression parts.....	44
Table 2.2. Maximum width-to-thickness ratios for compression parts (outstand flanges).....	45
Table 2.3. Maximum width to thickness ration for members in bending and/or compression.	45
Table 2.4. Selection of buckling curve for a cross section (source: EC3 1-1, 2005).	48
Table 3.1. Steel structural sections material properties.	61
Table 3.2. Concrete footing, reinforcing steel and bearing soil material properties.	62
Table 3.3. Self-weight of structural elements.	63
Table 3.4. Self-weight of non-structural elements.	63
Table 3.5. Categorization of roofs.	63
Table 3.6. Blast load parameters relative to the front face of the building.	65
Table 3.7. Solicitations of the column.	67
Table 3.8. Properties of IPE 330.	67
Table 3.9. Column design.	68
Table 3.10. Solicitations of the purling.....	68
Table 3.11. Properties of IPE 120.....	69
Table 3.12. Purling design.	69
Table 3.13. Properties of 273x6.3 CHS.	70
Table 3.14. Design of the element in tension for the roof's reticular structure.	71
Table 3.15. Design of the element in compression for the roof's reticular structure.....	71
Table 3.16. Properties of 80x80x5.....	72
Table 3.17. Design of the roof's bracing system.	72
Table 3.18. Properties of 100x100x5.....	72
Table 3.19. Design of the column's bracing system.	72
Table 3.20. Foundation design.	73
Table 3.21. Bolt's solicitations	73
Table 3.22. Bolt design.	74
Table 3.23. Results of blast loads of charge weight 50kg of TNT.....	76
Table 3.24. DCR value due to the application of blast loads of charge weight 50kg on column 1.....	79

Table 3.25. DCR value due to the application of blast loads of charge weight 50kg on column 4.....	82
Table 3.26. DCR value due to the application of blast loads of charge weight 50kg after column 4 removal.	85
Table 3.27. DCR value due to the application of blast loads of charge weight 100kg on column 4.....	87
Table 3.28. DCR value due to the application of blast loads of charge weight 100kg after column 4 removal.	88
Table 3.29. Properties of HE 200B.....	91
Table 3.30. DCR value due to the application of blast loads of charge weight 100kg on column 4.....	94

TABLE OF CONTENTS

DEDICATION	i
ACKNOWLEDGEMENTS	ii
LIST OF ABBREVIATIONS AND SYMBOLS	iii
ABSTRACT	vi
RESUME	vii
LIST OF FIGURES	viii
LIST OF TABLES	xi
TABLE OF CONTENTS	xiii
GENERAL INTRODUCTION	1
CHAPTER 1: LITERATURE REVIEW	2
Introduction	2
1.1. Steel	2
1.1.1. Steel raw materials	2
1.1.2. Manufacture of steel	2
1.1.2.1. The Bessemer Process	2
1.1.2.2. The Siemens-Martins process	3
1.1.2.3. The Thomas Process	3
1.1.3. Properties of steel	3
1.1.3.1. Physical properties of steel	4
1.1.3.2. Mechanical properties	4
1.1.3.3. Chemical properties	4
1.1.4. Typology of steels	5
1.1.4.1. Carbon steel	5
1.1.4.2. Alloy steel	5
1.1.4.3. Stainless steel	5
1.1.4.4. Tool steel	6
1.1.5. Field of use of steel	6

1.1.5.1. Buildings and Infrastructure	6
1.1.5.2. Mechanical Equipment	6
1.1.5.3. Automotive	6
1.1.5.4. Metal Products	6
1.1.5.5. Other Transport	7
1.1.5.6. Domestic Appliances.....	7
1.1.5.7. Electrical Equipment	7
1.1.6. Defects of steel.....	7
1.1.7. Steel defect treatment.....	7
1.1.7.1. Paint coatings	7
1.1.7.2. vitreous enamel coatings.....	8
1.1.7.3. Metallic coatings	8
1.2. Progressive collapse.....	8
1.2.1. Classification and typology of progressive collapse.....	9
1.2.1.1. Redistribution-type collapses.....	9
1.2.1.2. Impact-type collapses	9
1.2.1.3. Instability-type collapse.....	10
1.2.1.4. Mixed-type collapse	10
1.2.2. Typical triggering events.....	12
1.2.2.1. Blast.....	12
1.2.2.2. Fire.....	12
1.2.2.3. Impact	12
1.2.2.4. Seismic loads	13
1.2.2.5. Multi-hazard scenarios	13
1.3. Blast loading.....	13
1.3.1. Blast loads and explosion	13
1.3.1.1. Ideal blast wave characteristics.....	13
1.3.1.2. Scaling laws	16

1.3.1.3. Simple numerical formulas for blast load predictions.....	17
1.3.1.4. Simplified blast wave profile	18
1.3.1.5. Dynamic Pressure.....	18
1.3.1.6. Reflected blast wave characteristics.....	19
1.3.1.7. Mach Reflection	22
1.3.1.8. Parameters related to blast phenomenon	23
1.3.1.9. Standoff Distance	24
1.3.1.10. Explosion	25
1.3.1.11. Type of explosion.....	26
1.3.2. Analysis methods for blast loading.....	28
1.3.2.1. Equivalent static method.....	28
1.3.2.2. Single Degree of Freedom System (SDOF)	28
Conclusion	33
CHAPTER 2: METHODOLOGY	34
Introduction.....	34
2.1. Site recognition.....	34
2.2. Data collection.....	34
2.2.1. Architectural data.....	34
2.2.2. Structural data	35
2.3. Determination of loads acting on the building	35
2.3.1. Permanent loads.....	35
2.3.2. Variable loads	35
2.3.2.1. Imposed loads	35
2.3.2.2. Wind loads	35
2.3.3. Blast loads	37
2.4. Load combinations.....	41
2.4.1. Static loading case.....	41
2.4.2. Blast loading case	42

2.5. Structural analysis and design methods	42
2.5.1. Software used for modelling and analysis of the structure	42
2.5.2. Design of the steel structure	43
2.5.2.1. Classification of the sections	43
2.5.2.2. Ultimate limit states design checks for steel members (ULS).....	46
2.5.2.3. Serviceability limit states check for steel members (SLS).....	55
2.5.3. Blast analysis approach	56
2.6. Acceptance criteria for progressive collapse.....	57
Conclusion	58
CHAPTER 3: PRESENTATION OF RESULTS AND INTERPRETATION	59
Introduction.....	59
3.1. General presentation of the city of Edea.....	59
3.1.1. Geographical location	59
3.1.2. Climate	59
3.1.3. Hydrology.....	59
3.1.4. Vegetation.....	60
3.1.5. Economic parameters	60
3.2. Presentation of the project.....	60
3.2.1. Geometrical presentation of the model	60
3.2.2. Geometrical and material characteristics	61
3.3. Load determination	62
3.3.1. Permanent loads.....	63
3.3.2. Variable loads	63
3.3.2.1. Impose load.....	63
3.3.2.2. Wind load.....	63
3.3.2.3. Blast loads determination	65
3.4. Loads combinations	66
3.5. Static analysis of the structure.....	67

3.5.1. Design of the column	67
3.5.2. Design of the purling.....	68
3.5.3. Design reticular structure of the roof	70
3.5.3.1. Element in tension	70
3.5.3.2. Element in compression.....	71
3.5.4. Design of the bracing system.....	71
3.5.4.1. Bracing system of the roof.....	71
3.5.4.2. Bracing system of the column.....	72
3.5.5. Design of foundation.....	73
3.5.6. Design of connection.....	73
3.6. Results of the blast analysis	74
3.6.1. Results for the blast loads of charge weight 50Kg on all the columns	74
3.6.2. Results for blast loads of charge weight 50Kg on individual columns.....	76
3.6.2.1. Blast loading on column 1	77
3.6.2.2. Blast loading on column 4	80
3.6.3. Results for blast loads of charge weight 100Kg on individual columns.....	86
3.6.3.1. Blast loading on column 4 of section IPE330.....	86
3.6.3.2. Blast loading on column 4 of section HE200B.....	91
3.7. Some possible solutions	96
3.7.1. The bracing system	96
3.7.1.1. Cross bracing	96
3.7.1.2. single diagonal bracing.....	96
3.7.1.3. V-bracing	96
3.7.1.4. K-bracing	97
3.7.2. The section and characteristic of the structural element	97
3.7.3. Creating obstacles on the field.....	97
Conclusion	98
GENERAL CONCLUSION.....	100

WEBOGRAPHY.....	106
ANNEXES.....	107

GENERAL INTRODUCTION

During the last few decades, accidental explosions and premeditated attacks on structures have prompted building owners, governments and design professionals to pay more attention to the vulnerability and survivability of structures relative to blast events. High-rise buildings, commercial buildings, monuments, buildings near explosives manufacturing and storage facilities and other critical structural systems are most likely to be exposed to explosion threats. Such events usually cause local damage to the structure of buildings, which can lead to a complete collapse. This is where the term progressive collapse comes in, understood as the process by which local damage sets in motion a chain of failures, leading to the collapse of the entire building or a large part of it.

For an economic and safe design of structures against progressive collapse to blast loads, a reliable progressive collapse analysis is essential. Engineers need an accurate and concise methodology to produce trustworthy and timely results. International codes and specifications such as General Service Administration, Department of Defence, and Eurocode 1 recommend prescriptive strategies for limiting progressive collapse. However, none of these guidelines defines an explicit and simplified numerical performance-based approach for the evaluation of progressive collapse. Though, sudden column removal is recommended in design guidelines without stating the steps on how to achieve it considering different modelling software. Consequently, various researchers adopt different methods and approaches in assessing building structures for progressive collapse.

The main objective of this work is therefore clear, to investigate the progressive collapse of a steel building caused by the removal of one column under blast load. Given that large-scale experiments are expensive, dangerous and labour-intensive as compared to the numerical simulation of blast loads based on finite element analysis, only the numerical investigation is presented in this thesis, using reliable finite element software.

In order to achieve this objective, the study is divided in three parts. The first part (Chapter 1) consists of a literature review on steel, progressive collapse as well as blast loads. The second part (Chapter 2) presents the methodology of the study, it elaborates on the collection of data, analysis and design procedures used. The third part (Chapter 3) is the application of the detailed methodology outlined in chapter 2 that is using SAP2000 to obtain solicitations, static analysis of the structure and blast analysis results of the building.

CHAPTER 1: LITERATURE REVIEW

Introduction

This chapter reviews the available literature on steel that is steel's raw materials, Steel's manufacture, its properties, typology as well as the field of use. We will also see the defect of steel and its treatment. Furthermore, we will see the concept of progressive collapse, its classification and triggering event. Blast loads may cause damage or destruction of the load bearing elements in buildings. Consequently, over the last decades, various studies have been carried out in order to develop techniques relevant to the examination of the nature of the blast loads, the local and global behaviour of the structure under the blast impact. All the major parameters related to blast events, the blast wave profiles used to determine the blast loads on a structure and the blast wave interaction with structural elements are equally presented in this chapter. Finally, we will present the analysis methods for blast loading.

1.1. Steel

Steel is a widely used material in engineering and construction material. It is used in every aspect of our lives. A clear understanding of this material will be presented in this section.

1.1.1. Steel raw materials

Steel is an alloy consisting mostly of iron and less than 2% carbon, 1% manganese and small amounts of silicon, phosphorus, sulphur and oxygen. Iron ore is, therefore, essential for the production of steel, which in turn is essential in maintaining a strong industrial base. The ores used in making steel are iron oxides, which are compounds of iron and oxygen.

1.1.2. Manufacture of steel

Steel is obtained by the refining of cast irons. It can be done by the means of three processes namely the Bessemer process, the Siemens-Martins process and the Thomas process.

1.1.2.1. The Bessemer Process

Bessemer invented a pear-shaped receptacle referred to as a converter in which the iron could be heated, and oxygen could be blown through the molten metal. When oxygen passes through the molten metal, it would react with the carbon, releasing carbon dioxide and creating a purer iron. The process was both inexpensive and fast, it removed carbon and silicon from iron in only a few minutes but was still strong. By the end of the process, too much carbon was being removed and too much oxygen remained in the final product. To solve this, Bessemer ultimately found that if he added the right quantities of manganese, it would provide a solution,

so he began adding it to his conversion process with great success. There was still only one problem, Bessemer had failed to find a way to remove phosphorus from his end product, which made the steel brittle (The AISE Steel Foundation,1998)

1.1.2.2. The Siemens-Martins process

The open-hearth process, also called Siemens-martin process is a steelmaking technique that accounted for the major part of all steel made in the world for most of the 20th century. Here, natural gas or atomized heavy oils are used as fuel. Both air and fuel are heated before combustion. The furnace is charged with liquid blast-furnace iron and steel scrap together with iron ore, limestone, dolomite, and fluxes. The furnace itself is made of highly refractory materials such as magnesite bricks for the hearths and roofs. Capacities of open-hearth furnaces are as high as 600 tons, and they are usually installed in groups, so that the massive auxiliary equipment needed to charge the furnaces and handle the liquid steel can be efficiently employed (The AISE Steel Foundation,1998).

1.1.2.3. The Thomas Process

The Thomas converter is similar in design to the Bessemer converter, except that it is larger. The essential difference between the two is in the lining. The basic lining of the Thomas converter, thoroughly calcined dolomite, makes it possible to charge the furnace with lime (about 12–15 percent of the volume of pig iron) for slagging and the removal of phosphorus. After charging, molten pig iron at a temperature of 1180°-1250°C is poured into the converter, which is tipped up to its vertical operating position and the blast is turned on. During the blow, Si and Mn are fully oxidized and Fe, C, and P are partially oxidized. The blow is continued until a carbon content of 0.05 percent is achieved, since intensive oxidation of phosphorus (up to 0.04–0.05 percent) does not begin until near the end of carbon oxidation. Sulphur is only partially removed from the metal. During the Thomas-Gilchrist process it is often necessary to cool the metal by adding ore, scale, or scrap. The yield of acceptable metal is 85–89 percent, and the yield of Thomas slag, which is used as phosphorus fertilizer, is 18–20 percent of the weight of the metal. The smelted steel is used for rolled stock, sheet, roofing iron, wire, and rails.

1.1.3. Properties of steel

These properties can be distinguished in 3 groups which are physical properties, mechanical properties and chemical properties.

1.1.3.1. Physical properties of steel

Steel has an attractive outer appearance. It is silvery in colour with a shiny, lustrous outer surface. Others Physical properties can be summarized in the following table 1.1.

Table 1.1.Physical properties of steel.

Physical properties	Value
density, ρ (kg/m ³)	7,850
Specific Heat Capacity, c_p (J/(kg-K))	502.416
thermal conductivity, k (W/Km)	45
Coefficient of thermal expansion, α (/°C)	1.2 x 10 ⁻⁵
Resistivity at 20 °C; ρ ($\Omega\cdot m$)	4.60×10 ⁻⁷
Conductivity at 20 °C; σ (S/m)	2.17×10 ⁶
Permeability (μ)-(H/m):	1.26×10 ⁻⁴
Relative permeability (μ / μ_0):	100

1.1.3.2. Mechanical properties

One of the useful mechanical properties of steel is its ability to change shape on the application of force to it, without resulting in a fracture. This property is known as ductility. Steel is equally malleable and can be deformed under compression. Others mechanical properties can be summarized in the following table 1.2.

Table 1.2.Mechanical properties of steel.

Mechanical properties	Value
Modulus of elasticity, E (GPA)	210
shear modulus, G (GPA)	81
Poisson's ratio, ν	0.3
Elongation percentage (%)	5-40

1.1.3.3. Chemical properties

The hardness of this alloy is high, reflecting its ability to resist strain. It is long-lasting and greatly resistant to external wear and tear. Hence it is considered a very durable material. Also, concerning the rust resistance, the addition of certain elements, makes some types of steel resistant to rust. Stainless steel for instance contains nickel, molybdenum and chromium which improve its ability to resist rust.

1.1.4. Typology of steels

According to the American Iron & Steel Institute (AISI), steel can be categorized into four basic groups based on the chemical compositions namely carbon steel, alloy steel, stainless steel and tool steel (Aakanksha Gaur,2019).

1.1.4.1. Carbon steel

Carbon steel refers to an iron-carbon alloy with a carbon content of less than 2% and containing a small amount of impurity elements such as silicon, phosphorus, sulphur and oxygen. According to its carbon content, these types of steel can be divided into four types:

- Low carbon steel, also known as iron or mild steel, has a carbon content of 0.04-0.30%
- Medium carbon steel, with a carbon content of 0.30 – 0.60%.
- High carbon steel, carbon content is 0.60-1.25%.
- Ultra high carbon steel with a carbon content of 1.25-2.00%

1.1.4.2. Alloy steel

Alloy steel refers to a steel that is refined on the basis of carbon steel by adding some alloying elements (such as chromium, nickel, molybdenum, tungsten, vanadium, titanium, etc.) in order to improve the properties of the steel. According to the type of alloying elements, these types of steel can be divided into:

- chrome steel,
- manganese steel,
- chromium manganese steel,
- chrome nickel steel,
- chromium molybdenum steel and
- silicon manganese steel.

1.1.4.3. Stainless steel

Stainless steels generally contain between 10-20% chromium as the main alloying element and are valued for high corrosion resistance. With over 11% chromium, steel is about 200 times more resistant to corrosion than mild steel. These steels can be divided into three groups based on their crystalline structure:

- Austenitic steels that are non-magnetic and non-heat-treatable, and generally contain 18% chromium, 8% nickel and less than 0.8% carbon

- Ferritic steels that contain trace amounts of nickel, 12-17% chromium, less than 0.1% carbon, along with other alloying elements, such as molybdenum, aluminium or titanium.
- Martensitic steels that contain 11-17% chromium, less than 0.4% nickel, and up to 1.2% carbon.

1.1.4.4. Tool steel

Tool steels contain tungsten, molybdenum, cobalt and vanadium in varying quantities to increase heat resistance and durability, making them ideal for cutting and drilling equipment.

1.1.5. Field of use of steel

Steel is both the most widely used and most recycled metal material on Earth. Steel applications can be divided into seven primary market sectors namely Buildings and infrastructure, Mechanical equipment, Automotive, Metal products, Other transport, Domestic appliances, Electrical equipment (Bell, 2020)

1.1.5.1. Buildings and Infrastructure

More than half of the steel produced annually is used to construct buildings and infrastructure such as bridges. According to the WSA, most of the steel used in this sector is found in reinforcing bars (44%), sheet products, including those used in roofs, internal walls, ceilings (31%) and structural sections (25%). In addition to those structural applications, steel is also used in items such as stairs, rails, and shelving. It is also widely used in utility infrastructure in the form of underground pipes for water or natural gas.

1.1.5.2. Mechanical Equipment

This second-greatest use of steel includes (among many other things) bulldozers, tractors, machinery that makes car parts, cranes, and hand tools such as hammers and shovels. It also includes the rolling mills that are used to shape steel into various shapes and thicknesses.

1.1.5.3. Automotive

On average, almost 2,000 pounds, or 900 kilograms, of steel is used to make a car, according to the WSA. About a third of that is used in the body structure and exterior, including the doors. Another 23% is in the drive train, and 12% is in the suspension.

1.1.5.4. Metal Products

This market sector includes various consumer products such as furniture, packaging for food and drinks, and razors. Foods packaged in steel cans don't need to be refrigerated.

1.1.5.5. Other Transport

Steel is used in ships, trains and train cars, and parts of planes. Hulls of large ships are almost all made of steel, and steel ships carry 90% of global cargo, the WSA says. Steel is important for sea transportation in one other way: almost all of the world's approximately 17 million shipping containers are made of steel. Besides the cars, steel shows up in trains in the wheels, axels, bearings, and motors. In airplanes, steel is crucial for engines and landing gear.

1.1.5.6. Domestic Appliances

Clothes washers and dryers, ranges, microwave ovens, dishwashers, and refrigerators all contain steel in varying amounts, including the motors, when applicable. According to the American Iron and Steel Association, a front-loading washer generally contains 84.2 pounds of steel, while a top-bottom refrigerator-freezer contains 79 pounds.

1.1.5.7. Electrical Equipment

The last major steel market sector involves applications in the production and distribution of electricity. That means transformers, which have a magnetic steel core; generators; electric motors; pylons; and steel-reinforced cables.

1.1.6. Defects of steel

Steel oxidize in the air (atmospheric corrosion), especially if the air is very humid. They are also attacked by contact with more or less aggressive materials. lime parts are more easily attacked than forged parts.

Steel are attacked by plaster. It is therefore absolutely necessary to protect these metals with a protective layer. Before applying any protective layer, the metal must be free of all traces of rust and grease (Mbessa,2005)

1.1.7. Steel defect treatment

Steel gets easily corroded and are attacked by plaster. In other to protect the steel, various means of treatment such as paint coatings, vitreous enamel coatings and metallic coatings can be applied.

1.1.7.1. Paint coatings

It usually comprises a sequential coating application of paints or alternatively paints applied over metallic coatings to form a duplex coating system. Protective paint systems usually consist of primer, intermediate/build coats and finish coats. Each coating 'layer' in any protective

system has a specific function, and the different types are applied in a particular sequence of primer followed by intermediate/build coats in the shop, and finally the finish coat (or top coat) either in the shop or on site (Qian et al., 2015).

1.1.7.2. vitreous enamel coatings

Enamel refers to a glassy, vitreous and usually opaque substance that is used in protective or decorative coating on metal, glass or ceramic ware. It is bonded to the steel substrate by thermal fusion. This coating is applied for the protection of steel products from surrounding environments. This coating provides not only an aesthetic exterior but also provides outstanding engineering properties, such as mechanical strength of the enamelled surface, multiplicity and stability of colour, corrosion resistance, resistance to wear and abrasion, chemical and heat resistance, resistance to thermal shock and fire, hygiene and ease of cleaning. (Song et al., 2018)

1.1.7.3. Metallic coatings

There are four commonly used methods of applying metal coating to steel surfaces. These are hot-dip galvanizing, thermal spraying, electroplating and sherardizing. The latter two processes are not used for structural steelwork but are used for fittings, fasteners and other small items.

For the hot-dip galvanizing method, it is a process involving the immersion of the steel component to be coated in a bath of molten zinc (at about 450°C) after pickling and fluxing, and then withdrawing it.

The thermally spraying method is a thermally sprayed coatings of zinc, aluminium, and zinc-aluminium alloys that can provide long-term corrosion protection to steel structures exposed to aggressive environments. The metal, in powder or wire form, is fed through a special spray gun containing a heat source, which can be an electric arc.

1.2. Progressive collapse

Progressive collapse is a relatively rare occurrence as a result of sudden loading on a structure that causes local damage in that structure and then extends to other structural parts (Kiakojoury et al., 2020). The first time that researchers looked at the issue of progressive collapse was the structural failure of a 22-story building at Ronan Point (1968). The underlying characteristic of progressive collapse is that the final state of failure is disproportionately larger than the initial local failure (Ellingwood et al., 2007).

1.2.1. Classification and typology of progressive collapse

The first and widely accepted classification of progressive collapse was provided by Starossek. The author focused on structural response after initial failure and did not consider the triggering event. Based on different characteristic features, progressive collapse can be categorized in four different types as described below (Starossek, 2007).

1.2.1.1. Redistribution-type collapses

The redistribution-type collapses are further classified into 2 categories namely the zipper-type collapse and section-type collapse.

a. Zipper-type collapse

This type of collapse is initiated by rupture of one cable and propagating by overloading and rupture of adjacent cables. Example of this type of collapse is collapse of original Tacoma Narrows Bridge in 1940 (Strom & Ebeling, 2002).

b. Section-type collapse

This type of collapse is initiated when a member under bending moment or axial tension is cut. The internal forces transmitted by that part are redistributed in to the remaining cross section. The corresponding increase in stress at some locations can cause the rupture of further cross sectional parts, and in the same manner, a failure progression throughout the entire cross section (Smith JW, 2006).

1.2.1.2. Impact-type collapses

The impact-type collapses are further classified into pancake-type collapse and domino-type collapse.

a. Pancake-type collapse

The failure sequence followed in this type of collapse is, initiating event, separation of structural components, release of potential energy and the occurrence of impact forces. Depending on the size of the falling components, the potential energy of falling components can far exceed the strain energy stored in the structure. The collapse of WTC towers of New York in Sept. 2001 is example of this type of collapse where collapse is said to be initiated by weakening of the floor joists due to fire that resulted from the aircraft impact (Analysis et al., 2002).

b. Domino-type collapse

The mechanism behind this type of collapse is, initial overturning of one element, fall off that element in angular rigid-body motion around a bottom edge, transformation of potential energy into kinetic energy, lateral impact of the upper edge of that element on the side face of

an adjacent element where the horizontal pushing force transmitted by that impact is of both static and dynamic origin because of the tilting and the motion of the impacting element, overturning of the adjacent element due to the horizontal loading from the impacting element and collapse progression in the overturning direction. This type of failure can occur in row of temporary scaffolding towers. It is also common in overhead transmission line towers.

1.2.1.3. Instability-type collapse

Instability of structure is characterized by small imperfection which leads to large deformations or collapse. For example, the failure of a bracing element due to some small triggering event can make a system unstable and result in collapse. Another example is failure of a plate stiffener leading to local instability and failure of the affected plate, and possibly to global collapse. Here propagating destabilization occurs when the failure of destabilized elements leads to the failure of stabilizing elements.

1.2.1.4. Mixed-type collapse

This type of collapse can be assigned to the structure where one or more possible failure reasons fall in to different category of progressive collapse. For example, the partial collapse of the Murrah Federal Building (Oklahoma City) seems to have involved features of both a pancake-type and domino-type scenario. The horizontal forces, induced by an initial failure, that lead to overturning of other elements. This horizontal tensile force could have been induced by falling components and transmitted to other elements through continuous reinforcing bars. Another example is collapse of cable-stayed bridges which fall in to category of zipper-type and instability-type failure.

The hierarchical classification based on Starossek's suggestion is presented in figure 1.1. and is suitable for all type of structures.

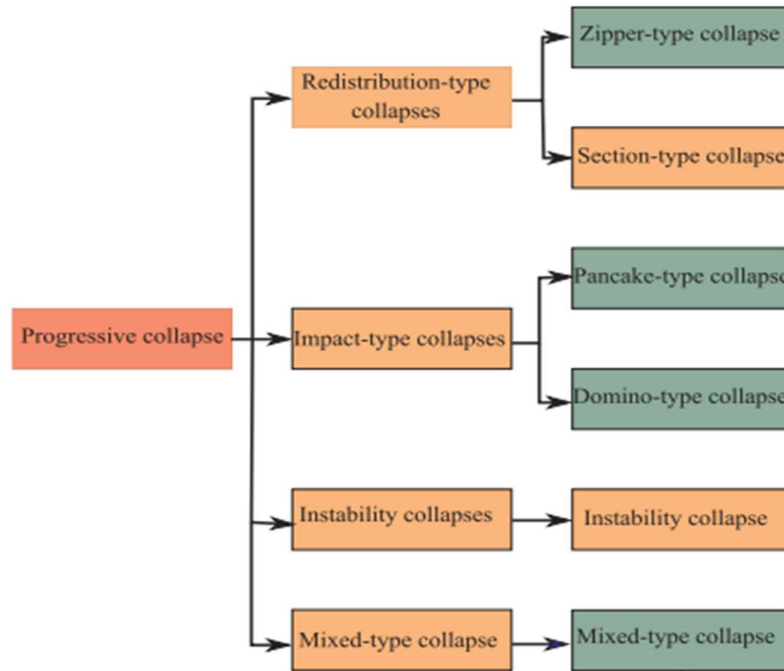


Figure 1.1. Typology of progressive collapse (Starossek, 2007).

Figure 1.2. below represents of the sketches of the most common propagation types that can be observed in frame structures. Red circle represents the plastic hinges. Blue arrow represents the direction of collapse propagation.

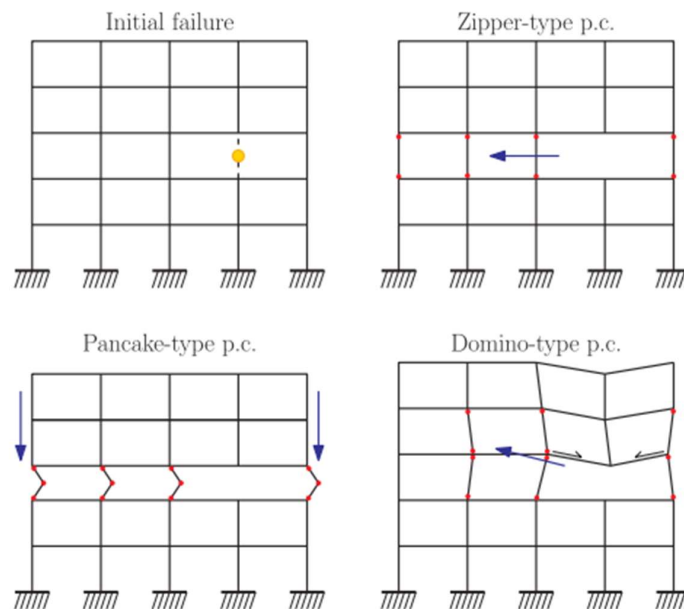


Figure 1.2. Visual sketches of the propagation types (Smith JW, 2006).

1.2.2. Typical triggering events

Based on Ellingwood et al. (Ellingwood et al., 2007), potential circumstances which could trigger progressive collapse are aircraft impact, design or construction error, fire, gas explosions, overload due to occupant misuse, transportation and storage of hazardous materials, vehicular collision and bomb explosions, earthquake. However, this is a limited literature on progressive collapse and, therefore, this section is focus on the main events which are blast, fire, impact and earthquake, as triggering events.

1.2.2.1. Blast

Blast has historically been considered as the main triggering event in progressive collapse study. Actually, most of the major progressive collapse disasters are induced by or accompanied with blast. The guidelines and codes implicitly consider a near-field small blast (that is, briefcase/suitcase bombs) as source of initial failure (General Services Administration Alternate Path Analysis & Design Guidelines for Progressive Collapse Resistance, 2013). In real blast and progressive collapse scenarios, more than one member is usually affected (Jeyarajan et al., 2015).

1.2.2.2. Fire

In a large number of structural failures, fires acted as a triggering event to initiate the progressive collapse. The effects of fire on RC and steel structures have a long research history, but the focus on fire-induced progressive collapse has been boomed after September, 11 attacks. The first research works were case studies on WTC towers(Z. P. Bažant & Zhou, 2001; Zdeněk P. Bažant & Verdure, 2007; Lane, 2003). In recent years, more and more researchers focused on progressive collapse under different fire scenarios such as localized fire (B. Jiang et al., 2015; J. Jiang & Li, 2017b), compartment fire(J. Jiang et al., 2015; J. Jiang & Li, 2017) and extreme fire when entire story or multiple stories are involved (Lu et al., 2017).

1.2.2.3. Impact

Research works on the impact-induced collapse can be categorized into two main groups; debris impact on the underlying floor (Behnam et al., 2019; Vlassis et al., 2009; Yankelevsky et al., 2020) and vehicle/aircraft impact (Kang et al., 2013; Nöldgen et al., 2012). Generally, the former cannot be considered as true triggering event because it occurs during collapse after original triggering event, that is, blast or fire. Research on aircraft impact on framed structures are mainly limited to case studies, especially on World Trade Center towers(Karim & Fatt, 2005). It should be noticed that, for vehicle impact, when only a single column affected, structural response can be completely different compared with threat-independent dynamic column removal.

1.2.2.4. Seismic loads

Most of the real seismic collapse incidents are in progressive manner, therefore, these earthquake-induced collapses can be categorized as progressive collapse (Gurley, 2008). While numerous research works discussed the seismic collapse of framed structures, studies that focused on seismic progressive collapse and its special characteristics are rare. Influences on seismic detailing and seismic design on the progressive collapse response are well-known fact (Jr et al., 2005; Kim & Kim, 2009; Ronagh, 2011). Potential of progressive collapse is decreased by increasing the design seismic level (Ronagh, 2011).

1.2.2.5. Multi-hazard scenarios

In many real collapse scenarios, more than one event contributed in the collapse progression and in the failure mechanism, that is, in the collapse of WTC, impact, blast and fire were involved. Moreover, fire can initiate blast and blast can cause fire in certain circumstances. Experimental tests on multi-hazards are mostly limited to structural members especially on columns.

1.3. Blast loading

This section focuses on the review of blast loads and explosion as well as analysis for blast loading.

1.3.1. Blast loads and explosion

In this part, we will do the review of the available literature on blast-related parameters and type of explosions.

1.3.1.1. Ideal blast wave characteristics

An explosion can be defined as a very fast chemical reaction involving a solid, dust or gas, during which a rapid release of hot gases and energy takes place. The phenomenon lasts only some milliseconds and it results in the production of very high temperatures and pressures. During detonation the hot gases that are produced expand in order to occupy the available space, leading to wave type propagation through space that is transmitted spherically through an unbounded surrounding medium. Along with the produced gases, the air around the blast (for air blasts) also expands and its molecules pile-up, resulting in what is known as a blast wave and shock front. The blast wave contains a large part of the energy that was released during detonation and moves faster than the speed of sound.

Figure 1.3. shows the idealized profile of the pressure in relation to time for the case of a free air blast wave, which reaches a point at a certain distance from the detonation. The pressure

surrounding the element is initially equal to the ambient pressure P_0 , and it undergoes an instantaneous increase to a peak pressure P_{SO} at the arrival time t_A , when the shock front reaches that point. The time needed for the pressure to reach its peak value is very small and for design purposes it is assumed to be equal to zero. The peak pressure P_{SO} is also known as side-on overpressure or peak overpressure. The value of the peak overpressure as well as the velocity of propagation of the shock wave decrease with increasing distance from the detonation center. After its peak value, the pressure decreases with an exponential rate until it reaches the ambient pressure at t_A+t_0 , to being called the positive phase duration. After the positive phase of the pressure-time diagram, the pressure becomes smaller (referred to as negative) than the ambient value, and finally returns to it. The negative phase is longer than the positive one, its minimum pressure value is denoted as P_{SO}^- and its duration as t_0^- . During this phase the structures are subjected to suction forces, which is the reason why sometimes during blast loading glass fragments from failures of facades are found outside a building instead in its interior.

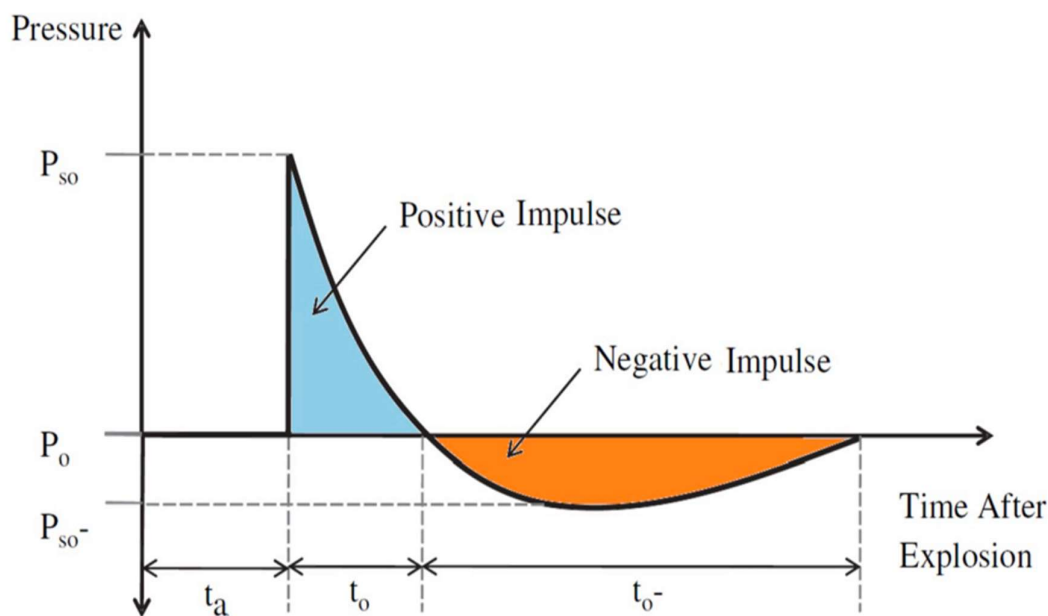


Figure 1.3. Ideal blast wave's pressure time history (Shirbhate & Goel, 2020).

The negative phase of the explosive wave is usually not taken into account for design purposes as it has been verified that the main structural damage is connected to the positive phase. Additionally, the pressures that are produced from the negative phase of the blast wave are relatively small compared to those of the positive phase and since these are in the opposite direction, it is usually on the safe side to assume that they do not have a big impact on the structural integrity of buildings under blast loads. However, the pressures that are below the

ambient pressure value should be taken into account if the overall structural performance of a building during a blast is assessed and not only its structural integrity. As can be seen from figure 1.3, the positive incident pressure decreases exponentially. The following form of Friedlander's equation has been proposed (Baker W.E.,1973), and is widely used to describe this rate of decrease in pressure values:

$$P_s(t) = P_{S0} \left(1 - \frac{t}{t_0}\right) e^{-b \frac{t}{t_0}} \quad (1.1)$$

where:

P_{S0} is the peak overpressure

t_0 is the positive phase duration

b is a decay coefficient of the waveform

t is the time elapsed, measured from the instant of blast arrival

The decay coefficient b can be calculated through a non-linear fitting of an experimental pressure time curve over its positive phase. Besides the peak pressure, for design purposes an even more important parameter of the blast wave pulse is its impulse because it relates to the total force (per unit area) that is applied on a structure due to the blast. It is defined as the shaded area under the overpressure-time curve of figure 1.3. The impulse is distinguished into positive i_s and negative i_s^- , according to the relevant phase of the blast wave time history. Equation (1.2) gives the expression in the case of the positive impulse, which is more significant than its negative counterpart in terms of building collapse prevention,

$$i_s = \int_{t_A}^{t_A+t_0} P_s(t) dt \quad (1.2)$$

For the above Friedlander equation (1.1), the positive impulse can be analytically calculated as

$$i_s = \frac{P_{S0} t_0}{b^2} [b - 1 + e^{-b}] \quad (1.3)$$

This equation constitutes an alternative way for solving iteratively for the decay parameter b when the values of the i_s , P_{S0} and t_0 are known from experimental data.

1.3.1.2. Scaling laws

One of the most critical parameters for blast loading computations is the distance of the detonation point from the structure of interest. The peak pressure value and velocity of the blast wave, which were described earlier, decrease rapidly by increasing the distance between the blast source and the target surface, as shown in Figure 1.4. In the figure only the positive phases of the blast waves are depicted, whose durations are longer whenever the distance from the detonation point increases.

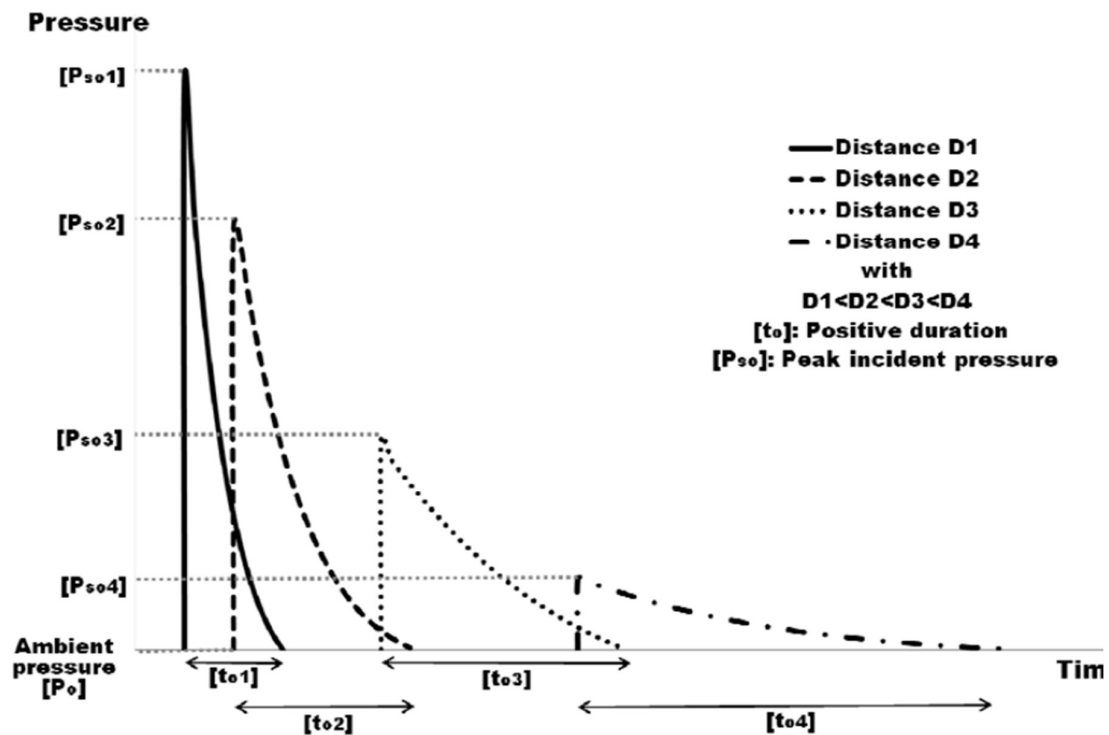


Figure 1.4. Influence of distance on the blast positive pressure phase (Karlos & Solomos, 2013).

The effect of distance on the blast characteristics can be taken into account by the introduction of scaling laws. These laws have the ability to scale parameters, which were defined through experiments, in order to be used for varying values of distance and charge energy release. The experimental results are, in this way, generalized to include cases that are different from the initial experimental setup. The most common blast scaling laws are the ones introduced by Hopkinson-Cranz and Sachs. The idea behind both formulations is that during the detonation of two charges of the same explosive that have similar geometry but different weight and are situated at the same scaled distance from a target surface, similar blast waves are produced at the point of interest as long as they are under the same atmospheric conditions. Sachs scaling is also suitable in the case of different atmospheric conditions. According to

Hopkinson-Cranz law, a dimensional scaled distance is introduced as described by Equation (1.4) (Karlos & Solomos, 2013)

$$Z = \frac{R}{\sqrt[3]{W}} \quad (1.4)$$

where:

R : is the distance from the detonation source to the point of interest [m]

W: is the weight (more precisely: the mass) of the explosive [kg]

The scaled distance (Z) or the proximity factor is in units of distance per mass to the power one third ($\text{m/kg}^{1/3}$). Although the use of scaling laws directly relates pressure of different explosions, it must be noted that, other properties (impulse, particle velocity and dynamic pressure) are not linearly proportional to the scaled distance. Scaling can also be applied to time parameters (Beshara, 1994). The scaled time τ_{sc} is defined by equation (1.5).

$$\tau_{sc} = \frac{t}{W^{1/3}} \quad (1.5)$$

1.3.1.3. Simple numerical formulas for blast load predictions

Blast wave parameters for conventional high explosive materials have been the focus of a number of studies during the 1950s and 1960s. Estimations of peak overpressure due to spherical blast based on the scaled distance $Z = R/W^{1/3}$ were introduced by Brode (1955) as:

$$P_{so} = \frac{6.7}{Z^3} + 1 \text{ bar}; (P_{so} > 10 \text{ bar}) \quad (1.6)$$

$$P_{so} = \frac{0.975}{Z} + \frac{1.455}{Z^2} + \frac{5.85}{Z^3} - 0.019 \text{ bar}; (0.1 \text{ bar} < P_{so} < 10 \text{ bar}) \quad (1.7)$$

Newmark and Hansen (1961) introduced a relationship to calculate the maximum blast overpressure, P_{so} , in bars, for a high explosive charge that detonates at the ground surface as:

$$P_{so} = 6784 \frac{W}{R^3} + 93 \left(\frac{W}{R^3} \right)^{\frac{1}{2}} \text{ (bars)} \quad (1.8)$$

Another expression of the peak overpressure in kPa is introduced by Mills (1987), in which W is expressed as the equivalent charge weight in kilograms of TNT, and Z is the scaled distance:

$$P_{so} = \frac{1772}{Z^3} - \frac{144}{Z^2} + \frac{108}{Z} \text{ (kPa)} \quad (1.9)$$

1.3.1.4. Simplified blast wave profile

The blast overpressure-time profile is simplified with an adequate assumption when determining blast load parameters for conventional practice and design (Yandzio et al.,1999). The overpressure is assumed to decay linearly during the positive phase as shown in figure 1.5 (Yandzio et al.,1999).

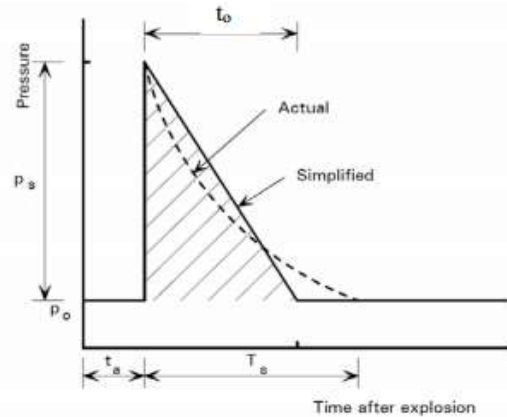


Figure 1.5.Simplified blast wave overpressure profile (Yandzio et al.,1999).

This simplified relationship is expressed numerically by equation 1.10.

$$P(t) = P_o + P_s \left(1 - \frac{t}{t_o}\right) \quad (1.10)$$

The simplified formula is sufficient to predict the blast pressure as the positive phase is significant on structural response (Yandzio et al.,1999)

1.3.1.5. Dynamic Pressure

The shock pressure directly created by the blast is represented by the incident overpressure-time profile. In addition, there is another type of shock wave formed following the explosion called the dynamic pressure. While the gas particles behind the front wave are in motion at lower velocities, the flow of the air mass behind creates a wind. Dynamic pressure is associated with this wind behind the shock front. It is a function of air density and wind velocity. In the low overpressure range with normal atmospheric conditions, the peak dynamic pressure q_o can be determined using the empirical formula developed by Newmark (Ngo et al. 2007)

$$q_o = \frac{2.5P_{s0}^2}{7P_o + P_{s0}} \quad (1.11)$$

Where

P_{so} : is the peak side-on overpressure

P_o : is the normal atmospheric pressure

The net dynamic pressure on a particular structure can be calculated by multiplying the peak dynamic pressure, q_o by the drag coefficient, C_D which is a parameter that depends on the shape and the orientation of the structure (Remennikov,2003).

1.3.1.6. Reflected blast wave characteristics

When blast waves hit an obstacle, they reflect with a maximum pressure which is greater than the peak pressure of the incident waves. There are three types of reflection phenomena namely the face-on reflection, regular reflection and mach reflection (TM5-1300,1990). The characteristics of each type are discussed below.

a. Face on reflection

The maximum reflected pressure is denoted by P_r and it is a function of the incident angle α , and the incident pressure P_{so} . The incident pressure is the blast overpressure at the reflecting surface before the reflection. The incident angle is the angle created between direction of the blast and the reflecting surface. The reflected pressure's value decreases as the angle of incidence α increases. Its minimum value is equal to the incident pressure and is created on surfaces perpendicular to the shock front ($\alpha = 90^\circ$). Equation (1.12) gives us the maximum reflected overpressure in the case of reflections at zero angle:

$$P_r = 2P_{so} \left(\frac{7P_o + 4P_{so}}{7P_o + P_{so}} \right) \quad (1.12)$$

Figure 1.6 shows an illustration the reflected overpressure.

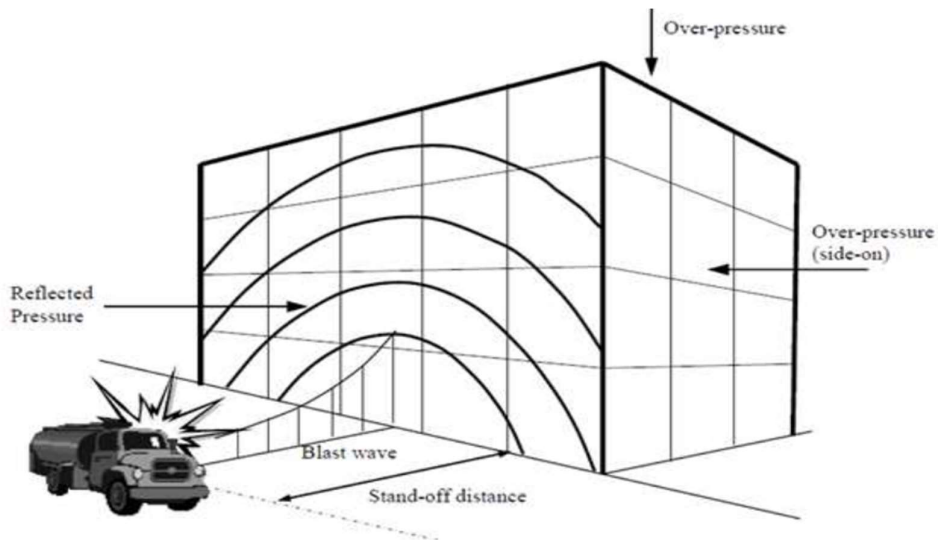


Figure 1.6.Reflected overpressure (Remennikov,2003).

Normal or face-on reflection occurs when the reflecting surface is located in such a way that the direction of the blast wave is perpendicular to the surface as shown in figure 1.7 (Yandzio et al.,1999).

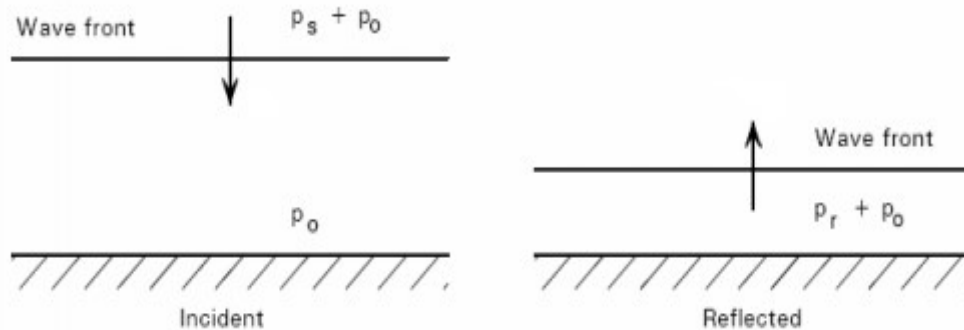


Figure 1.7.Face-on reflection (Yandzio et al.,1999).

The duration of the reflected blast wave is assumed to be equal to the incident pressure profile. Figure 1.8 shows the blast overpressure-time profile for the reflected blast wave.

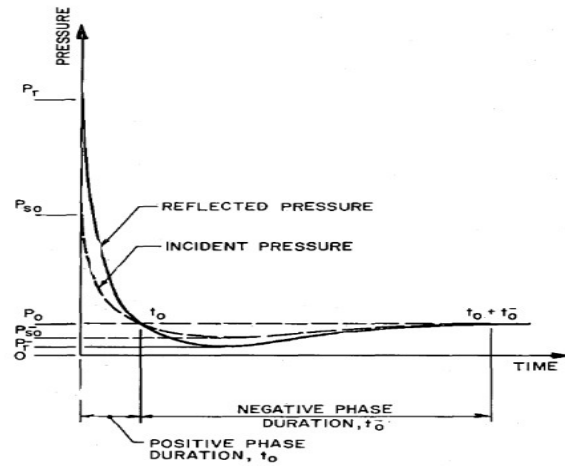


Figure 1.8.Last overpressure-time profile for a face-on reflected wave (Yandzio et al.,1999).

b. Regular Reflection

Regular reflection occurs when the blast wave strikes with an incident angle α which varies from 0° to approximately 40° (see Figure 1.9.) (Yandzio et al.,1999).

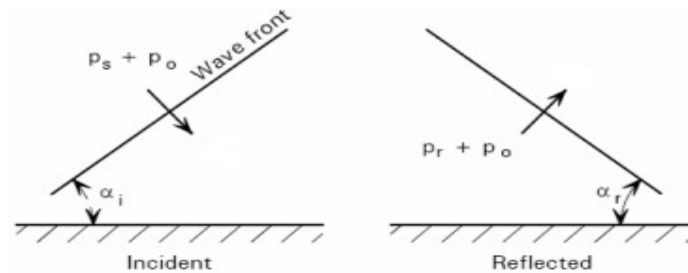


Figure 1.9.Regular reflection (Yandzio et al.,1999).

The regular reflection pressure is greater than the face-on reflection pressure. However, the angle of reflection α_r is not equal to the incident angle. The magnitude of the reflected pressure is determined using the reflection coefficient, C_r together with the incident pressure, P_{so} . The peak reflected pressure, P_r is defined in equation 1.13.

$$P_r = C_r P_{so} \quad (1.13)$$

C_r depends on the peak overpressure and the incident angle of the wave front to the reflecting surface. The values of C_r can be taken from Figure 1.10

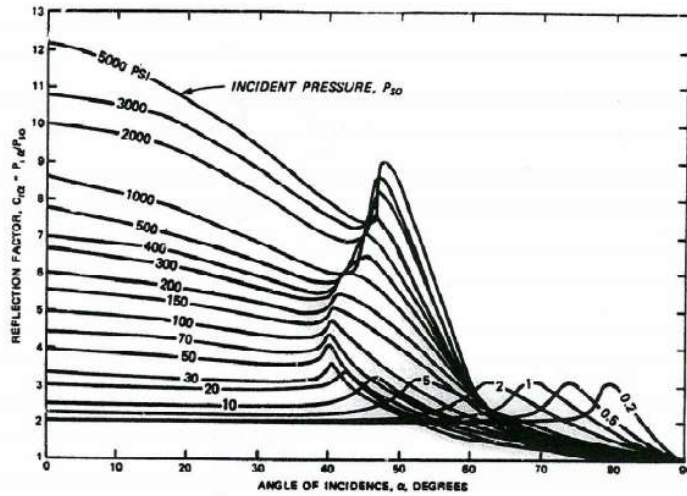
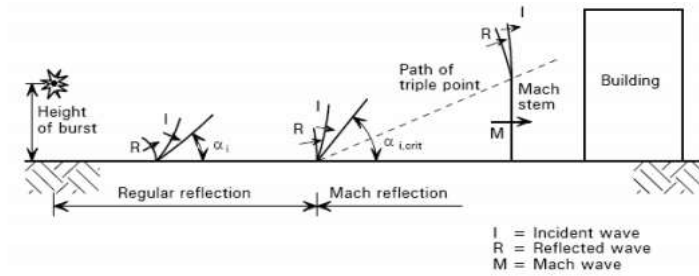


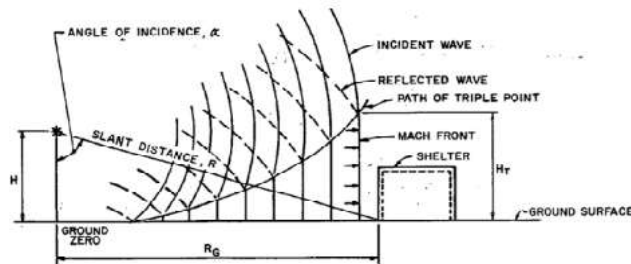
Figure 1.10. Reflection coefficients vs. angle of incidence. (Yandzio et al., 1999).

1.3.1.7. Mach Reflection

The regular reflection is converted to Mach reflection as the incident angle α for a given reflected pressure exceeds the limit angle, at approximately 40° . The mechanism that leads to the creation of the Mach reflection is illustrated in figure 1.11 (Yandzio et al., 1999).



(a) Region of Mach reflection (Yandzio et al. 1999)



(b) Parameters related to Mach reflection (TM5-1300 1990)

Figure 1.11. Mach reflection (Yandzio et al. 1999).

1.3.1.8. Parameters related to blast phenomenon

Blast wave consists of shock wave with high pressure and high-speed wind. The air moving behind the shock front with some pressure difference is termed as blast wind (Cullis, 2001). The parameters related to the blast phenomenon such as TNT equivalence, angle of incidence and standoff distance are explained in the following subsections.

a. TNT Equivalence

Blast load primarily depends on energy output of the explosives. Explosive energy of the detonating materials is determined with respect to equivalent weight of Trinitrotoluene (TNT). In addition to explosive energy, TNT equivalence depends on charge shape (cylindrical, spherical, flat, square etc.), charge weight, confinement of explosive (casing, containers etc.) and the range of the pressure (close-in, intermediate or far ranges etc.) (Army, Navy, 1990; Oswald & Zehrt, 2010; Ullah et al., 2017).

To know the energy output of explosion, one reference explosive TNT is used as standard explosive known as explosion bench mark. Conversion factor based on specific energy of explosive is multiplied to the specific energy of TNT to get the energy output of explosive under consideration and these factors are reported in Table 1.3. (Jeremić & Bajić, 2006; Neff & Fiume, 1999). The table 1.3 shows the type of explosives and TNT equivalent.

Table 1.3.Type of explosives and TNT equivalent.

Explosive type	Mass specific energy Q_x (kJ/kg)	TNT equivalent Q_x / Q_{TNT}
Compound B (60% RDX 40% TNT)	5190	1.148
RDX (cyclonite)	5360	1.185
HMX	5680	1.256
Nitroglycerien (liquid)	6700	1.481
TNT	4520	1.000
Blasting gelatin (91% Nitroglycerin, 7.9% nitrocellulose, 0.9% antacid, 0.2% water)	4520	1.000
60% Nitroglycerine dynamite	2710	1.000
Semtex	5660	1.250
Pentolite 50/50	5860	1.129
PETN (90/10)	6406	1.23
Pentrite	6400	1.13

In case of unconfined explosions, charge weight of explosive under consideration is calculated with reference to weight of TNT explosive and is represented by Equation (1.14) (Army, Navy, 1990).

$$W = \frac{Q_X}{Q_{TNT}} W_X \quad (1.14)$$

Where

W represents effective charge weight in TNT

W_X is weight of explosive

Q_X is the mass specific energy of the explosive

Q_{TNT} is the mass specific energy of TNT

$\frac{Q_X}{Q_{TNT}}$ represents TNT equivalent based on detonation heat

b. Angle of incidence

When the explosive charge gets detonated, incident blast wave is generated and it strikes the ground surface at an angle of incidence. The angle made by tangent to the blast wave and the ground varies from 0° to 90° and is known as angle of incidence (Eichinger, 1985; Karzova et al., 2015; Rigby et al., 2015). Incidence angle influences blast pressure variation and impulse pattern on the structure. It also affects the reflection process and the value of reflection pressure. Reflected pressure reaches to maximum value when the reflected surface is perpendicular to the blast wave whereas, reflected pressure reduces to minimum value if the reflected surface is parallel to the blast wave. Reflected pressure will be moderate for an angle of incidence ranging between 40° and 55° . Within this range of angle of incidence, a coalescent wave resulting to Mach stem could be formed (Gedeon, 2003; Löfquist, 2016).

1.3.1.9. Standoff Distance

The direct, unobstructed distance between asset and midpoint of charge weight is termed as the standoff distance and is shown in Figure 1.12 The main purpose of standoff distance is to keep the threat away from the structure. With increasing standoff distance, the intensity of blast overpressure reduces (Verma et al., 2015). Standoff distance is not a fixed quantity but it is dependent on the type of explosion, type of structure to be protected and the protection level to be achieved. Standoff distance is an important and most economic parameter of blast mitigation strategy, as the intensity of blast overpressure can be reduced with provision of more standoff

distance. The standoff distance can be created by proper entry control point, vehicle barriers, fencing, planters, knee walls, bollards and other physical barriers (Activity, 2014; Gedeon, 2003; Hao et al., 2016).

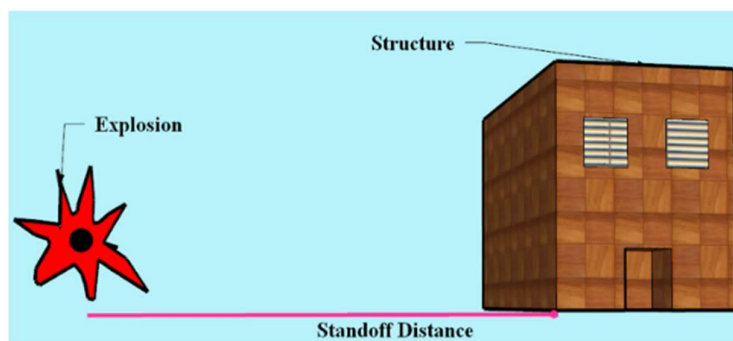


Figure 1.12.Standoff distance of the explosion from the structure. (Shirbhate & Goel, 2020).

1.3.1.10. Explosion

An explosion is a rapid release of stored energy characterized by a bright flash and an audible blast. Part of the energy is released as thermal radiation (flash) and part is coupled into the air as air blast and into the soil (ground) as ground shock, both as radially expanding shock waves.

Explosions can be categorised as physical, nuclear or chemical events. Examples of physical explosions include the catastrophic failure of a cylinder of compressed gas, the eruption of a volcano or the violent mixing of two liquids at different temperatures. In a nuclear explosion, the energy released arises from the formation of different atomic nuclei by the redistribution of the protons and neutrons within the interacting nuclei. A chemical explosion involves the rapid oxidation of fuel elements forming part of the explosive compound. The oxygen needed for the reaction is also contained within the compound so that air is not necessary for the reaction to occur. To be an explosive, the material will have the following characteristics (Anatol & Mniszewski, 1996):

- They must contain a substance or mixture of substances that remains unchanged under ordinary conditions, but undergoes a fast chemical change upon stimulation.
- This reaction must yield gases whose volume under normal pressure, but at the high temperature resulting from an explosion is much greater than that of the original substance.
- The change must be exothermic in order to heat the products of the reaction and thus to increase their pressure.

1.3.1.11. Type of explosion

The blast loading on structures can be divided into two main groups based upon the confinement of the explosive charge (Army, Navy, 1990).

Table 1.4.Explosion load categories (Army, Navy, 1990).

Charge confinement	Categories
Unconfined	Free air burst
	Air burst
	Surface burst
Confined	Full ventilation
	Partially confined
	Fully confined

a. Unconfined Explosions

This group can be distinguished in three basic types, which depend on the relative position of the explosive source and the structure to be protected that is on the height above ground, where the detonation of a charge occurs, and on the horizontal distance between the projection of the explosive to the ground and the structure. These three explosion types are:

i. Free Air Burst Loads

The explosive charge is detonated in the air, the blast waves propagate spherically outwards and impinge directly onto the structure without prior interaction with other obstacles or the ground as illustrated in Figure 1.13.

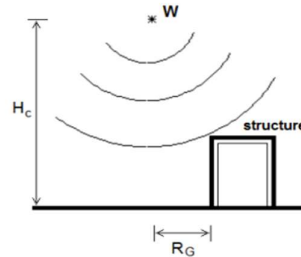


Figure 1.13.Free-air bursts loads (Army, Navy, 1990).

ii. Air Burst Loads

The explosive charge is detonated in the air, the blast waves propagate spherically outwards and impinge onto the structure after having interacted first with the ground; a Mach wave front is created

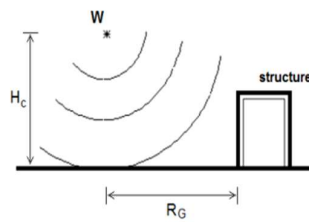


Figure 1.14.Air Burst Loads (Army, Navy, 1990).

iii. Surface Burst Loads

The explosive charge is detonated almost at ground surface, the blast waves immediately interact locally with the ground and they next propagate hemispherically outwards and impinge onto the structure

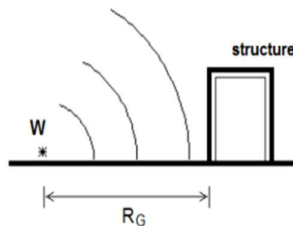


Figure 1.15.Surface Burst Loads (Army, Navy, 1990).

b. Confined Explosions

When a detonation occurs within a structure, the explosion can be further categorised as fully vented, partially vented or fully confined. A fully vented confined explosion is created within structures which have one or more opening surfaces to the atmosphere. If the vented surfaces are more limited than a fully confined case, it is said to be a partially vented confined explosion. If it happens in a fully covered volume, it becomes a fully confined explosion. Figure 1.16 illustrates each of these with simple individual diagrams (Yandzio et al.,1999)

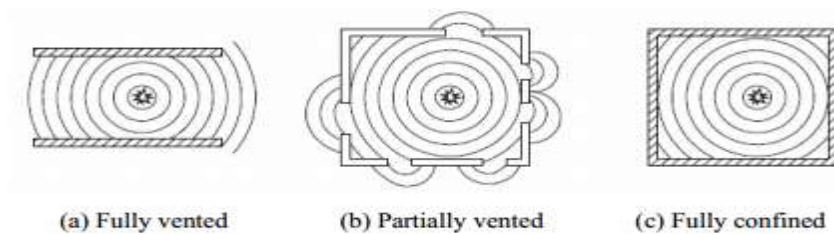


Figure 1.16.Types of confined explosions (Yandzio et al.,1999).

1.3.2. Analysis methods for blast loading

Blast loading is a short duration load also called impulsive loading. Mathematically blast loading is treated as triangular loading. The ductility and natural period of vibration of a structure governs its response to an explosion. Several analysis methods are used for blast resistance design ranging from simple hand calculations and graphical solutions to more complex computer dynamic based applications. Common methods/approaches for blast analysis are discussed below.

1.3.2.1. Equivalent static method

One method of blast analysis which had been commonly used in the past, but which is no longer advocated is the equivalent static method. The method employs a static analysis with an approximate applied load to simulate the dynamic response. Dynamic parameters such as time varying loads, rapid strain rate material strengths, load amplification factors, mass, stiffness, period of vibration, and allowable plastic deformations are not used. The primary difficulty with this method is determining an appropriate static loading which will yield reasonable results. This method is not recommended for general use except for cases where the structure is far removed from the blast source, such that the blast loading resembles a wind gust.

1.3.2.2. Single Degree of Freedom System (SDOF)

Complexity in analysing the dynamic response of blast-loaded structures involves the effect of high strain rates, the non-linear inelastic material behaviour, the uncertainties of blast load calculations and the time-dependent deformations. Therefore, to simplify the analysis, a number of assumptions related to the response of structures and the loads has been proposed and widely accepted. To establish the principles of this analysis, the structure is idealized as a single degree of freedom (SDOF) system and the link between the positive duration of the blast load and the natural period of vibration of the structure is established. This leads to blast load idealization and simplifies the classification of the blast loading regimes (Ngo et al., 2007).

a. Elastic SDOF Systems

The simplest discretization of transient problems is by means of the SDOF approach. The actual structure can be replaced by an equivalent system of one concentrated mass and one weightless spring representing the resistance of the structure against deformation. Such an idealized system is illustrated in Figure 3-1. The structural mass, M , is under the effect of an external force, $F(t)$, and the structural resistance, R , is expressed in terms of the vertical displacement, y , and the spring constant, K .

The blast load can also be idealized as a triangular pulse having a peak force F_m and positive phase duration t_d , illustrated in Figure 1.17. The forcing function is given as

$$F(t) = F_m \left(1 - \frac{t}{t_d}\right) \quad (1.15)$$

The blast impulse is approximated as the area under the force-time curve, and is given by

$$I = \frac{1}{2} F_m t_d \quad (1.16)$$

The equation of motion of the un-damped elastic SDOF system for a time ranging from 0 to the positive phase duration, t_d , is given by Biggs (M. Biggs, 1964.) as:

$$M\ddot{y} + Ky = F_m \left(1 - \frac{t}{t_d}\right) \quad (1.17)$$

The general solution for displacement $y(t)$ and velocity $\dot{y}(t)$ can be expressed as

$$y(t) = \frac{F_m}{K} (1 - \cos \omega t) + \frac{F_m}{K t_d} \left(\frac{\sin \omega t}{\omega} - t\right) \quad (1.18)$$

$$\dot{y}(t) = \frac{dy}{dt} = \frac{F_m}{K} \left[(\omega \sin \omega t) + \frac{1}{t_d} (\cos \omega t - 1) \right] \quad (1.19)$$

In which ω is the natural circular frequency of vibration of the structure and T is the natural period of vibration of the structure which is given by equation (1.20).

$$\omega = \frac{2\pi}{T} = \sqrt{\frac{K}{M}} \quad (1.20)$$

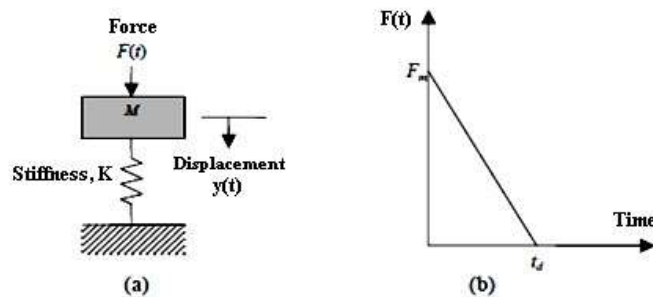


Figure 1.17.(a) SDOF system and (b) blast loading (Ngo et al., 2007).

The maximum response is defined by the maximum dynamic deflection y_m which occurs at time t_m . The maximum dynamic deflection y_m can be evaluated by setting dy/dt in Equation 8

equal to zero, that is when the structural velocity is zero. The dynamic load factor, DLF, is defined as the ratio of the maximum dynamic deflection y_m to the static deflection y_{st} which would have resulted from the static application of the peak load F_m , which is shown as follows:

$$DLF = \frac{y_{max}}{y_{st}} = \frac{y_{max}}{F_m/K} = \psi(\omega t_d) = \psi\left(\frac{t_d}{T}\right) \quad (1.21)$$

The structural response to blast loading is significantly influenced by the ratio $\frac{t_d}{T}$ or ωt_d ($\frac{t_d}{T} = \frac{\omega t_d}{2\pi}$) Three loading regimes are categorized as follows:

- $\omega t_d < 0.4$: impulsive loading regime.
- $\omega t_d > 40$: quasi-static loading regime.
- $0.4 < \omega t_d < 40$: dynamic loading regime.

b. Elasto-Plastic SDOF Systems

Structural elements are expected to undergo large inelastic deformation under blast load or high velocity impact. Exact analysis of dynamic response is then only possible by step-by-step numerical solution requiring nonlinear dynamic finite- element software. However, the degree of uncertainty in both the determination of the loading and the interpretation of acceptability of the resulting deformation is such that solution of a postulated equivalent ideal elasto-plastic SDOF system is commonly used (Ngo et al., 2007) Interpretation is based on the required ductility factor $\mu = y_m/y_e$ shown in Figure 1.18.

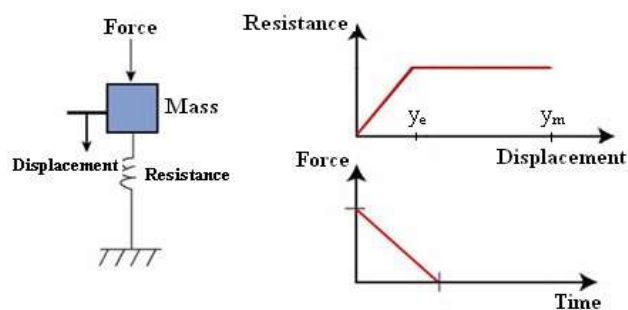


Figure 1.18. Simplified elasto-plastic SDOF model for blast load (Ngo et al., 2007).

The response of the ideal bilinear elasto-plastic system can be evaluated using:

i. Graphical Presentation of Solutions

Analytical solutions for SDOF systems may be very cumbersome, even for simple loading functions. Such computations become much harder for nonlinear resistance functions and complicated loading pulses. To simplify such computations in support of design activities, one may use dynamic response charts that enable an analyst to estimate the values of key parameters for assessing the suitability of a tentative structural design. For the triangular load pulse comprising rapid rise and linear decay, with maximum value F_1 and duration t_d . The result for the maximum displacement is generally presented in chart form (TM 5-1300), as a family of curves for selected values of R_u/F_1 showing the required ductility μ as a function of t_d/T , in which R_u is the structural resistance of the beam and T is the natural period. See Figure 1.19.

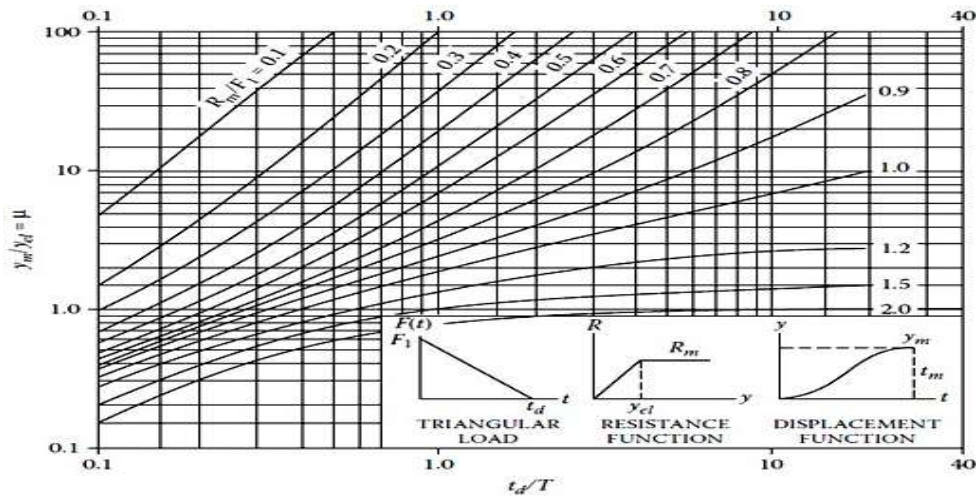


Figure 1.19. Maximum response of elasto-plastic SDOF systems under triangular load pulse with zero rise time (Ngo et al., 2007).

ii. Closed Form Solutions

They are available only for some simple loading cases of SDOF systems. Published solutions exist for both elastic and elastic-plastic responses, and for triangular and rectangular load pulses. The analysis can also be greatly simplified when the duration of the loading, t_d , is either very short or extremely long compare to the period, t_n .

iii. Numerical Integration

The closed form solution of the equation of motion by the approach described earlier may not be possible for highly nonlinear cases. In this case numerical time integration method can be used. This method is also known as the time history method. Most text on structural dynamics (Bigges 1964, Chopra 2001, Paz 1991) provides extensive coverage on numerical solution methods for nonlinear SDOF systems.

It is necessary to derive an efficient numerical integration procedure to solve dynamic equation that will be valid for a wide range of cases. One such technique is the Newmark numerical integration method, which is commonly used to obtain the time history response for nonlinear SDOF systems. For a dynamic equilibrium equation N.M. Newmark developed a family of time stepping solution based on the following equations (Chopra, 2011):

$$[M]\ddot{y} + [C]\dot{y} + [K]y = F_t \quad (1.22)$$

$$\dot{y}_{i+1} = \dot{y}_i + [(1 - \gamma)\Delta t]\ddot{y} + (\gamma\Delta t) + \ddot{y}_{i+1} \quad (1.23)$$

$$y_{i+1} = y_i + (\Delta t)\dot{y}_i + [(0.5 - \beta)(\Delta t^2)]\ddot{y}_i + [\beta(\Delta t^2)]\ddot{y}_{i+1} \quad (1.24)$$

It is most commonly used with either constant-average or linear acceleration approximations within the time step. An incremental solution is obtained by solving the dynamic equilibrium equation for the displacement at each time step. Results of pervious time steps and the current time step are used with recurrence formulas to predict the acceleration and velocity at the current time step. To insure an accurate and numerically stable solution, a small time increment must be selected.

On the other hand, the accuracy obtainable from a SDOF approximation depends on how well the deformed shape of the structure and its resistance can be represented with respect to time. The properties of the equivalent SDOF system are also based on load and mass transformation factors, which are calculated to cause conservation of energy between the equivalent SDOF system and the component assuming a deformed component shape and that the deflection of the equivalent SDOF system equals the maximum deflection of the component at each time.

c. Finite element analysis method

A finite element analysis method is recommended when one or more of the following conditions exist:

- The ratio of a member's natural frequency to the natural frequency of the support system is in range of 0.5 to 2.0, such that an uncoupled analysis approach may yield significant inaccurate result.
- Overall structural behaviour is to be evaluated with regard to structural stability, gross displacements and P-delta effects.
- The structure has unusual features such as unsymmetrical or no uniform mass and stiffness characteristics.

Many commercial finite element programs are available for nonlinear dynamic analysis. Computational methods of computer modelling used by that software's for blast analysis can be categorized as coupled or uncoupled analysis (Ngo et al., 2007). In coupled analysis, both blast load prediction and structural modelling are achieved together in one model. Uncoupled analysis models analyses structures by applying pre-determined loads separately. Coupled analysis tends to be less accurate due to software limitations (Ngo et al., 2007).

Conclusion

In this chapter, the concept of steel, progressive collapse, blast loading and explosions has been introduced, presenting a review of the previous research carried out. We defined progressive collapse, explained the different typology of progressive collapse then finally, the different triggering events that can lead to a progressive collapse. Concerning the blast loading, we talked about blast and its parameter, the scaling law, the dynamic pressure and reflected blast waves. We moved on to explosion and type of explosion and finally the analysis methods for the blast loading. Recent incidents show that a great majority of the blast events occur close to the buildings. It is therefore necessary to carry out in-depth investigations on the blast loads in order to assess the vulnerability of the buildings when they are subjected to near-field blast events. The next chapter presents the method and theories involved in the progressive collapse of steel building subjected to blast loads.

CHAPTER 2: METHODOLOGY

Introduction

Following the literature review done in the previous chapter which enabled us to have a broad knowledge on the concept of progressive collapse and blast loads, this chapter will focus on the description of the methodology of work. The methodology is the part of the study that establishes the research procedure after the definition of the problem, so as to achieve the set objectives. It is partitioned in different sections, the first being a general recognition of the site done by a documentary research. This is followed by data collection that will enable the modelling and analysis of a hangar. Thereafter, this chapter will focus on the description of the design procedures and the governing equations used by analytical and numerical procedures which are intended to be used for the study of the progressive collapse of the steel structure. For our study, the definition of loads and the design of the structural members will be done using the European norms. The modern software makes it possible to analyse ever increasing number of structural problems. However, the results of these analyses are strongly dependent on the assumptions made and the understanding of the working principles of the software used, so care is always recommended when adopting numerical solutions. Therefore, finite element modelling (FEM) and analytical techniques have been extensively employed using the computer codes SAP2000 version 22 and RC blast.

2.1. Site recognition

Recognition of the site was done through research from available documents in order to know on one hand the general physical characteristics (geographical location, climate, hydrology and geology) as well as the economic activities of the region.

2.2. Data collection

The main type of data required for the purpose of this research is the architectural and structural data of the building.

2.2.1. Architectural data

These data collected gives information on the geometry of the building, the surface area and the specific use of the building.

2.2.2. Structural data

These data collected gives information on the sections properties of structural elements, the characteristic of materials used as well as the load applied on the structure.

2.3. Determination of loads acting on the building

Different types of actions act on the building. Regarding our study, we will focus on permanent, variable and blast loads.

2.3.1. Permanent loads

These are also known as static or dead loads. These are actions that act on the whole nominal life of the structure with a negligible variation of their intensity in time. We have the self-weight of the structural elements such as beams, columns, slabs etc... and the self-weight of the non-structural elements.

2.3.2. Variable loads

These are actions on structures with instantaneous values which can significantly vary in time. We have imposed loads and wind loads.

2.3.2.1. Imposed loads

These are loads arising from building occupancy and maintenance (roof elements). They include the loads induced by the normal use by persons, the furniture and moveable objects, vehicles etc. According to Eurocode 1, different categories of areas exist. These categories are presented in Annex 3.

2.3.2.2. Wind loads

Wind load shall be considered for the structure. The response of a building to high wind pressures depends not only upon the geographical location and proximity of other obstructions to airflow but also upon the characteristics of the structure like the size, shape and dynamic properties of the structure. The effect of wind on the structure as a whole is determined by the combined action of external and internal pressures acting upon it. In all cases, the calculated wind loads act normal to the surface to which they apply. The pressures created inside a building due to access of wind through openings could be suction (negative) or pressure (positive) of the same order of intensity while those outside may also vary in magnitude with possible reversals. Thus the design value shall be taken as the algebraic sum of the two in appropriate or concerned direction.

a. Basic wind velocity

The norm used for wind load computation is BS-EN1991 E_2002 (EN 1994 1-4) .The Basic wind velocity, V_b , will be calculated from equation (2.1)

$$V_b = C_{dir} \times C_{season} \times V_{b,0} \quad (2.1)$$

C_{dir} and C_{season} are respectively the directional and seasonal factor. EN 1994 1-4 recommend this value to be taken as 1.

b. Peak and Basic velocity pressure

The peak and basic velocity will be calculated as follows:

- Basic velocity pressure, q_b , is given by equation (2.2)

$$q_b = \frac{1}{2} \rho_{air} V_b^2 \quad (2.2)$$

- Peak velocity pressure, q_p , will be calculated from equation (2.3)

$$q_p(z_e) = C_e(z_e) q_b \quad (2.3)$$

Where:

Terrain factor, K_r , is given by equation (2.4)

$$K_r = 0.19 \left(\frac{z_0}{0.05} \right)^{0.07} \quad (2.4)$$

Orography factor, $C_0 = 1$

Turbulence intensity, I_v , is obtained from equation (2.5)

$$K_i = 1, \quad I_v(z) = \frac{K_i}{C_0 \ln \left(\frac{z}{z_0} \right)} \quad (2.5)$$

Exposure factor $C_e(z)$, is given by equation (2.6)

$$C_e(z) = C_e(z_{min}) = K_r^2 C_0 \ln \left(\frac{z}{z_0} \right) \left(7 + C_0 \ln \left(\frac{z}{z_0} \right) \right), \quad z \leq 10 \text{ m} \quad (2.6)$$

c. Wind pressure on surfaces

Considering a conservative case, the pressure coefficients can be computed and the wind pressure can be obtained following the Figure 2.1.

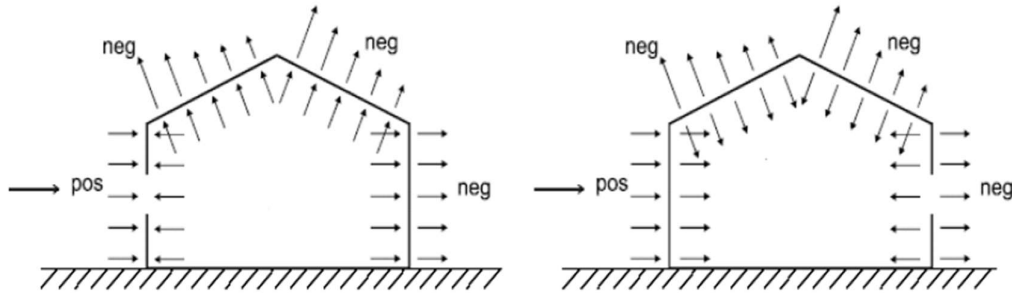


Figure 2.1. Wind pressure on external surfaces (source: BS-EN1991 E_2002).

On windward side, $W_e(w) = C_{pe}(w)C_sC_dq_p$

On leeward side, $W_e(l) = C_{pe}(l)C_sC_dq_p$

With, $C_sC_d = 1.0$ (framed buildings with structural walls less than 100 m high)

2.3.3. Blast loads

The necessary blast load parameters are established using available standard sources based on empirically developed equations and experiments in the field of explosions. Empirical equations developed by Kingery et al. (1984) and charts provided by TM5-1300 1990, are used in this thesis assuming infinite target dimensions for the building. Air pressure is the dominant cause of critical damage to the building, and ground borne shock resulting from the bomb blast and its transmission to the foundations of the building have not been investigated in this thesis (Horoschun 2007).

Recent blast explosions revealed that commercial buildings on city streets are common targets by a small truck or a car bomb often positioned a little above the ground level. Therefore, it is reasonable to assume a hemispherical surface blast environment as a conservative type of external blast scenario on a building. It is shown in figure 2.2.

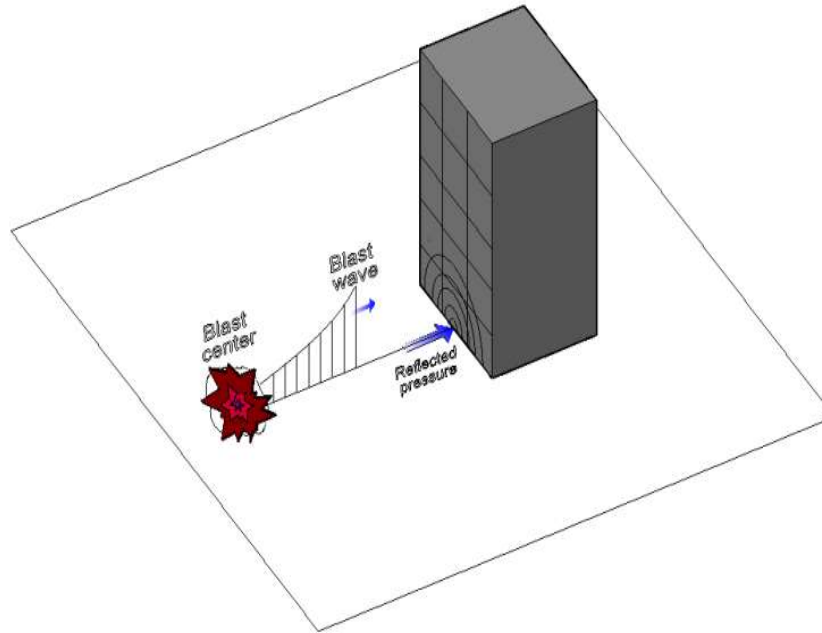


Figure 2.2. Hemispherical blast wave propagation (Remennikov, 2003).

Considering figure 2.3, the method used to determine the blast load parameters at point A is illustrated, when A is at different locations on the loading surface as described in each sample procedure.

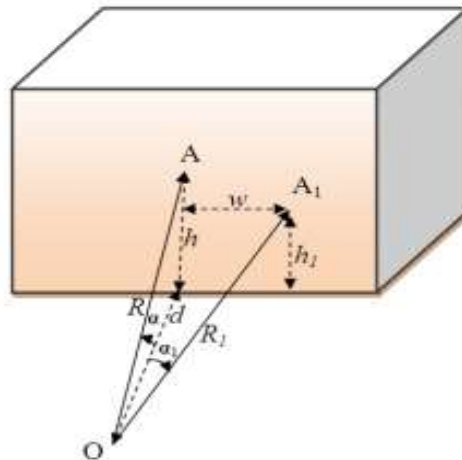


Figure 2.3. Simple diagram for blast load determination (Karlos & Solomos, 2013).

The blast origin is point O in figure 2.3. Point A is the point where the blast parameters need to be calculated. It is located relative to point O at a horizontal distance d and at a height h . The angle of incidence is α which is the angle made between the shock wave and the line perpendicular to the target surface. The distance in the transverse direction is w between the

point of origin and the point of application of the blast when the target point of the blast load is point A1.

According to Pythagoras theorem, the standoff distance R is given by equation (2.7)

$$R = \sqrt{(d^2 + h^2)} \quad (2.7)$$

From trigonometry, the angle of incidence is given by equation (2.8)

$$\alpha = \cos^{-1}\left(\frac{d}{R}\right) = \tan^{-1}\left(\frac{h}{d}\right) \quad (2.8)$$

From the scaling laws, the scaled distance Z is given by equation (2.9)

$$Z = \frac{R}{W^{1/3}} \quad (2.9)$$

Figure 2.4 shows all the required positive phase parameters in metric units with respect to the scaled distance Z.

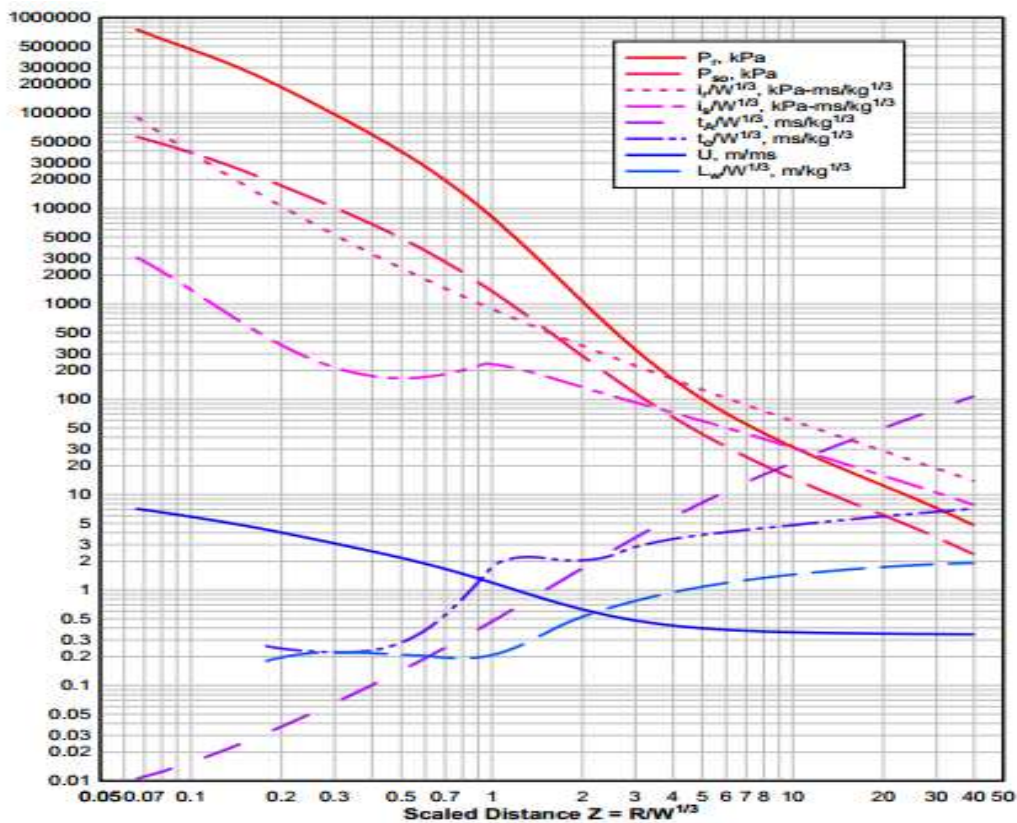


Figure 2.4. Positive phase parameters of shock hemispherical wave of TNT charges from surface bursts (TM5-1300 1990).

The maximum reflected pressure P_r , the design duration t_o and the arrival time t_a are obtained from the graph. The software RC-Blast will be used in order to have the pressure-time graph.

Figure 2.4 is only valid in the case of normal reflections. If there is an angle of incidence α between the wave propagation direction and the loading surface, the process of reflection may be quite different. This angle affects the resulting reflection and, consequently, the blast loading on the structure. The reflection coefficient $C_{r\alpha}$ can be obtained based on figure 2.5, knowing P_{so} and α . The value of the peak reflected overpressure can then be deduced from equation (2.10.)

$$P_{r\alpha} = c_{r\alpha} * P_{so} \quad (2.10)$$

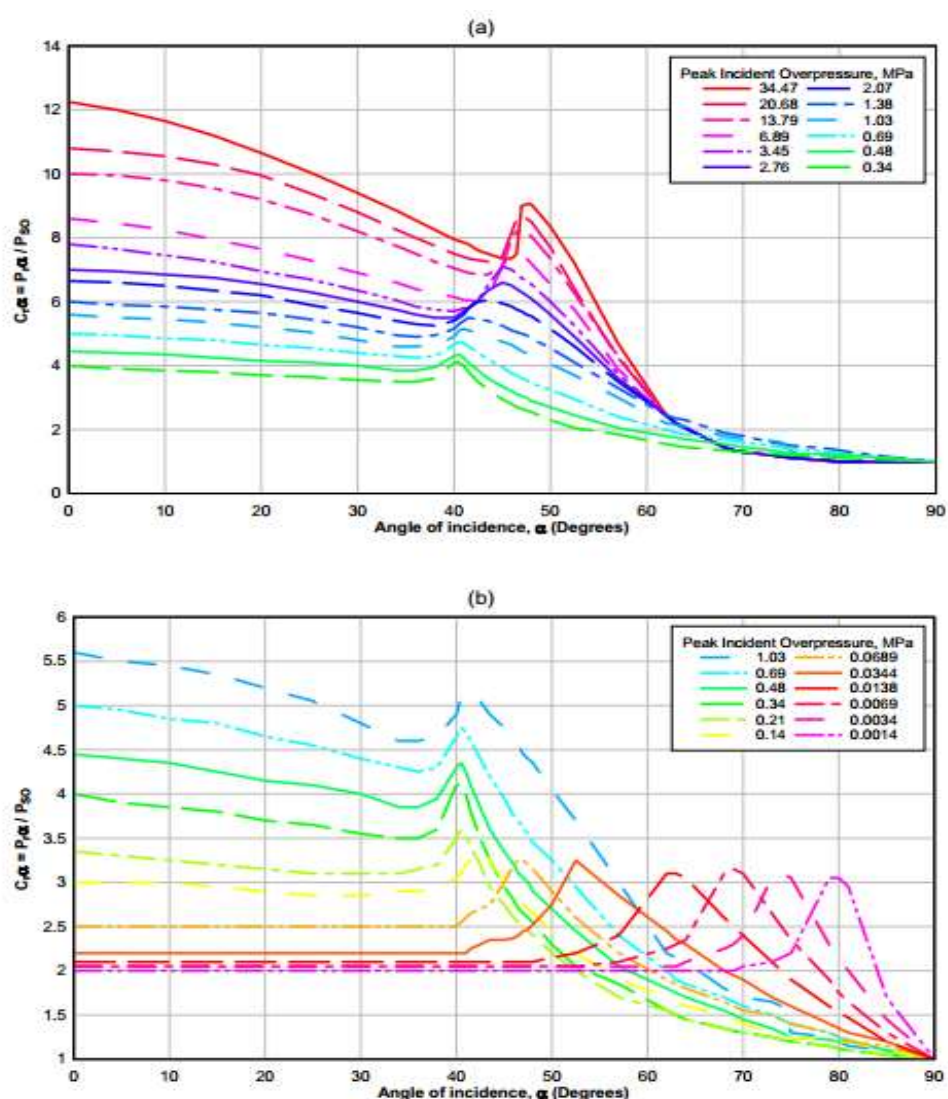


Figure 2.5. Reflected pressure coefficients versus angle of incidence (a) for larger and (b) for smaller values of incident overpressure (TM5-1300 1990).

2.4. Load combinations

A load combination defines a set of values used for the verification of the structural reliability for a limit state under the simultaneous influence of different loads. The static and blast loading cases are discussed in the section below.

2.4.1. Static loading case

A combination of actions defines a set of values used for the verification of the structural reliability for a limit state under the simultaneous influence of different actions. In the case of a building, they are defined by:

- The fundamental combination, used for the Ultimate Limit State (ULS) associated with collapse or other similar forms of structural failure is given by equation (2.11)

$$\sum_{j \geq 1} \gamma_{G,j} G_{k,j} + \gamma_p P + \gamma_{Q,1} Q_{k,1} + \sum_{i \geq 1} \gamma_{Q,i} \Psi_{0,i} Q_{k,i} \quad (2.11)$$

- For SLS the load combinations, this include characteristic (rare) combination, frequent and quasi permanent combinations. These combinations are represented respectively in the following equations.

$$\sum_{j \geq 1} G_{k,j} + P + Q_{k,1} + \sum_{i \geq 1} \Psi_{0,i} Q_{k,i} \quad (2.12)$$

$$\sum_{j \geq 1} G_{k,j} + P + \Psi_{1,1} Q_{k,1} + \sum_{i \geq 1} \Psi_{2,i} Q_{k,i} \quad (2.13)$$

$$\sum_{j \geq 1} G_{k,j} + P + \Psi_{2,1} Q_{k,1} + \sum_{i \geq 1} \Psi_{2,i} Q_{k,i} \quad (2.14)$$

Where:

$G_{k,j}$ is the characteristic value of the permanent action j

$Q_{k,1}$ is the characteristic value of the leading variable action 1

$Q_{k,i}$ is the characteristic value of the accompanying variable action i

$\Psi_{0,i}$ is the combination coefficient and its values are given in annex 2

γ is the safety factor for permanent and variable loads and its values are obtained from annex 2

2.4.2. Blast loading case

The load combinations that have to be applied for a building designed for an accidental load, such as blast load, are included in Eurocode EN-1990. According to its provisions, the self-weight of the structure should be included, as well as the frequent and quasi-permanent values of the live load. The wind and seismic loads may be neglected as their simultaneous presence with the accidental load is highly unlikely. The load combination formulated in Eurocode EN-1990 has been made with the assumption that the loading event is accidental. Internal explosions that could be produced from a gas leakage are considered as random events in time. On the other hand, a terrorist blast attack is not a strictly random event, since it is not based on random conditions, but could be the outcome of human planning. For this reason, the designer should consider the probability of having to increase the safety factors proposed in Eurocode EN-1990, so as to take into account the individual requirements of the project under investigation, such as the expected occupancy of the structure during the blast event, the type and use of the building etc. The general formula proposed by the Eurocode EN-1990 for the loads that have to be considered for the accidental combination is presented in equation (2.15).

$$E_d = \sum_{j \geq 1} G_{k,j} + A_d + \sum_{i \geq 1} \Psi_{2,i} Q_{k,i} \quad (2.15)$$

Where:

A_d is the design value of the accidental load (in this case the blast load)

The values of ψ_1 and ψ_2 depend on the relevant accidental design situation. In case of potentially targeted building structures, the value of ψ_1 ranges from 0.5 (for office and residential areas) to 0.7 (for congregation and shopping areas), while ψ_2 ranges from 0.3 (for office and residential areas) to 0.6 (for congregation and shopping areas).

2.5. Structural analysis and design methods

In this section, we will present the software used for the modelling, the verifications that has to be made for the static analysis and finally the blast analysis approach.

2.5.1. Software used for modelling and analysis of the structure

Numerical modelling in civil engineering is used as a tool that facilitates the engineers to evaluate the behaviour of structures. The numerical methods are convenient, and less time-consuming for the analysis of redistribution of stresses and designing of structures. Numerical methods give the exact mathematical solution for the problem based on the engineering judgment and input parameters like physical and strength parameters of steel building.

To study the progressive collapse of the steel building due to blast loads, RC blast and SAP2000 version 22 will be used. The pressure-time curve information's will be obtained on RC Blast and the modelling of the structure will be done on SAP2000 version 22. Modelling will consist of creating the appropriate material, section properties, loads and combinations. The steel elements shall be drawn according to plan and the supports conditions assigned to be fixed and pinned where concerned. The structure shall be loaded with respect to specific load patterns discussed in section 2.3. The load combinations will be defined prior to the analyses to satisfy the ULS and SLS conditions discussed in section 2.4.1.

2.5.2. Design of the steel structure

The structure will be designed according to the corresponding limit states in such a way to sustain all actions acting upon it during its intended life. This implies it will be designed having adequate structural stability (ultimate limit states) and remain fit for the use it is required (serviceability). Before any element is designed, it needs to be classified according to its capacity to develop plastic hinges and rotation deformations. We shall use the classification proposed by EC3 1-1.

2.5.2.1. Classification of the sections

The sections of the members to be design are going to be classified as class 1, 2, 3, or 4. The norm defines these classes as follow:

- Class 1 cross-sections are those which can form a plastic hinge with the rotation capacity required from plastic analysis without reduction of the resistance.
- Class 2 cross-sections are those which can develop their plastic moment resistance, but have limited rotation capacity because of local buckling.
- Class 3 cross-sections are those in which the stress in the extreme compression fibre of the steel member assuming an elastic distribution of stresses can reach the yield strength, but local buckling is liable to prevent development of the plastic moment resistance.
- Class 4 cross-sections are those in which local buckling will occur before the attainment of yield stress in one or more parts of the cross-section.

The sections are going to be classified according to Table 2.1, 2.2 and 2.3.

Table 2.1.Maximum width-to-thickness ratios for internal compression parts.

Internal compression parts						
				Axis of bending		
				Axis of bending		
Class	Part subject to bending	Part subject to compression	Part subject to bending and compression			
Stress distribution in parts (compression positive)						
1	$c/t \leq 72\epsilon$	$c/t \leq 33\epsilon$	when $\alpha > 0,5$: $c/t \leq \frac{396\epsilon}{13\alpha - 1}$ when $\alpha \leq 0,5$: $c/t \leq \frac{36\epsilon}{\alpha}$			
2	$c/t \leq 83\epsilon$	$c/t \leq 38\epsilon$	when $\alpha > 0,5$: $c/t \leq \frac{456\epsilon}{13\alpha - 1}$ when $\alpha \leq 0,5$: $c/t \leq \frac{41,5\epsilon}{\alpha}$			
Stress distribution in parts (compression positive)						
3	$c/t \leq 124\epsilon$	$c/t \leq 42\epsilon$	when $\psi > -1$: $c/t \leq \frac{42\epsilon}{0,67 + 0,33\psi}$ when $\psi \leq -1^*$: $c/t \leq 62\epsilon(1 - \psi)\sqrt{(-\psi)}$			
$\epsilon = \sqrt{235/f_y}$	f_y	235	275	355	420	460
	ϵ	1,00	0,92	0,81	0,75	0,71

*) $\psi \leq -1$ applies where either the compression stress $\sigma \leq f_y$, or the tensile strain $\epsilon_y > f_y/E$

Table 2.2.Maximum width-to-thickness ratios for compression parts (outstand flanges).

Outstand flanges						
		Rolled sections		Welded sections		
Class	Part subject to compression	Part subject to bending and compression				
		Tip in compression		Tip in tension		
Stress distribution in parts (compression positive)						
1	$c/t \leq 9\epsilon$	$c/t \leq \frac{9\epsilon}{\alpha}$	$c/t \leq \frac{9\epsilon}{\alpha}$	$c/t \leq \frac{9\epsilon}{\alpha\sqrt{\alpha}}$	$c/t \leq \frac{9\epsilon}{\alpha\sqrt{\alpha}}$	$c/t \leq \frac{9\epsilon}{\alpha\sqrt{\alpha}}$
2	$c/t \leq 10\epsilon$	$c/t \leq \frac{10\epsilon}{\alpha}$	$c/t \leq \frac{10\epsilon}{\alpha}$	$c/t \leq \frac{10\epsilon}{\alpha\sqrt{\alpha}}$	$c/t \leq \frac{10\epsilon}{\alpha\sqrt{\alpha}}$	$c/t \leq \frac{10\epsilon}{\alpha\sqrt{\alpha}}$
Stress distribution in parts (compression positive)						
3	$c/t \leq 14\epsilon$	$c/t \leq 21\epsilon\sqrt{k_{\sigma}}$ For k_{σ} , see EN 1993-1-5				
$\epsilon = \sqrt{235/f_y}$	f_y	235	275	355	420	460
	ϵ	1,00	0,92	0,81	0,75	0,71

Table 2.3.Maximum width to thickness ratio for members in bending and/or compression.

Angles						
Refer also to "Outstand flanges" (see sheet 2 of 3)					Does not apply to angles in continuous contact with other components	
Class	Section in compression					
Stress distribution across section (compression positive)						
3	$h/t \leq 15\epsilon : \frac{b+h}{2t} \leq 11,5\epsilon$					
Tubular sections						
Class	Section in bending and/or compression					
1	$d/t \leq 50\epsilon^2$					
2	$d/t \leq 70\epsilon^2$					
3	$d/t \leq 90\epsilon^2$					
NOTE For $d/t > 90\epsilon^2$ see EN 1993-1-6.						
$\epsilon = \sqrt{235/f_y}$	f_y	235	275	355	420	460
	ϵ	1,00	0,92	0,81	0,75	0,71
	ϵ^2	1,00	0,85	0,66	0,56	0,51

2.5.2.2. Ultimate limit states design checks for steel members (ULS)

Ultimate limit states are those that relate to the failure of a structural member or a whole structure. Design verifications that relate to the safety of the people in and around the structure are ultimate limit state verifications. The design verifications will be done with respect to EC3 1-1, 2005.

a. Design of tension or compression members

The design for a tension or compression member must be such that the design actions are lower than the resisting forces and moments.

i. Tension member

For a tension member, we will check that,

$$\frac{N_{Ed}}{N_{t,Rd}} \leq 1 \quad (2.16)$$

Where, N_{Ed} is the design tension load and $N_{t,Rd}$ is the resisting tensile force of the element and is the minimum between $N_{pl,Rd}$ and $N_{u,Rd}$ given in equations (2.17) and (2.18).

$$N_{pl,Rd} = \frac{Af_y}{\gamma_{M0}} \quad (2.17)$$

$$N_{u,Rd} = \frac{0.9A_{net}f_u}{\gamma_{M2}} \quad (2.18)$$

ii. Compression member

For a compression member, we will check that,

$$\frac{N_{Ed}}{N_{c,Rd}} \leq 1 \quad (2.19)$$

Where $N_{c,Rd}$ should be determined by equation (2.20).

$$N_{c,Rd} = \frac{Af_y}{\gamma_{M0}} \quad \text{For class 1, 2 and 3 cross sections} \quad (2.20)$$

The steel element shall also be checked for buckling. To do so, the design compressive force should be lower than the buckling resistance force.

$$\frac{N_{Ed}}{N_{b,Rd}} \leq 1 \quad (2.21)$$

Where, $N_{b,Rd}$ is the design buckling resistance of the compression member and is given by equation (2.22) and (2.23).

$$N_{b,Rd} = \frac{\chi A f_y}{\gamma_{M1}} \quad \text{For class 1, 2 and 3 cross sections} \quad (2.22)$$

$$N_{b,Rd} = \frac{\chi A_{eff} f_y}{\gamma_{M1}} \quad \text{For class 4 cross sections} \quad (2.23)$$

Where, χ is the buckling factor which reduces the resisting axial force of the whole element. To determine χ , we first need to select the appropriate buckling curve (see Figure 2.6) which is given according to Table 2.4 with respect to the section's characteristics and steel type.

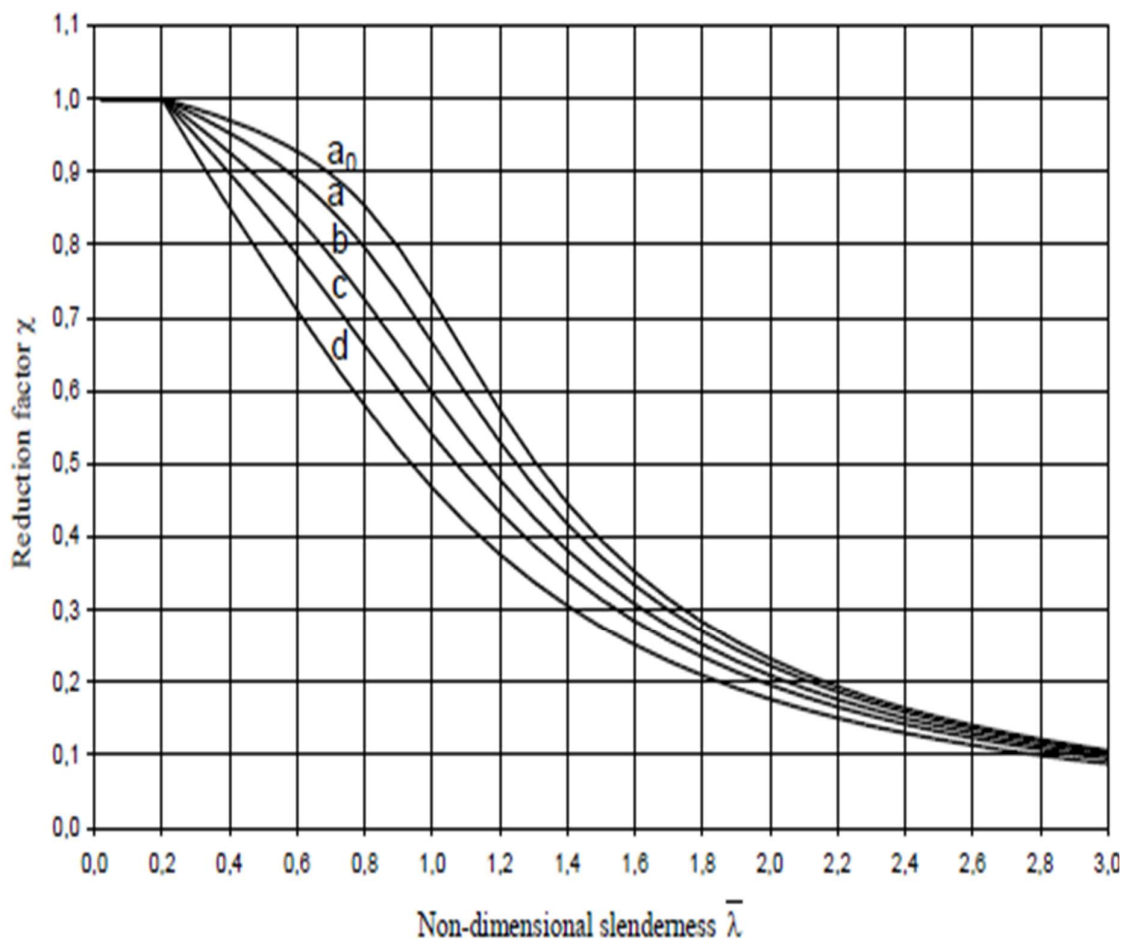
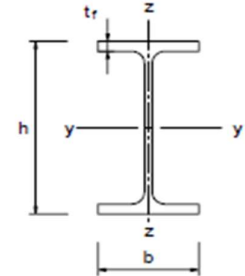
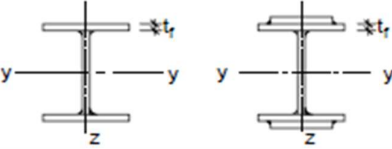

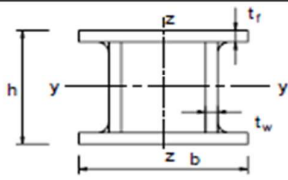
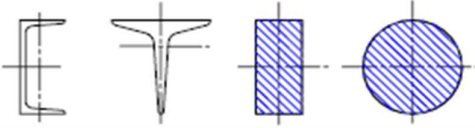
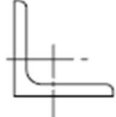


Figure 2.6.Buckling curves (source: EC3 1-1 , 2005).

Table 2.4. Selection of buckling curve for a cross section (source: EC3 1-1, 2005).

Cross section		Limits	Buckling about axis	Buckling curve	
				S 235 S 275 S 355 S 420	S 460
Rolled sections		$h/b > 1,2$	$t_r \leq 40 \text{ mm}$	y-y z-z	a a ₀
			$40 \text{ mm} < t_r \leq 100$	y-y z-z	b c
		$h/b \leq 1,2$	$t_r \leq 100 \text{ mm}$	y-y z-z	b c
			$t_r > 100 \text{ mm}$	y-y z-z	d c
Welded I-sections		$t_r \leq 40 \text{ mm}$	y-y z-z	b c	
		$t_r > 40 \text{ mm}$	y-y z-z	c d	
Hollow sections		hot finished	any	a	a ₀
		cold formed	any	c	c
Welded box sections		generally (except as below)	any	b	b
		thick welds: $a > 0,5t_r$ $b/t_r < 30$ $h/t_w < 30$	any	c	c
U-, T- and solid sections			any	c	c
L-sections			any	b	b

The non-dimensional slenderness, $\bar{\lambda}$ is computed using equation (2.24) and equation (2.25).

$$\bar{\lambda} = \sqrt{\frac{Af_y}{N_{cr}}} = \frac{l_{cr}}{i} \left(\frac{1}{\lambda_1} \right) \quad \text{For class 1, 2 and 3 cross sections} \quad (2.24)$$

$$\bar{\lambda} = \sqrt{\frac{A_{eff}f_{yk}}{N_{cr}}} = \frac{l_{cr}}{i} \frac{\sqrt{A_{eff}}}{\lambda_1} \quad \text{For class 4 cross sections} \quad (2.25)$$

Where:

l_{cr} is the buckling length in the buckling plane considered

i is the radius of gyration about the relevant axis

$$\lambda_1 = 93.9\varepsilon.$$

N_{cr} is the elastic critical force for the relevant buckling mode based on the gross cross sectional properties and is given by equation (2.26).

$$N_{cr} = \frac{\pi^2 EJ}{l_0^2} \quad (2.26)$$

b. Design of beams-columns

The design procedure for the beam-column elements will be done as follow:

i. Bending and axial check, bending and axial interaction

The design value of bending moment at each cross-section shall satisfy:

$$\frac{M_{Ed}}{M_{C,Rd}} \leq 1 \quad (2.27)$$

Where M_{Ed} is the design moment and $M_{C,Rd}$ is the resisting moment.

For class 1 or 2 sections

$$M_{C,Rd} = M_{pl,Rd} = \frac{W_{pl} f_y}{\gamma_{M0}} \quad (2.28)$$

For class 3 sections

$$M_{C,Rd} = M_{el,Rd} = \frac{W_{el,min} f_y}{\gamma_{M0}} \quad (2.29)$$

For class 4 sections

$$M_{C,Rd} = M_{el,Rd} = \frac{W_{eff,min} f_y}{\gamma_{M0}} \quad (2.30)$$

Where:

f_y is the yielding strength

W_{pl} is the plastic section modulus

$W_{el,min}$ is the elastic section modulus

$W_{eff,min}$ is the effective section modulus

As earlier defined, beam-column are subjected to axial and flexural load. In a more conservative approach, the design proposal states that the condition given by equation (2.31) should hold.

$$\frac{N_{Ed}}{N_{c,Rd}} + \frac{M_{Ed}}{M_{c,Rd}} \leq 1 \quad (2.31)$$

In which N_{Ed} is the design axial force and M_{Ed} the design moment acting on the element at the cross-section under consideration, $N_{c,Rd}$ is the cross-section axial resistance, and $M_{c,Rd}$ is the cross-section moment resistance.

$$\frac{N_{Ed}}{N_{c,Rd}} \leq 1 \quad (2.32)$$

Where $N_{c,Rd}$ is given by equation (2.33)

$$N_{c,Rd} \leq \frac{Af_y}{\gamma_{M0}} \quad (2.33)$$

For a given section, there is no reduction to the major axis plastic moment resistance provided the conditions hold:

$$N_{Ed} \leq 0.25N_{pl,Rd} \quad (2.34)$$

$$N_{Ed} \leq \frac{0.5 h_w t_w f_y}{\gamma_{M0}} \quad (2.35)$$

ii. Shear check, shear and bending moment interaction

The design value of the shear force, V_{Ed} at each cross-section shall satisfy equation (2.36).

$$\frac{V_{Ed}}{V_{c,Rd}} \leq 1 \quad (2.36)$$

For plastic design (which shall be the one considered), $V_{c,Rd}$ is the design plastic shear resistance, $V_{pl,Rd}$ given by equation (2.37)

$$V_{pl,Rd} = \frac{A_v \left(\frac{f_y}{\sqrt{3}} \right)}{\gamma_{M0}} \quad (2.37)$$

Where:

f_y is the yielding strength

A_v is the shear area

If the shear force is less than half the plastic shear resistance ($V_{Ed} < 0.5V_{pl,Rd}$), its effect on the moment resistance may be neglected. If V_{Ed} exceeds 50% of $V_{pl,Rd}$, the reduced plastic shear resistance is calculated using a reduced yield strength given by equation (2.38).

$$f'_y = (1 - \rho)f_y \quad (2.38)$$

$$\text{Where, } \rho = \left(\frac{2V_{Ed}}{V_{pl,Rd}} - 1 \right)^2.$$

The column elements shall also be checked for buckling since they are subjected to compressive force. The stability of the column is given by the equation (2.39).

$$\frac{N_{Ed}\gamma_{M1}}{\chi_{min}A f_y} + \frac{M_{eq,Ed}\gamma_{M1}}{W_{pl}f_y \left(1 - \frac{N_{Ed}}{N_{cr}}\right)} \leq 1 \quad (2.39)$$

Where:

$$M_{eq,Ed} = 0.75M_{max}$$

χ_{min} is the buckling factor

N_{cr} is the elastic critical force for the relevant buckling mode

c. Foundation design of the steel structure

With respect to the structural system used for the columns, the type of foundation used is pad footing. To design these elements, it shall satisfy the following equations.

The bearing capacity is verified by equation (2.40).

$$\sigma_{sol} \leq \sigma_{adm} \quad (2.40)$$

With σ_{sol} is the pressure exerted by the footing on the ground and it is calculated using equation (2.41).

$$\sigma_{sol} = \frac{N + \gamma * A * B * H}{A * B} \quad (2.41)$$

Where:

N is the axial force solicitation at the level of the column base connection

A and B are the dimensions of the section of the concrete footing

H is the height of the concrete footing

γ is the unit weight of concrete

Afterwards, the compressive resistance of the concrete block is verified with the help of equation (2.42).

$$\sigma \leq f_{ck} \quad (2.42)$$

Where:

f_{ck} is the characteristic compressive cylinder strength of concrete

σ is the compression constraint exerted on the concrete bloc calculated using equation (2.43)

$$\sigma \leq \frac{N}{ab} \quad (2.43)$$

With a and b being the length and width of the steel plate.

The bending resistance verification is given by equation (2.44).

$$M_{Ed} \leq M_{lim} \quad (2.44)$$

Where:

$$M_{lim} = 0.167f_{ck}bd^2 \quad (2.45)$$

$$M_{Ed} = 0.5ql^2 \quad (2.46)$$

The longitudinal reinforcement of the footing is given by equation (2.47) and (2.48)

$$\frac{M_{Ed}}{0.87f_{yk}z} \leq A_s \quad (2.47)$$

$$A_{s,min} \leq A_s \quad (2.48)$$

With:

$$A_{s,min} = \frac{0.15bd}{100} \quad (2.49)$$

The concrete footings being designed; we need to design the column base plate. To do so, we start by determining the geometry of the plate. The section of the plate will be calculated with equation (2.50).

$$A_p = \frac{N_{Ed}}{f_{cd}} \quad (2.50)$$

Where f_{cd} is the characteristic resistance of the concrete footing.

Admitting that the part of the plate at the edge of the columns will be subjected to an uplift due to the reactions from the foundations, it will bend according to the tangent lines 1 and 2 shown in Figure 2.7. The extended part of the plate from these lines will be calculated as cantilever and will be verified that it can resist the uplift moment exerted by the concrete.

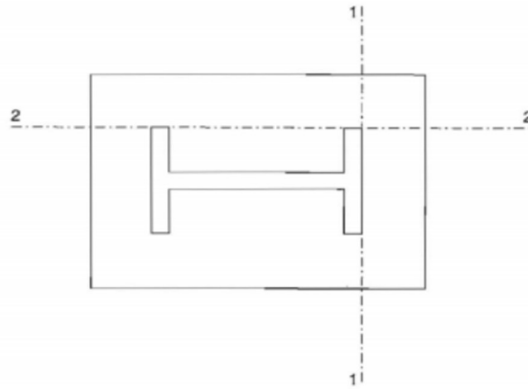


Figure 2.7. Tangent lines on the base plate which determine uplift (Morel, 2005).

The thickness of the plate, t_p should not be less than the value computed in equation (2.51)

$$t_p \geq \mu \sqrt{\frac{3\sigma}{f_y}} \quad (2.51)$$

Where:

μ is the perpendicular distance from the edge of the beam flange to the edge of the column (lever arm)

σ is the compression constraint exerted on the concrete bloc calculated as

$$\sigma = \frac{N_{Ed}}{ab} \quad (2.52)$$

With a and b being the length and width of the plate

d. Design of the connections

In this structure, bolted connections were used the most.

i. Shear resistance for one bolt

The design resistance for a bolt in shear is given by equation (2.53)

$$F_{v,Rd} = \frac{\alpha_v f_{ub} A_b}{\gamma_{Mb}} \quad (2.53)$$

Where:

$$\alpha_v = \begin{cases} 0,6 & \text{for classes 4.6, 5.6 and 8.8} \\ 0,5 & \text{for classes 4.8, 5.8 and 10.9} \end{cases}$$

f_{ub} is the ultimate tensile stresses of the bolt

A_b is the gross area of the bolt given by $\frac{\pi d^2}{4}$

γ_{Mb} is the partial safety factor for bolts = 1,25

ii. Traction resistance for one bolt

The design resistance for a bolt in tension is given by equation (2.54)

$$F_{t,Rd} = \frac{0,9 f_{ub} A_s}{\gamma_{Mb}} \quad (2.54)$$

With A_s being the resisting area of the bolt

If shear and traction are present on the bolt, the following verification must be made:

$$\frac{F_{v,Ed}}{F_{v,Rd}} + \frac{F_{t,Ed}}{1.4F_{t,Rd}} \leq 1 \quad (2.55)$$

iii. Bearing resistance for the plate

For the plate involved in the connection, the bearing resistance is given by Equation (2.56)

$$F_{b,Rd} = \frac{K_1 \alpha_b f_u d_0 t}{\gamma_{M2}} \quad (2.56)$$

Where:

$$\alpha_b = \min \left\{ \left(\frac{p_1}{3d_0} - 0,25 \right); \frac{f_{ub}}{f_u}; 1 \right\}$$

$$K_1 = \min \left\{ \left(\frac{2,8e_2}{d_0} - 1,7 \right); 2,5 \right\}$$

f_u is the ultimate tensile strength for the plate

d_0 is the hole diameter

t is the thickness of the plate

e_1, e_2, p_1, p_2 are the constructive dispositions on the plate and are represented in Figure 2.8

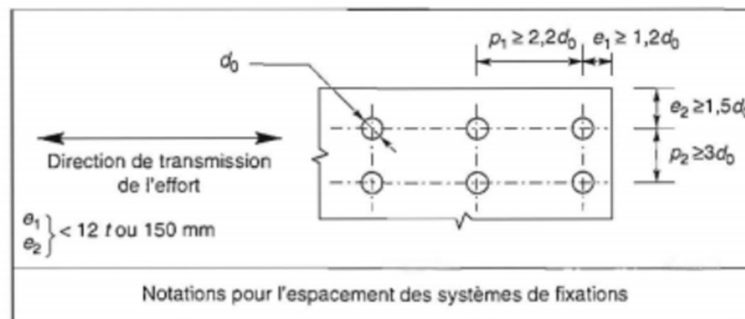


Figure 2.8. Spacing of the holes on the plate (Morel, 2005).

2.5.2.3. Serviceability limit states check for steel members (SLS)

Serviceability limit states concern the functioning of the structure under normal use, the comfort of the people using the structure and the appearance of the structure. Serviceability limit states may be irreversible or reversible.

Irreversible limit states occur where some of the consequences remain after the actions that exceed the limit have been removed, e.g. there is permanent deformation of a beam or cracking of a partition wall. Reversible limit states occur when none of the consequences remains after the actions that exceed the limit have been removed, i.e. the member stresses are within its elastic region.

Criteria that are considered during serviceability limit state design checks are:

- Deflections that affect the appearance of the structure, the comfort of its users and its functionality,
- Vibrations that may cause discomfort to users of the structure and restrict the functionality of the structure,
- Damage that may affect the appearance or durability of the structure and,
- Stress limitation in the section

The Eurocodes do not specify any limits for serviceability criteria, but limits may be given in the National Annexes. The limits should be defined for each project, based on the use of the member and the Client's requirements. For our structure and requirements, we shall consider the following checks:

- For the stress limitation, we will consider $\sigma \leq 0.8f_y$,
- Deflection, $d < l/250$ where, l is the span length and $d < h/300$ for columns

2.5.3. Blast analysis approach

The blast loads will be applied to the columns since our study is focus on the progressive collapse of the structure due to column removal. The reflection areas of the structural components are assumed big enough in order that there is no blast wave diffraction around the structure. A global structural analysis for the complete building is performed using the commercially available graphical user interface FEM code SAP2000 version 22. The complete structure is modelled and time-history loads are applied as joint loads and distributed loads.

The blast analysis is carried out with gravitational loads under the serviceability limit state. Blast load segments applied on the structural components are defined individually as the intensity of blast loads vary rapidly with the distance from the blast source. Therefore, each blast load segment following the explosion has its own magnitude and arrival time to the structure. SAP2000 provides an excellent capability to input the loads with time history variations (SAP2000 user manual 2017).

Individual blast load segments are linked to one single analysis load case that represents a complete blast loading of the structure. Since blast loads deal with time histories following an

explosion, a time-history analysis will provide a true outcome of the structure's response, during and after the investigation.

Time-history analysis of a structure involves solving the dynamic equilibrium. The direct integration more efficiently solves the linear impact and wave propagation problems. Numerical direct integration is therefore used to solve the dynamic equilibrium equation step-by-step in order to obtain the dynamic response of structural systems. A number of integration methods are available each with different defined algorithms. The constant acceleration method, the linear acceleration method, the Newmark beta method, Wilson theta method and the Hilber-Hughes-Taylor-alpha (HHT) method are the available methods in the computer code SAP2000 (SAP2000 user manual 2017). The HHT method is an implicit method used successfully in the field and therefore, will be used for dynamic analyses along with SAP2000 in this thesis.

2.6. Acceptance criteria for progressive collapse

One of the acceptance criteria for progressive collapse is the demand-to-capacity ratios (DCR) based on the recommendations of GSA guidelines (GSA,2003). DCR for a given structural component is the ratio of maximum demand D (e.g. maximum moment, M_{\max}) of the beam or column to its expected capacity C (e.g. ultimate moment capacity, M_p) which is calculated as the product of plastic section modulus and yield strength. In M_p calculations for columns, the effect of the axial load is neglected because the column axial loads were relatively small and did not significantly affect the moment capacity of the cross section.

$$DCR = \frac{D}{C} = \frac{M_{\max}}{M_p} \quad (2.53)$$

If a DCR value is greater than 1.0, theoretically the member has exceeded its ultimate capacity at that location. However, this alone does not signify failure of the structure as long as other members are capable of carrying the forces redistributed after the initial plastic hinge formation or failure. According to GSA (2003), if DCR values for steel columns and beams exceed 2.0 and 3.0, respectively, the members are to be considered failed members, resulting in severe damage or potential partial or total collapse of the structure.

Conclusion

The aim of this chapter was to present in a chronological manner, the steps necessary to demonstrate the progressive collapse due to blast loads on steel structures. We started off by establishing the procedure of collecting data from the field to material properties. In order to perform righteous analyses, a clear methodology to obtain the loads acting on the structures and the various loads combination was done. The software used for this thesis was shown. The design at limit state follows a clear procedure and for the case study, the standard to satisfy these limit states were explained. We moved on to the blast analysis approach presentation and finally, we have explained the acceptance criteria for the progressive collapse for this thesis. In view of all the above, the rest of this work will consist in giving the detailed results of this methodology in the next chapter.

CHAPTER 3: PRESENTATION OF RESULTS AND INTERPRETATION

Introduction

This chapter presents the results obtained from the previously detailed methodology outlined in chapter 2. This application will integrate in particular the general presentation of Edea's city to which our case study belongs, followed by the presentation of the project. The case study to be modelled and its corresponding material properties with respect to the methodology discussed will be presented. The loads acting on the structure are computed to obtain the solicitations and deflections. The various data collected will allow static analysis and blast analysis followed by the results obtained for each of these analysis. We will equally interpret our result as we gradually proceed with their presentation and finally, the last part of this chapter will be devoted to some possible solutions.

3.1. General presentation of the city of Edea

The presentation of the city of Edea will be the subject of this section. The city will be presented geographically, the climate, the hydrology and economic conditions in order to know the different conditions which generally have a major influence on the design of structures.

3.1.1. Geographical location

Edea is a city located along the Sanaga River in Cameroon's Littoral Region. It lies on the Douala–Yaoundé railway line. It is the capital of the Sanaga-Maritime department in the Littoral region of Cameroon and it's located on the national road 3, 61 km south-east of the regional capital of Douala. the city is one of the few crossing points allowing the crossing of the Sanaga between Douala and Yaoundé.

3.1.2. Climate

As for its climate, Edea features a tropical monsoon climate, with relatively consistent temperatures throughout the course of the year, through the city experiences somewhat cooler temperatures in July and August. It is located at an altitude of 67m The average temperature in Edea is 25.6 ° C. The average annual precipitation is 2606 mm.

3.1.3. Hydrology

Edea is a city located along the Sanaga River and is irrigated by it. The flow of the river was observed in Edea and the average annual flow or modulus observed was 1,985 m³/s for a

territory of 131,520 km², that is almost the entire watershed of the river. Its main tributaries are Lom (300 km), Sélé (50 km), Mbam (425 km). It empties, by two main arms, into the Gulf of Guinea, 58 km south of the port city of Douala and face to the Bioko's island, 32 km from the coast of Cameroon and part of Equatorial Guinea.

3.1.4. Vegetation

The vegetation of the Edea are characterized by the presence of large trees under the feet of species such as *Coula edulis*, *Irvingia gabonensis* and *Baillonella toxisperma*. The specific composition is about 500 species identified with a wide dominance of Rubiaceae, Euphorbiceae, Cesalpiniaceae and Fabaceae. The canopy is high and there are several strata. Three species dominate the leaf canopy namely *Coula edulis* and *Lophira alata* in Mvia and *Baillonella toxisperma* in Yavi and Yatou.

3.1.5. Socio-economic parameters

Edea is populated by indigenous Bakoko or Elog Mpo'o populations (Yassoukou, Adié, Ndonga, Yakalag, Bisso'o), Malimba, Pongo-Songo, Bonangasse and Bassa but also several other ethnic groups from all of Cameroon.

The Edea Urban Community covers an area of 180,000 km², 60% of which is allocated to agricultural activity and the rest to industrial activity. The Edea industrial zone reflected by its hydroelectric dam commissioned in 1954 and the Cameroonian Aluminum Company (Alucam) factory producing aluminum since 1957, which constitute one of the first industrial sites in Central Africa.

3.2. Presentation of the project

For the presentation of the project, we will first present our case study followed by a presentation of the element section's and the material used.

3.2.1. Geometrical presentation of the model

The case study is a hangar in Edea. The building occupies a surface area of 1000 m² and is 7m high. The building is a steel structure as shown in Figure 3.1. It is a 50 m long by 20 m large. It is closed and covered with Aluminium 8/10 sheets. The distribution plan is shown in Annex 4.

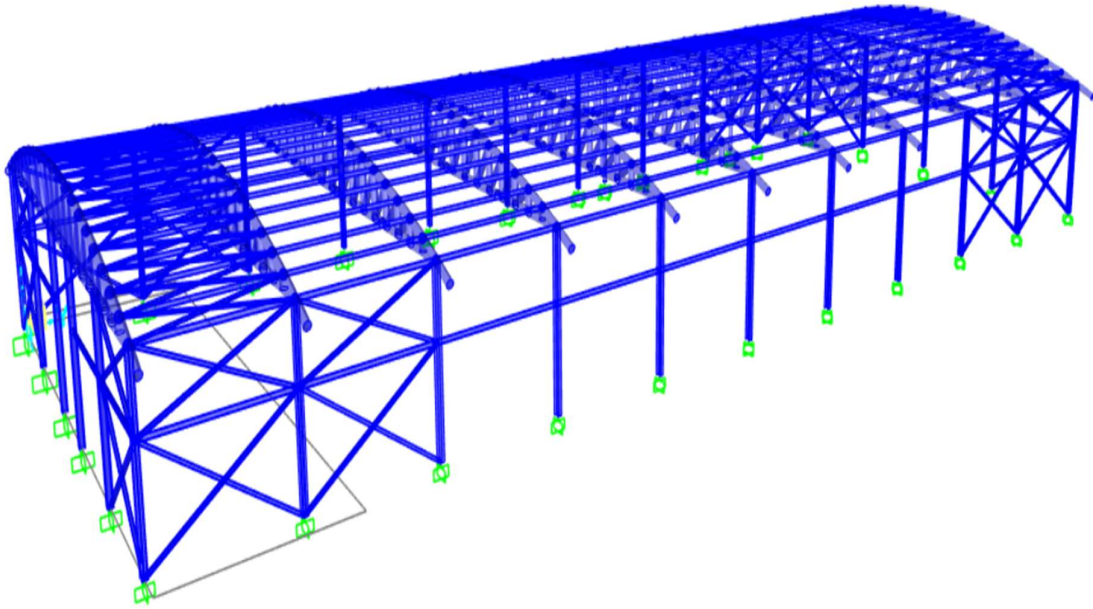


Figure 3.1.3D-view of the steel hangar.

3.2.2. Geometrical and material characteristics

In this building, the supporting structure is entirely made of steel profiles. The columns are IPE 330, the mains beams are IPE 140. Concerning the purling of the building, an IPE 120 section was used and the entire reticular structure of the roof is made with steel section 273x6.3 CHS. The bracing system of the roof has a section of 80x80x5 while bracing system of the column 100x100x5.

The structure is made of two main material, steel grade S235 as presented in Table 3.1 for the structural elements and Table 3.2 for concrete C25/30 for the footing.

Table 3.1.Steel structural sections material properties.

Property	Value	Unit	Definition
Steel grade	S235	-	Gives the steel resistance
f_y	235	N/mm ²	Characteristic yield strength
f_u	360	N/mm ²	Characteristic ultimate strength
E	210 000	N/mm ²	Young modulus
G	80769.231	N/mm ²	Shear modulus
ν	0.3	-	Poisson's ratio

α	0.000012	perK	Coef. of thermal expansion
γ_{M0}	1	-	Safety factor for resistance whatever the section
γ_{M1}	1	-	Safety factor for resistance of members to instability
γ_{M2}	1.25	-	Safety factor for cross section in tension
$f_{ya} = \sigma_{0.2}$	940	N/mm ²	proof strength of bolt grade
f_{ua}	1000	N/mm ²	Ultimate strength of the anchor

Table 3.2.Concrete footing, reinforcing steel and bearing soil material properties.

Property	Value	Unit	Definition
Concrete class	C25/30	-	Concrete class
f_{ck}	25	N/mm ²	Cylindrical crushing strength
E_{cm}	31476	N/mm ²	Static (secant) modulus of concrete
ϵ_{cu2}	0.35%	-	Ultimate compressive strain of concrete
ϵ_{cu3}	0.35%	-	Ultimate compressive strain of concrete
γ_c	1.5	-	Safety factor for concrete
Reinf. Steel type	B500C	-	Reinforcement steel type
f_{yk}	500	N/mm ²	Characteristic yield strength of reinforcing steel
E_s	210000	N/mm ²	Modulus of elasticity of reinforcing steel
γ_s	1.15	-	Safety factor for steel
Q_{adm}	0.2	MPa	Admissible soil bearing capacity

3.3. Load determination

EN 1991-1-1 gives the general recommendations for loads acting on structures according to the building category. The categories ranges from category A to category D depending on the specific use. These categories are represented in appendix 8. This hangar belongs to building category C3, an area with low person mobility.

3.3.1. Permanent loads

The permanent loads acting on the building are of two categories and are presented in the Table 3.3 and Table 3.4.

Table 3.3.Self-weight of structural elements.

Nature	Description	Value	Unit
G1	Self-weight of structural component	78.5	kN/m ³

Table 3.4.Self-weight of non-structural elements.

Nature	Description	Value	Unit
G2	Aluminium roof 8/10 on steel elements	0.03	kN/m ²

3.3.2. Variable loads

For the variable loads, we will present the impose loads, the wind loads and the blast loads.

3.3.2.1. Impose load

The main variable loads on the structure will be the maintenance of roof. The roof is of category H (See table 3.5). The imposed loads q_k vary between 0 kN/m² and 1 kN/m². For our case, 0.5 kN/m² will be used.

Table 3.5.Categorization of roofs.

Categories of loaded area	Specific Use
H	Roofs not accessible except for normal maintenance and repair.
I	Roofs accessible with occupancy according to categories A to D
K	Roofs accessible for special services, such as helicopter landing areas

3.3.2.2. Wind load

The computation of the wind load acting on the building is divided in two main parts, the load acting on the rectangular walls' contours of the structure and that acting on the vaulted roof. As earlier mentioned in chapter 2, the norm used for wind load computation is BS-EN1991 E_2002. We introduce the following wind parameters considering the combination factors for the wind load to be $\varphi_0 = 0.6$ and $\varphi_2 = 0$.

a. Basic wind velocity

For the evaluation of the basic wind velocity, V_b , we have $C_{dir} = C_{season} = 1$ and $V_{b,0} = 22\text{m/s}$, hence we obtain $V_b = 22\text{m/s}$.

b. Peak and Basic velocity pressure

For the calculation of the peak and basic velocity pressure, we have the following:

- Terrain category II, $z_0 = 0.05$ and $z_{min} = 2$
- Terrain factor, $K_r = 0.19$,
- Orography factor, $C_0 = 1$
- Turbulence intensity, $I_v = 0.21$.
- Exposure factor $C_e(z)$ taking into account turbulence $z \leq 10$ m, $C_e(z) = 1.93$

Hence, we obtain:

- Basic velocity pressure (q_b) = 0.3025 kN/m^2
- Peak velocity pressure (q_p) = 0.5835 kN/m^2

c. Wind pressure external on surfaces

Here, we will evaluate the loads acting on the columns and on the roof.

i. the load acting on the rectangular walls

Considering a conservative case, the pressure coefficients can be computed and the wind pressure can be obtained following the Figure 3.2.

$$C_{pe}(\text{windward}, w) = +0.80 + 0.20 = +1.00 \quad C_{pe}(\text{leeward}, l) = -0.4 - 0.2 = -0.6$$

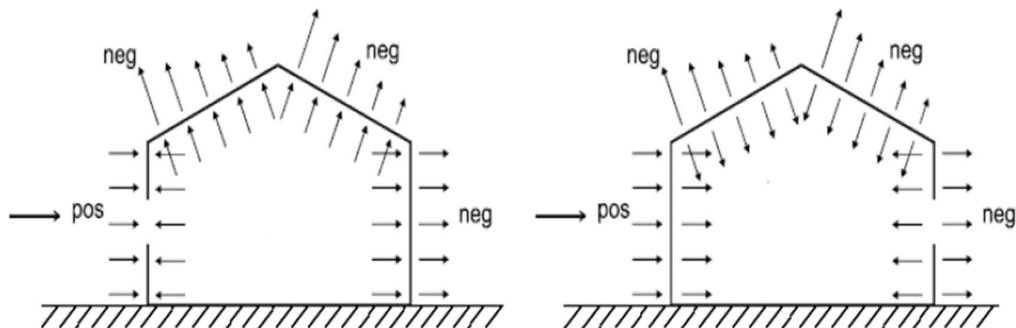


Figure 3.2. Wind pressure on external surfaces (source: BS-EN1991 E_2002).

With, $C_s C_d = 1.0$ (framed buildings with structural walls less than 100 m high), we obtained:

- On windward side, $W_e(w) = 0.3017 \text{ kN/m}^2$.
- On leeward side, $W_e(l) = -0.18 \text{ kN/m}^2$.

ii. The load acting on the roof

For the loads acting on the roof, we have $W_e = -0.18 \text{ kN/m}^2$. This loads will be applied in pressure.

3.3.2.3. Blast loads determination

The blast load parameters used in this global analysis were generated by explosions of charge weight 50kg and 100kg of TNT. A global analysis of the explosion impacting all the columns on the face has been done for the charge weight of 50kg. (see figure 3.3).

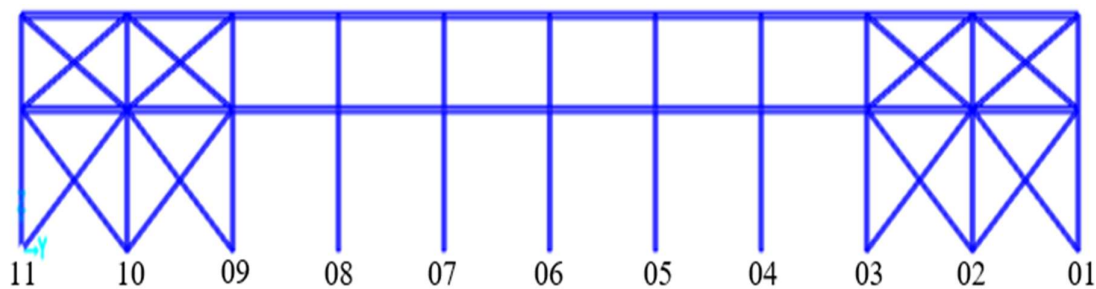


Figure 3.3.Columns on the front face of the building.

From section 2.4.3, we have calculated the various blast wave parameters. Table 3.6 shows the overall blast wave parameters for the front face of the building, given a charge weight of 50kg.

Table 3.6.Blast load parameters relative to the front face of the building.

Column	d (m)	w(m)	R (m)	Z(m/kg ^(1/3))	α	t_A (ms)
Column 01	5	15	15.81	4.29	71.57	350
Column 02	5	10	11.18	3.03	63.43	200
Column 03	5	5	7.07	1.92	45.00	100
Column 04	5	0	5.00	1.36	0.00	40
Column 05	5	5	7.07	1.92	45.00	200
Column 06	5	10	11.18	3.03	63.43	100

Column 07	5	15	15.81	4.29	71.57	350
Column 08	5	20	20.62	5.60	75.96	500
Column 09	5	25	25.50	6.92	78.69	750
Column 10	5	30	30.41	8.26	80.54	850
Column 11	5	35	35.36	9.60	81.87	1000

For a mass of 50kg on the 4th column, the scaled distance obtained for the blast $Z = 1.36 \text{ m/kg}^{(1/3)}$. Based on figure 3.4, we had as extrapolated values $P_r = 3412\text{kN/m}^2$, $t_A = 40\text{ms}$. Figure represents the Pressure-Time graph for a charge weight of 50 kg of TNT.

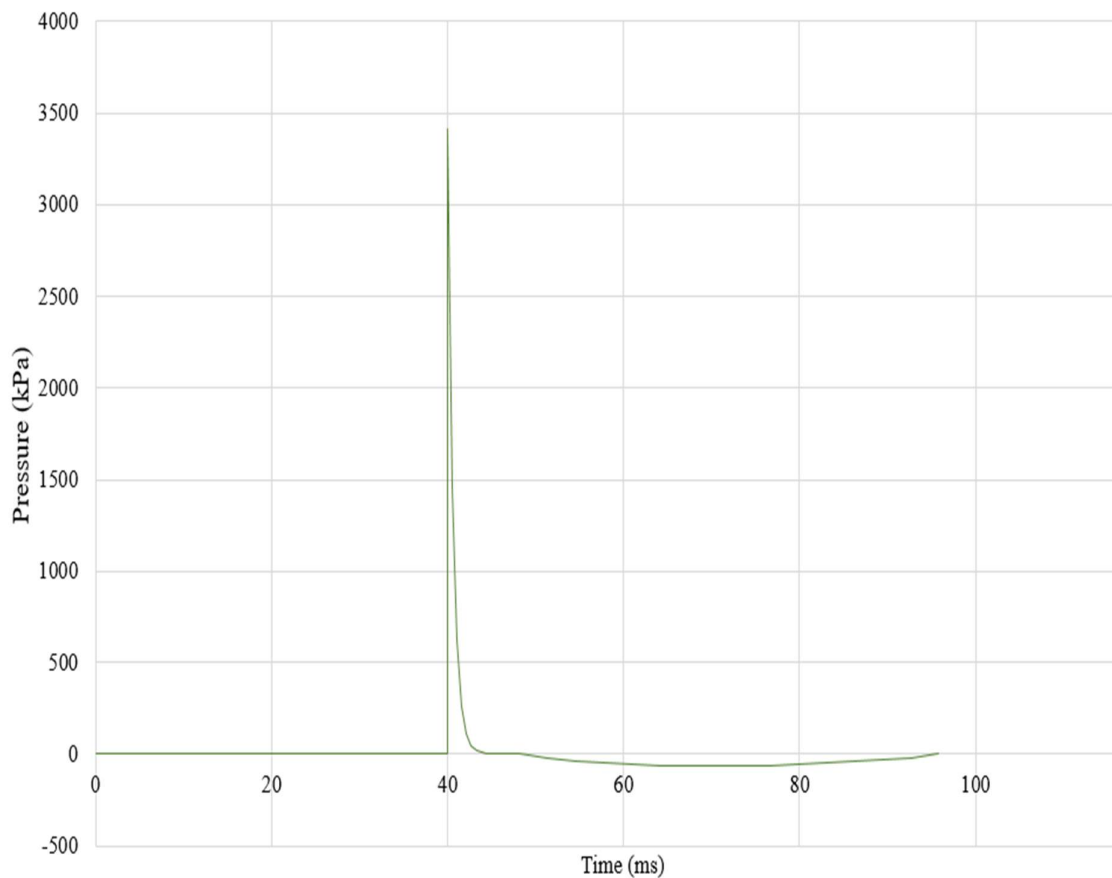


Figure 3.4. Pressure-Time graph for a charge weight of 50 kg of TNT.

3.4. Loads combinations

For the verification of the structure, the load combinations are divided in two groups, the Ultimate limit states(ULS) and serviceability state combinations(SLS). A load envelope is obtained for the ULS combinations to have the most unfavourable condition for an element.

$$ULS1: 1.35G_1 + 1.35G_2 + 1.5Qt + 0.9Qw \quad (3.1)$$

$$ULS2: 1.35G_1 + 1.35G_2 + 1.5Qw \quad (3.2)$$

$$SLS1: G_1 + G_2 + Q + 0.6Qw \quad (3.3)$$

For the blast loading, we have as combination

$$E_d = G_1 + G_2 + A_d \quad (3.4)$$

3.5. Static analysis of the structure

The static analysis of the building is done under the static action meaning considering only the permanent and the imposed loads. It consists of obtaining the design solicitations on the members of the structure and the deflections.

3.5.1. Design of the column

Here, the main interest will be to design the column element with maximum axial, shear forces and bending moment. The solicitations obtained are given in Table 3.7.

Table 3.7.Solicitations of the column.

Bending moment, M[kNm]	Shear force, V[kN]	Axial force, N[kN]	Deflection, f[mm]
-47.85	15.97	-100.66	2.1 mm

IPE 330 was used for the column's section. Its characteristics are given in Table 3.8.

Table 3.8.Properties of IPE 330.

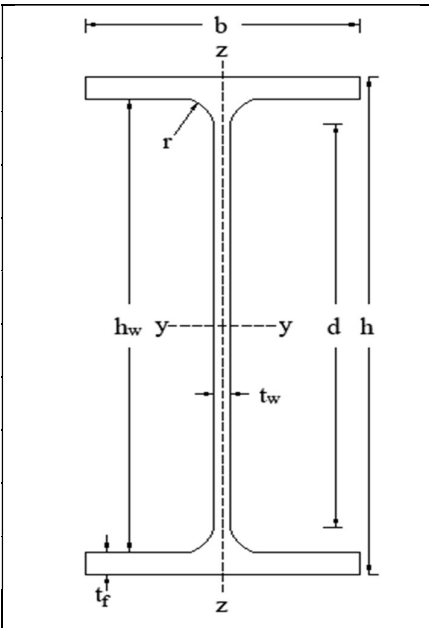
	G	49.1	Kg/m
	h	330	mm
	b	160	mm
	d	271	mm
	h_w	307	mm
	t_w	7.5	mm
	t_f	11.5	mm
	r	18	mm
	A	62.6	cm ²
	A_{vY}	30.8	cm ²
	I_Y	11770	cm ⁴
W_{PL,Y}	804	cm ³	

Table 3.9 shows the result obtained in the excel sheet for the column verification.

Table 3.9.Column design.

Designation	Value/Verification		Observation
Class verification	Web in bending	36.13 < 72	Class 1
	Flange in compression	5.06 < 9	Class 1
Deflection check (SLS)	2.1 cm < 16.67 cm		Verified
Resistance in bending, $M_{Ed} \leq M_{pl,Rd}$	47.85 kNm < 188.94 kNm		Verified
Resistance in shear, $V_{Ed} \leq V_{pl,Rd}$	15.97 kN < 417.87 kN		Verified
Moment and shear interaction, $V_{Ed} \leq 0.5V_{pl,Rd}$	7.98 kN < 417.87 kN		No bending moment reduction
Resistance in compression, $N_{Ed} \leq N_{pl,Rd}$	100.66 kN < 1471 kN		Verified
Bending and axial interaction	$\frac{N_{Ed}}{N_{c,Rd}} + \frac{M_{Ed}}{M_{c,Rd}} \leq 1$	0.31 < 1	No bending-axial interaction
	$N_{Ed} \leq 0.25N_{pl,Rd}$	100.7 kN < 367.5 kN	Axial forces doesn't affect moments
	$N_{Ed} \leq \frac{0.5 h_w t_w f_y}{\gamma_{M0}}$	100.7 kN < 270.5 kN	
Resistance to Buckling $\chi \leq 1$	0.85 < 1		verified
Stability of the column $\frac{N_{Ed}\gamma_{M1}}{\chi_{min}A_f y} + \frac{M_{eq,Ed}\gamma_{M1}}{W_{pl}f_y \left(1 - \frac{N_{Ed}}{N_{cr}}\right)} \leq 1$	0.35 < 1		verified

3.5.2. Design of the purling

Here, the main interest will be to design the purling element with maximum axial, shear forces and bending moment. The solicitations obtained are given in Table 3.10.

Table 3.10.Solicitations of the purling.

Bending moment, M[kNm]	Shear force, V[kN]	Axial force, N[kN]	Deflection, f[mm]
3.89	3.11	-10.371	13.22

IPE 120 was used for the column's section. Its characteristics are given in Table 3.11.

Table 3.11. Properties of IPE 120.

	G	10.4	Kg/m
	h	120	mm
	b	64	mm
	d	93.4	mm
	h_w	107.4	mm
	t_w	4.4	mm
	t_f	6.3	mm
	r	7	mm
	A	13.2	cm ²
	A_{vz}	6.31	cm ²
	I_y	318	cm ⁴
W_{PL,Y}	60.7	cm ³	

Table 3.12 shows the result obtained in the excel sheet for the purling verification.

Table 3.12. Purling design.

Designation	Value/Verification		Observation
Class verification	Web in bending	21.23 < 72	Class 1
	Flange in compression	3.6 < 9	Class 1
Deflection check (SLS)	13.22 cm < 20 cm		Verified
Resistance in bending, $M_{Ed} \leq M_{pl,Rd}$	3.89 kNm < 14.26 kNm		Verified
Resistance in shear, $V_{Ed} \leq V_{pl,Rd}$	3.11 kN < 85.62 kN		Verified
Moment and shear interaction, $V_{Ed} \leq 0.5V_{pl,Rd}$	3.11 kN < 42.81 kN		No bending moment reduction
Resistance in compression, $N_{Ed} \leq N_{pl,Rd}$	10.37 kN < 310.2 kN		Verified
Bending and axial interaction	$\frac{N_{Ed}}{N_{c,Rd}} + \frac{M_{Ed}}{M_{c,Rd}} \leq 1$	0.31 < 1	Verified
	$N_{Ed} \leq 0.25N_{pl,Rd}$	10.3 kN < 77.5 kN	No bending moment reduction

	$N_{Ed} \leq \frac{0.5 h_w t_w f_y}{\gamma_{M0}}$	10.3 kN < 55.5 kN	No bending moment reduction
--	---	-------------------	-----------------------------

3.5.3. Design reticular structure of the roof

To design the reticular structure of the roof, we will verify the elements in tension and in compression of the roof.

3.5.3.1. Element in tension

To design the elements in tension of the roof, we will verify the element with the maximum tension force. (see Figure 3.5).

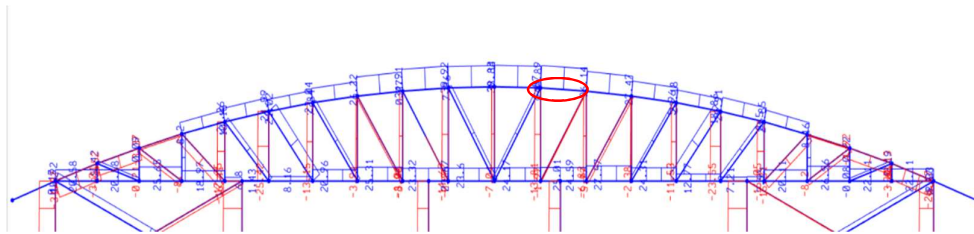


Figure 3.5.Element in tension to be designed on the reticular steel roof.

The axial force solicitations obtained is $N_{Ed} = 44.37$ KN. The section of the element under study is 273x6.3 CHS. Its characteristics are given in Table 3.13.

Table 3.13.Properties of 273x6.3 CHS.

	s	6.3	mm
	D	273	mm
	A	52.79	cm ²
	I	4696	cm ⁴
	W	344	cm ³

Table 3.14 shows the result obtained in the excel sheet for the verification of the element in tension of the roof's reticular structure.

Table 3.14.Design of the element in tension for the roof's reticular structure.

Designation	Value/Verification	Observation
Class verification	$43.3 < 50$	Class 1
Resistance in tension, $N_{Ed} \leq N_{pl,Rd}$	$44.37 \text{ kN} < 1240.57 \text{ kN}$	Verified

3.5.3.2. Element in compression

To design the elements in compression of the roof, we will verify the element with the maximum compressive force. (see figure 3.6).

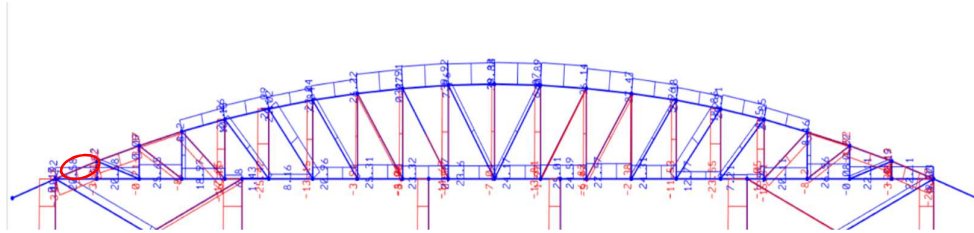


Figure 3.6.Element in compression to be designed on the reticular steel roof.

The axial force solicitations obtained $N_{Ed} = -34.78 \text{ kN}$. The section of the element under study is 273x6.3 CHS. Table 3.15 shows the result obtained in the excel sheet for the verification of the element in tension of the roof's reticular structure.

Table 3.15.Design of the element in compression for the roof's reticular structure.

Designation	Value/Verification	Observation
Class verification	$43.3 < 50$	Class 1
Resistance in tension, $N_{Ed} \leq N_{c,Rd}$	$34.78 \text{ kN} < 1240.57 \text{ kN}$	Verified
Resistance to buckling, $N_{Ed} \leq N_{b,Rd}$	$34.78 \text{ kN} < 868.4 \text{ kN}$	Verified

3.5.4. Design of the bracing system

In this section, we will design the bracing system of the roof and for the pillars.

3.5.4.1. Bracing system of the roof

For the bracing system of the roof, we will design the elements with the maximum tension force. The axial force solicitations obtained $N_{Ed} = 32.05 \text{ kN}$. The section of the element under study is 80x80x5. Its characteristics are given in Table 3.16.

Table 3.16. Properties of 80x80x5.

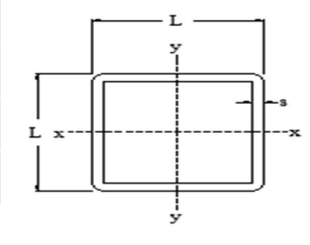
	s	5	mm
	L	80	mm
	A	14.14	cm ²
	I	128	cm ⁴
	W	31.99	cm ³

Table 3.17 shows the result obtained in the excel sheet for the verification of the roof bracing system's element.

Table 3.17.Design of the roof's bracing system.

Designation	Value/Verification	Observation
Class verification	15 < 72	Class 1
Resistance in tension, $N_{Ed} \leq N_{pl,Rd}$	32.05 KN < 332.29 KN	Verified

3.5.4.2. Bracing system of the column

To design the bracing system of the column, we will verify the elements with the maximum tension force. The axial force obtained solicitations obtained $N_{Ed} = 24.47$ KN. The section of the element under study is 100x100x5; its characteristics are given in Table 3.18.

Table 3.18. Properties of 100x100x5.

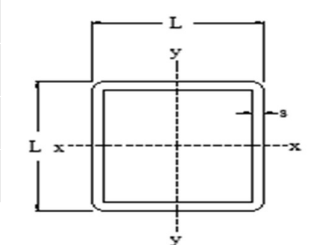
	s	5	mm
	L	100	mm
	A	18.14	cm ²
	I	265.7	cm ⁴
	W	53.14	cm ³

Table 3.19 shows the result obtained in the excel sheet for the verification of the column bracing system's element.

Table 3.19.Design of the column's bracing system.

Designation	Value/Verification	Observation
Class verification	18 < 72	Class 1
Resistance in tension, $N_{Ed} \leq N_{pl,Rd}$	24.47 KN < 426.29 KN	Verified

3.5.5. Design of foundation

We shall design the footing of the column with the maximum axial force. To do so, we follow the design procedure described in section 2.6.2.2. For the foundation, the section of footing used is a 100 cm x 100 cm x 50 cm the effective depth, d , 45 cm. The longitudinal reinforcement for the top and bottom mesh is 7 Phi 12 for each mesh. The steel plate used has as dimension 430 x 260 x 15mm. Table 3.21 shows the result obtained in the excel sheet for the foundation verification.

Table 3.20. Foundation design.

Designation	Value/Verification		Observation
bearing capacity, $\sigma_{sol} \leq \sigma_{adm}$	0.11 Mpa < 0.15 MPa		Verified
compressive resistance, $\sigma \leq f_{ck}$	0.9 Mpa < 25 Mpa		Verified
Resistance in bending, $M_{Ed} \leq M_{lim}$	25.84 kNm < 479.2 kNm		Verified
Longitudinal reinforcement of the footing	$\frac{M_{Ed}}{0.87f_{yk}Z} \leq A_s$	132 mm ² < 791.7 mm ²	Verified
	$A_{s,min} \leq A_s$	540 mm ² < 791.68mm ²	Verified
Thickness of the plate, $t_p \geq \mu \sqrt{\frac{3\sigma}{f_y}}$	15mm > 4.8mm		Verified

3.5.6. Design of connection

The design of the connection is done here by choosing one of the connection of the structure. The selected connection is the one forming a junction between a column and a beam. 4 bolts of class 10.9 and diameter 14mm were used for the beam-column connection Table 3.21 shows the solicitations obtained for the beam to column connection.

Table 3.21. Bolt's solicitations

Shear force, V[kN]	Axial force, N[kN]
9.65	53.49

Table 3.22 shows the result obtained in the excel sheet for the beam to column connection verification.

Table 3.22.Bolt design.

Designation	Value/Verification	Observation
Shear resistance for one bolt, $F_{v,Ed} \leq F_{v,Rd}$	9.65 KN < 246.3 KN	Verified
Traction resistance for one bolt, $F_{v,Ed} \leq F_{t,Rd}$	53.49 < 226.2	Verified
Shear and traction of the bolt interaction, $\frac{F_{v,Ed}}{F_{v,Rd}} + \frac{F_{t,Ed}}{1.4F_{t,Rd}} \leq 1$	0.21 < 1	Verified
Bearing resistance for the plate, $F_{v,Ed} \leq F_{b,Rd}$	53.49 < 423	Verified

3.6. Results of the blast analysis

This section presents the results obtained from the global structural analysis carried out on SAP2000. We will present the solicitations obtained during the blast loading on the column and progressive collapse assessment for the most vulnerable elements.

3.6.1. Results for the blast loads of charge weight 50Kg on all the columns

A push over analysis is first carried out in order to have the bearing capacity of the columns. The following results were obtained.

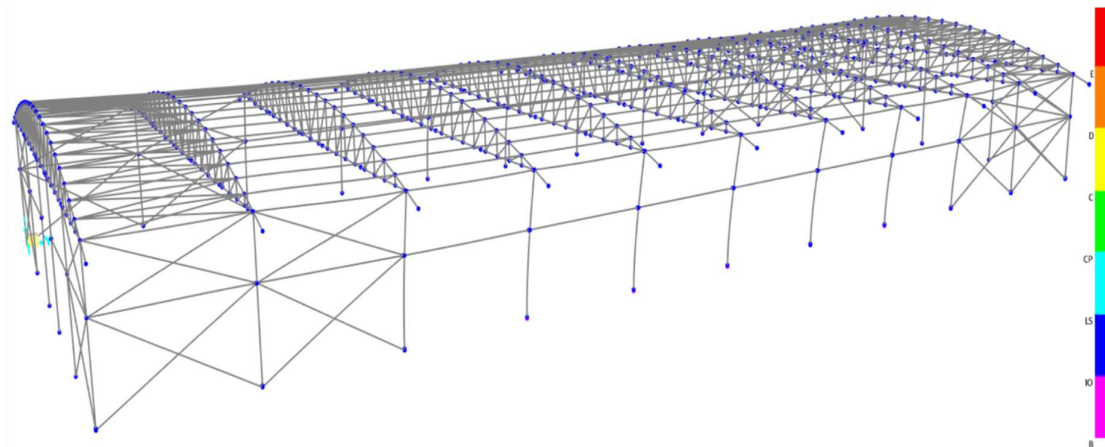


Figure 3.7.Results of the push-over analysis.

From Figure 3.7, we can observe that our hinges are blue and from the legend, our hinges fall in between the immediate occupancy zone (IO) and the life safety zone (LS). IO defines the beginning of the behavior beyond elasticity while the LS defines the limit of the behavior beyond elasticity that the section is capable of safely ensuring the strength. Figure 3.8 illustrates the moment-rotation curve in pushover analysis of one hinge.

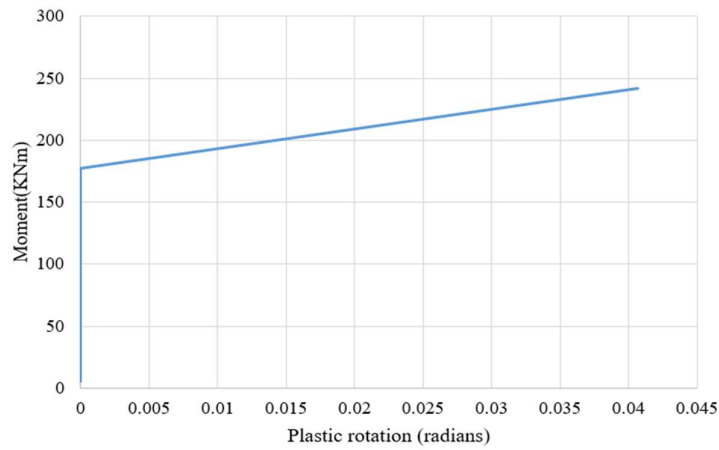


Figure 3.8.moment-rotation curve in pushover analysis of one hinge.

Moving to our Blast analysis, we first of all carried an analysis of a blast loading of mass 50kg that impinges the front face of the structure. From section 3.3.2.3, we have the different blast parameters of each column as well as their time of arrival. Figure 3.9 illustrates the pressure-time graph of these 11 columns.

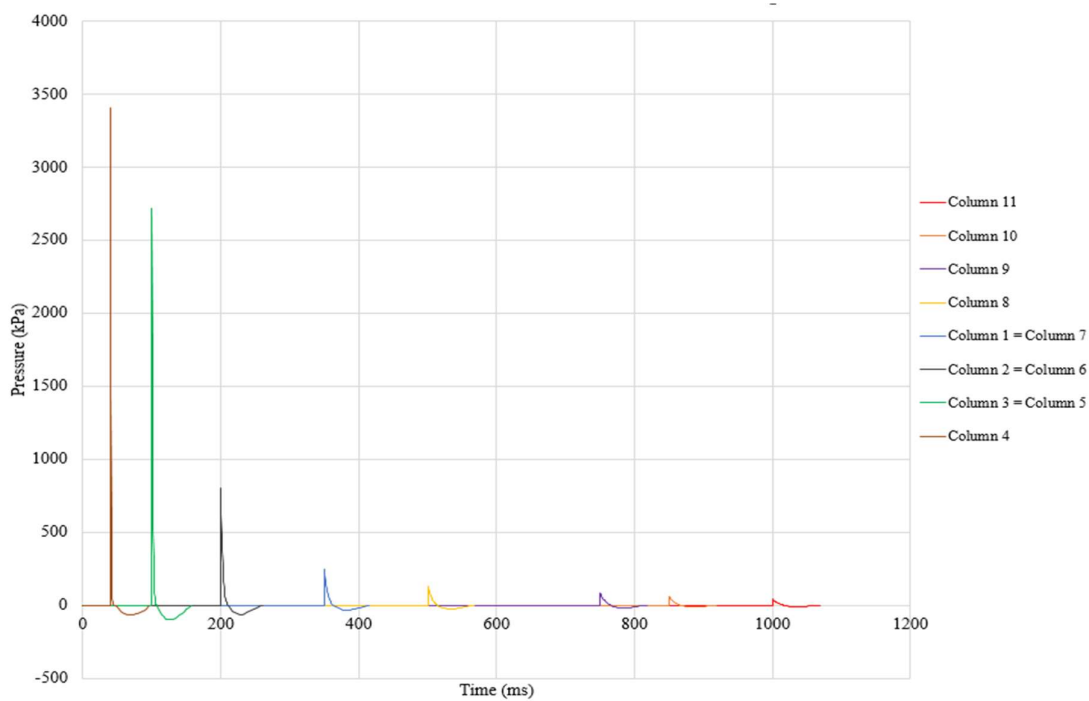


Figure 3.9.The pressure-time graph of the 11 columns.

The blast load pattern for each column was defined on sap and was associated with the corresponding time history function representing the pressure-time curve of the blast. The load cases for each load pattern was modified to a time-history analysis, a load combination of linear

add of this eleven load pattern was defined and the analysis was carried on. Table 3.23 displays the result obtained in the time arrival order.

Table 3.23.Results of blast loads of charge weight 50kg of TNT.

Columns	Time of arrival (ms)	Maximum moment (KNm)
Column 04	40	-544
Column 03	100	-92
Column 05	100	-115
Column 02	200	-17.3
Column 06	200	-71
Column 01	350	-5.2
Column 07	350	-37
Column 08	500	-25.2
Column 09	750	-13.75
Column 10	850	-1.25
Column 11	1000	-0.992

From this results, we observe that column 01 and 07 that were submitted to the same blast load patterns have different moments. This moment reduction of column 01 is due to the presence of the bracing system on it. The same interpretation applies on the couples of column 02 and 06 as well as column 03 and 05. Column 04 is the column that is highly damaged. This is because it is directly hit by the blast (angle of incidence is 0) and has a shorter time of arrival.

For our work thesis, our aim is to study the progressive collapse assessment due to the removal of one structural element (the column), caused by the application of a high impact load (blast loads). To do so, we will apply the blast loading on one column at an angle of 0°. We will proceed in the following section with the results obtained for the application of a blast load of mass 50kg and 100 kg respectively on individual columns.

3.6.2. Results for blast loads of charge weight 50Kg on individual columns.

Our column has an IPE330 section with a $M_{pl,rd}=188.94$ KNm. This section will show the results obtained for the analysis two cases, column 1 and column 4 each subjected to the blast

loads with mass 50kg. The blast load pattern defined on sap is associated with a time history function representing the pressure-time curve of the blast (See Figure 3.4) for the analysis.

3.6.2.1. Blast loading on column 1

Applying the blast effect on the corner column (column 1) as shown in Figure 3.10. The deformation results are shown in Figure 3.11.

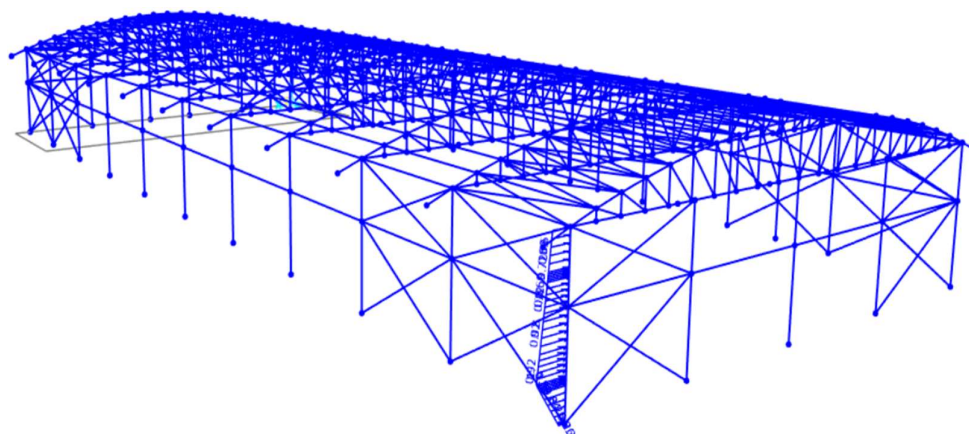


Figure 3.10. Application of blast loads on column 1.

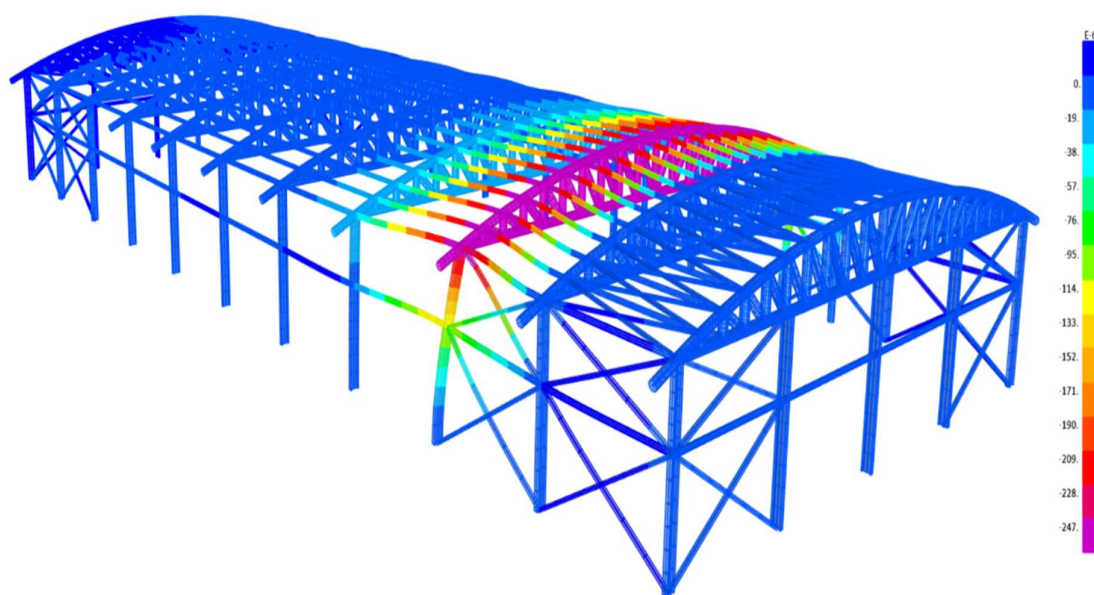


Figure 3.11. Deformation of structural elements due to the application of blast loads on column 1.

From Figure 3.11, We can observe that the brace system has caused column 03 to deform instead of column 01. Figure 3.12 and Figure 3.13 show the moment and displacement results

with time respectively components induced by the blast loading on column 1. The maximum moment can be observed at the time where the blast arrives on the structure.

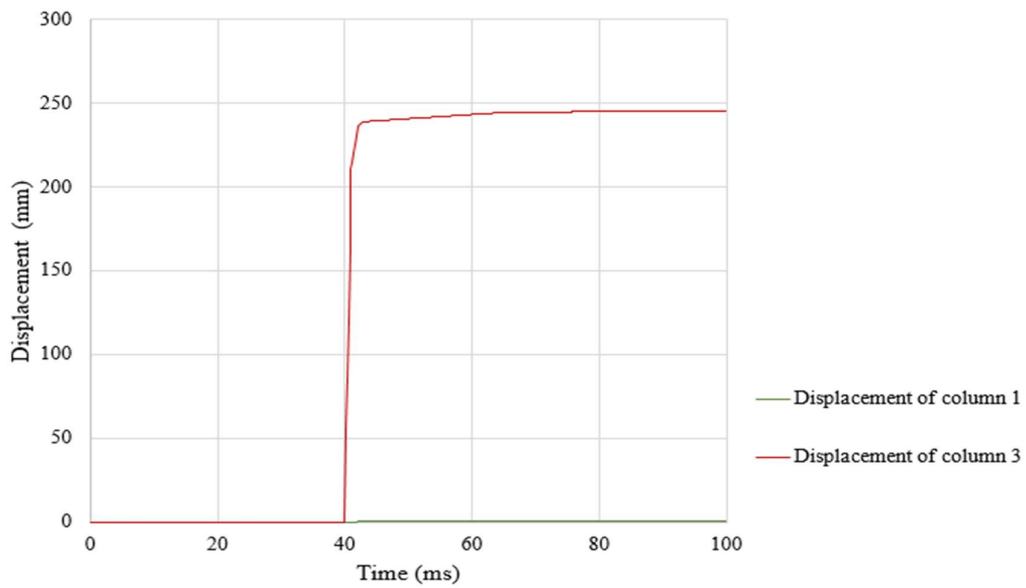


Figure 3.12. Displacement-time curve due to the application of blast loads of charge weight 50kg on column 1.

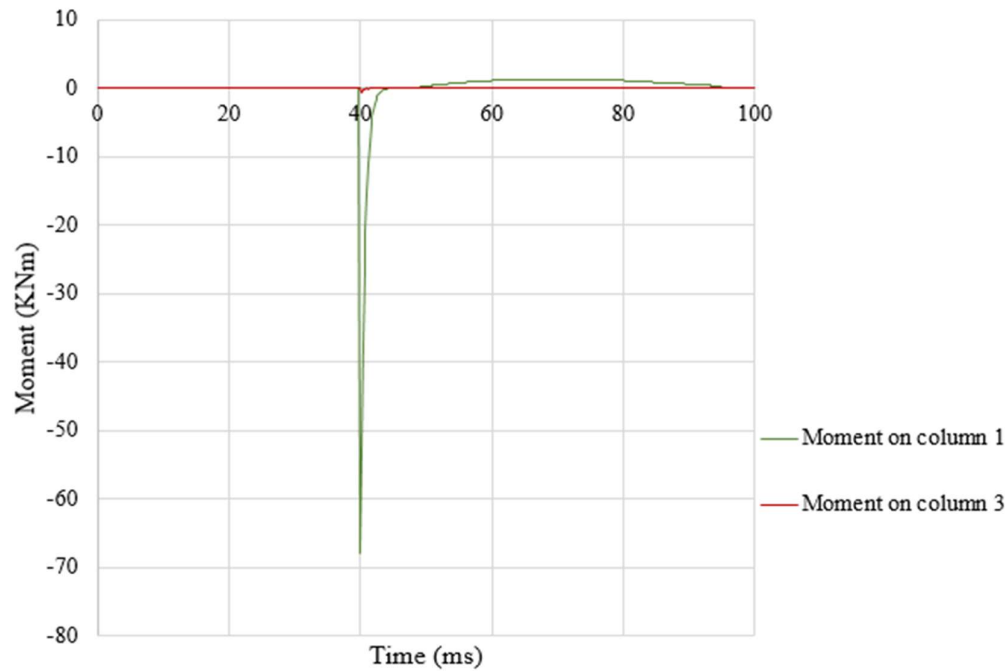


Figure 3.13. Moment-time curve due to the application of blast loads of charge weight 50kg on column 1.

As per GSA guideline, the DCR of each element should be less than 2. If the DCR value exceeds 2, the progressive collapse will occur. Table 3.24 shows the computation of the DCR values of two columns around column 1 and it is illustrated in Figure 3.14 and 3.15.

Table 3.24.DCR value due to the application of blast loads of charge weight 50kg on column 1.

Members	Mpl,rd IPE 330	Moment (KNm)		DCR Values	
		Before Blast (static condition)	After Blast	Before Blast	After blast
Column 1	188.94	-2.12	-74.4	0.01	0.53
Column 2	188.94	10	2.3	0.05	0.01
Column 3	188.94	-33.25	2.1	0.178	0.01

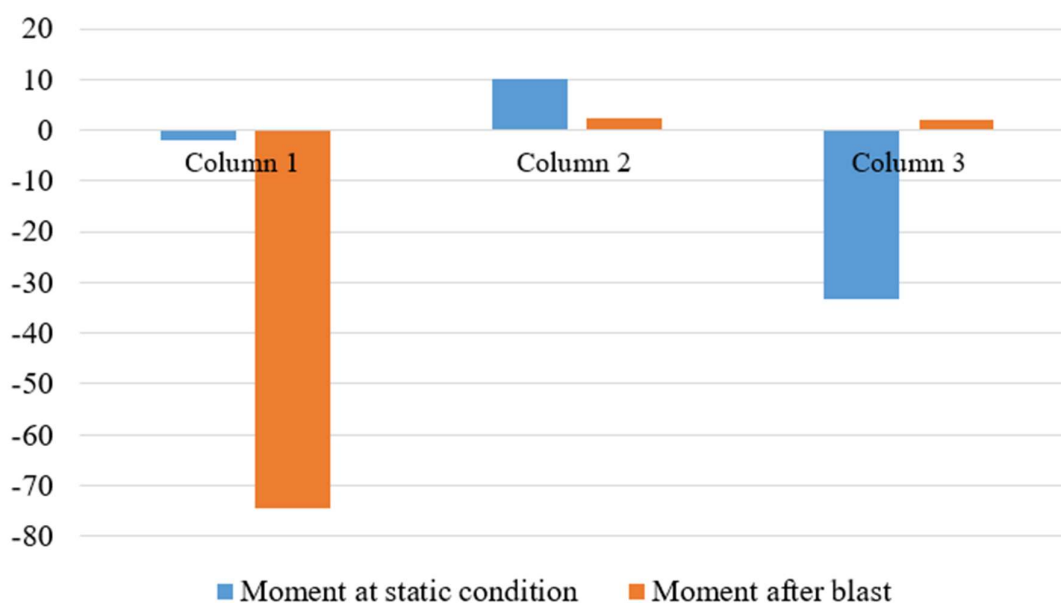


Figure 3.14.Moment results due to the application of blast loads of charge weight 50kg on column 1.

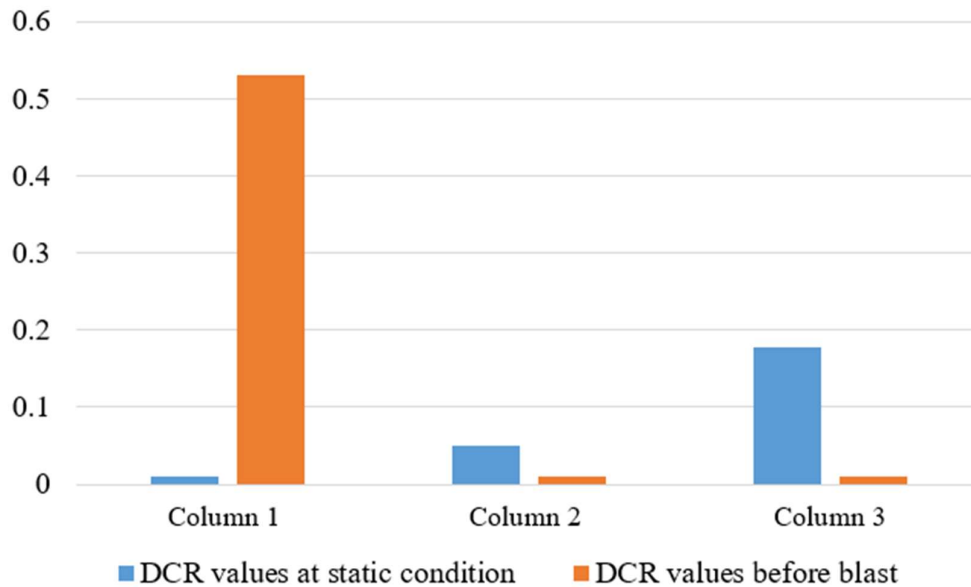


Figure 3.15.DCR values results due to the application of blast loads of charge weight 50kg on column 1.

Hence DCR values are within the limit, progressive collapse will not occur under blast load.

3.6.2.2. Blast loading on column 4

Applying the blast effect on the middle column (column 4) as shown in Figure 3.16. The deformation results are shown in Figure 3.17.

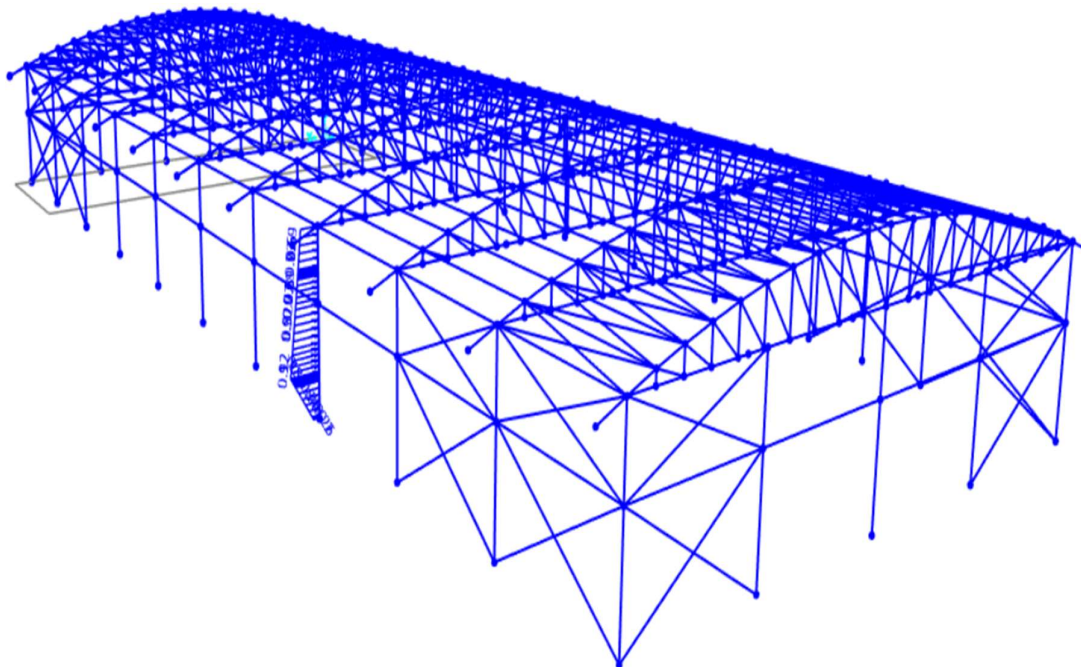


Figure 3.16.Application of blast loads on column 4.

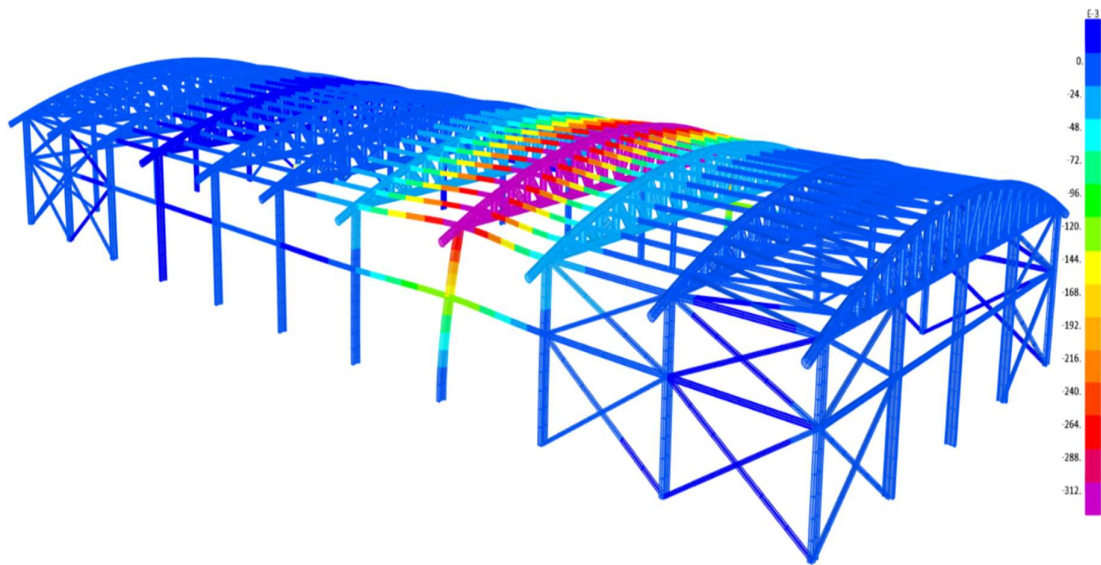


Figure 3.17. Deformation of structural elements due to the application of blast loads on column 4.

Figure 3.18 and Figure 3.19 show the moment and displacement results with time respectively components induced by the blast loading on column 4. The maximum moment can be observed at the time where the blast arrives on the structure.

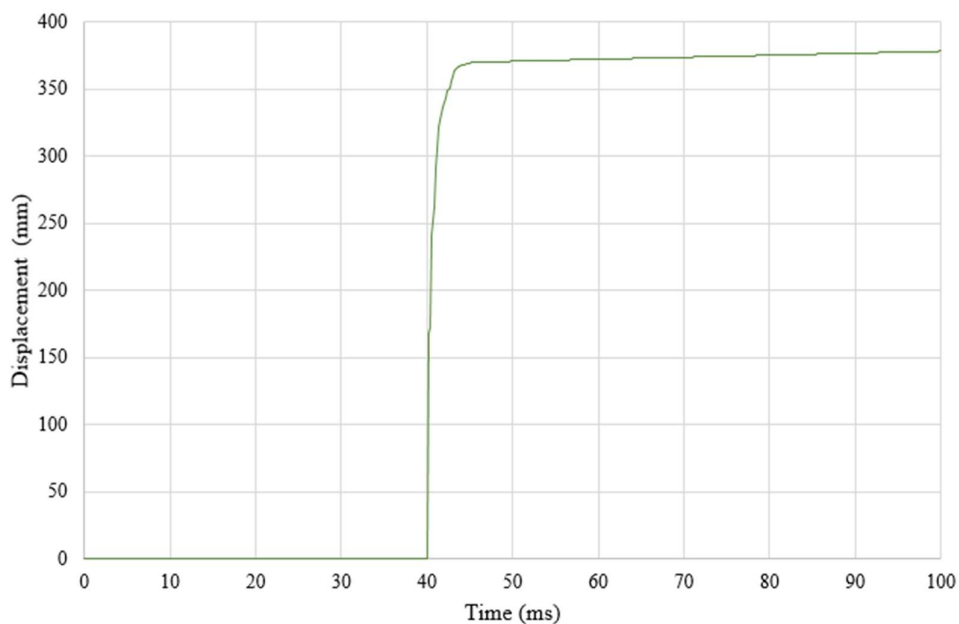


Figure 3.18. Displacement-time curve due to the application of blast loads of charge weight 50kg on column 4.

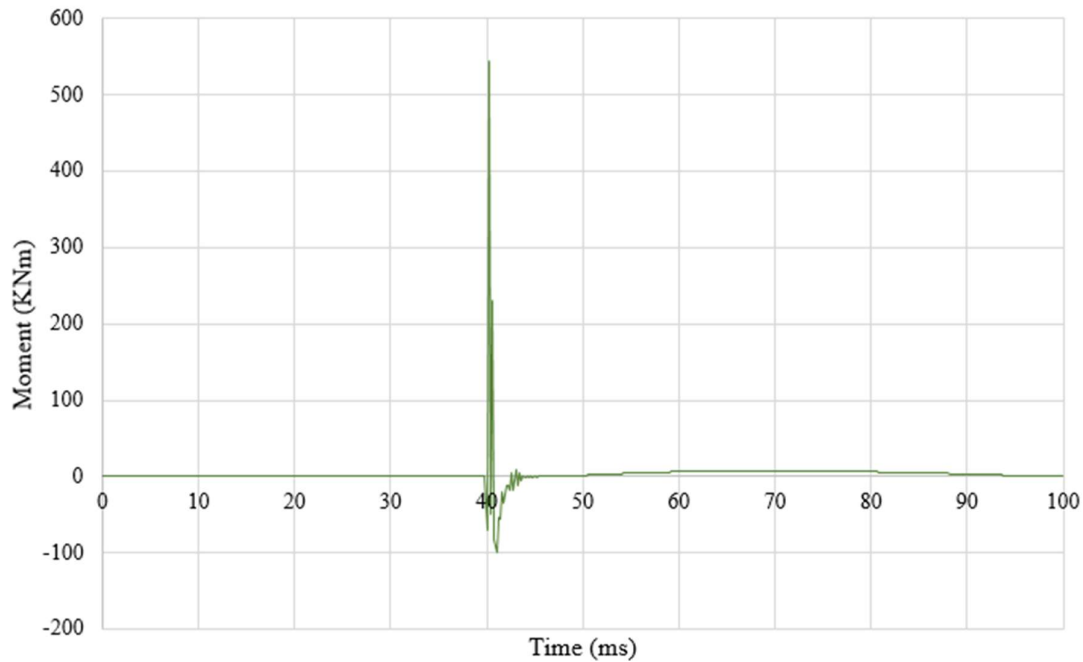


Figure 3.19. Moment-time curve due to the application of blast loads of charge weight 50kg on column 4.

For the progressive collapse assessment, The DCR value is calculated and if it exceeds 2, the progressive collapse will occur. Table 3.25 shows the computation of the DCR values of two columns surrounding column 4. It is illustrated in Figure 3.20 and 3.21.

Table 3.25. DCR value due to the application of blast loads of charge weight 50kg on column 4.

Members	Mpl,rd IPE 330	Moment (kNm)		DCR Values	
		Before Blast (static condition)	After Blast	Before Blast	After blast
Column 3	188.94	-33.25	-58.61	0.18	0.31
Column 4	188.94	-38.9	-543.58	0.21	2.88
Column 5	188.94	-38.6	-61.5	0.20	0.33

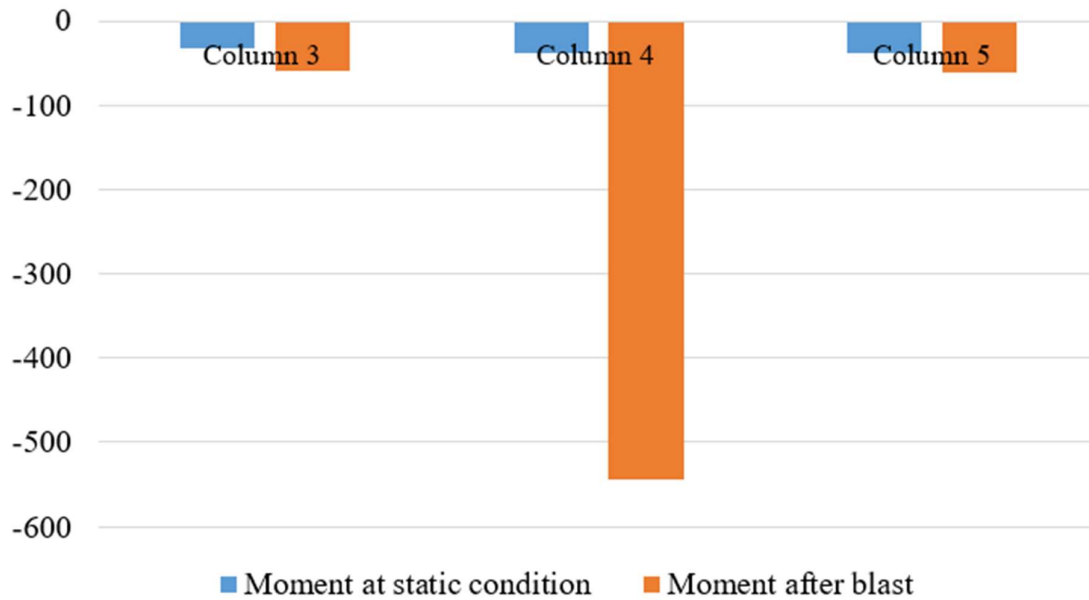


Figure 3.20. Moment results due to the application of blast loads of charge weight 50kg on column 4.

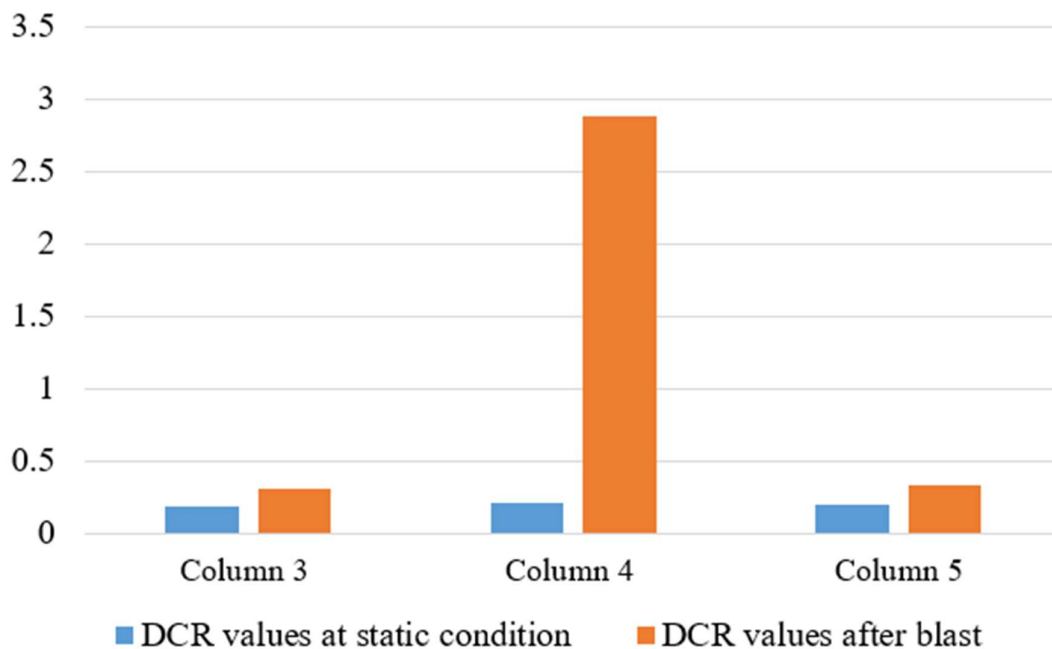


Figure 3.21. DCR values results due to the application of blast loads of charge weight 50kg on column 4.

The DCR Value of column 4 exceed 2, hence we have a progressive collapse. There will be the removal of the collapsed column. A second analysis is carried out in order to evaluate the impact of column 4 removal on its surrounding columns.

To realise it, we will create another model (see figure 3.22) in which the column is removed. Apply the column end forces, obtained during the analysis of blast load, to simulate the presence of the removed column.

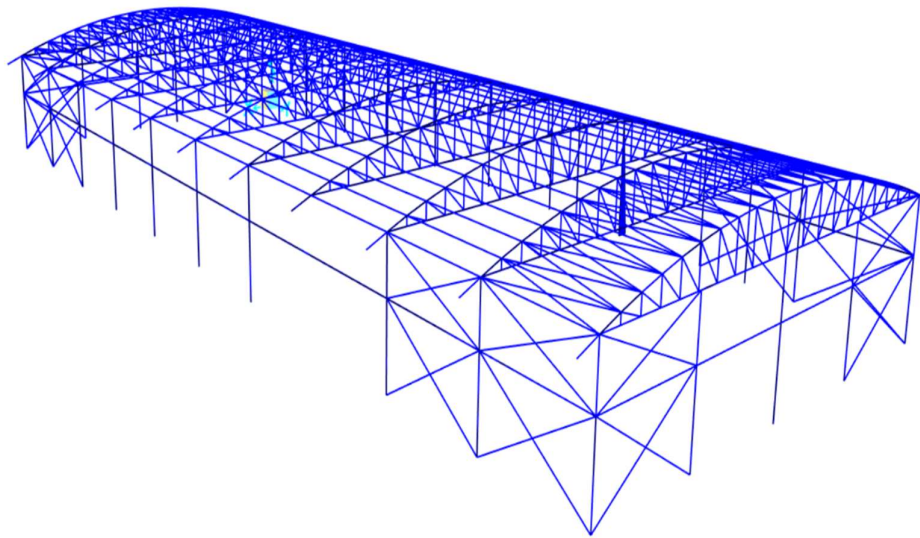


Figure 3.22.Column 4 removal.

The simulation of column removal is done by running a time-history analysis in which these equivalent column loads are reduced to zero over a short period of time. This is done by applying a ramp time function (see figure 3.23) in which loads opposite to those of the equivalent column loads are scaled from zero to the full value. The duration of this event should match the time in which the column is removed.

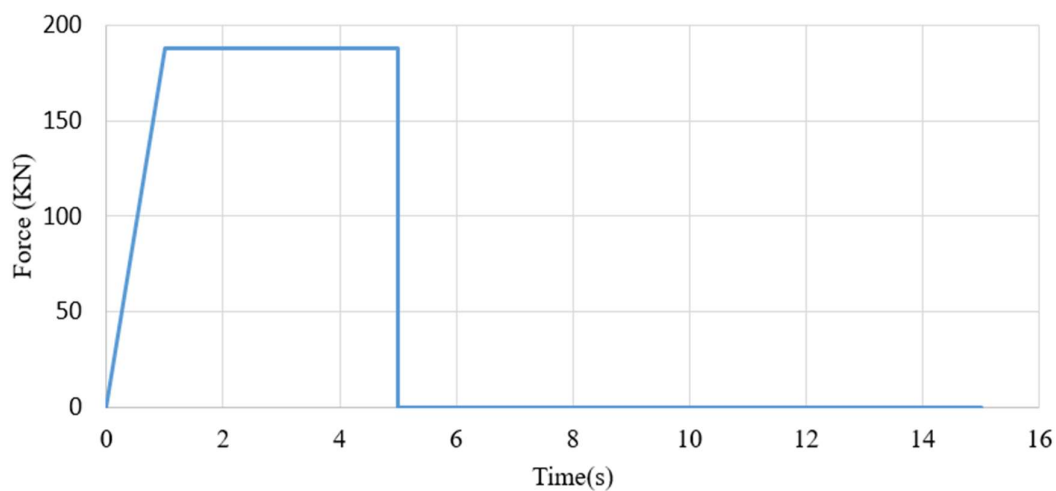


Figure 3.23.Rampth function for the column removal.

Table 3.26 shows the evaluation of the DCR values for this analysis. This results are displayed in figure 3.24 and 3.25.

Table 3.26.DCR value due to the application of blast loads of charge weight 50kg after column 4 removal.

Members	Mpl,rd IPE 330	Moment (KNm)		DCR Values	
		Before removal	After removal	Before removal	After removal
Column 3	188.9 4	-58.61	292.5	0.31	1.5
Column 4	REMOVED				
Column 5	188.94	-61.5	325.97	0.33	1.7

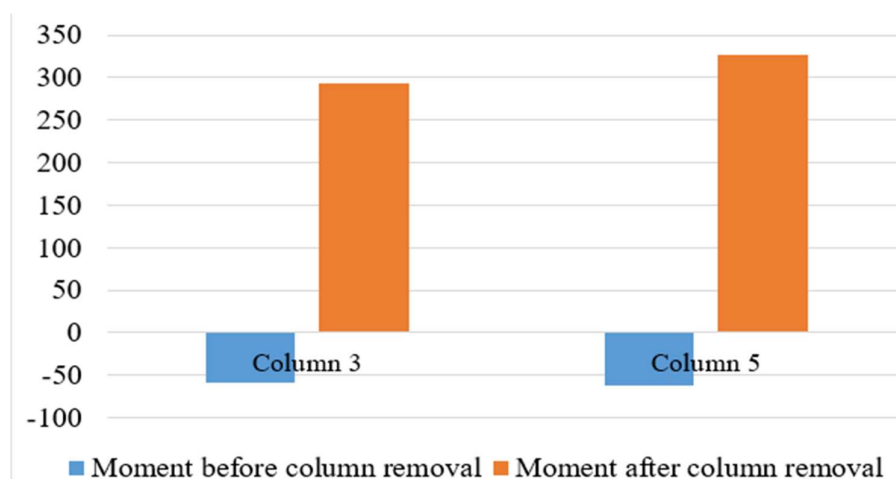


Figure 3.24.Moments results due to the application of blast loads of charge weight 50kg after column 4 removal.

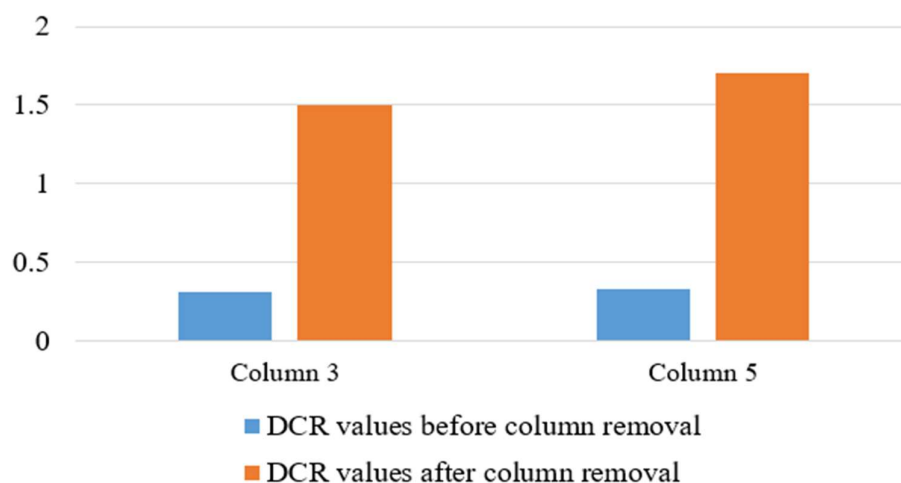


Figure 3.25.DCR values results due to the application of blast loads of charge weight 50kg after column 4 removal.

We can observe that after the column removal, thus the moment of column 3 and 5 increases considerably, they will not collapse.

3.6.3. Results for blast loads of charge weight 100Kg on individual columns.

This section will show the results obtained for the analysis of column 4 subjected to the blast loads with mass 100kg. We will analyze two cases, one in which the section used is the IPE 330 and the other one where the section used is the HE200B.

3.6.3.1. Blast loading on column 4 of section IPE330

Our column has an IPE330 section with a $M_{pl,rd}=188.94$ KNm. This section will show the results obtained for the analysis of the column. The blast load pattern defined on sap is associated with the corresponding time history function representing the pressure-time curve of the blast for the analysis. the deformation result is illustrated on figure 3.26.

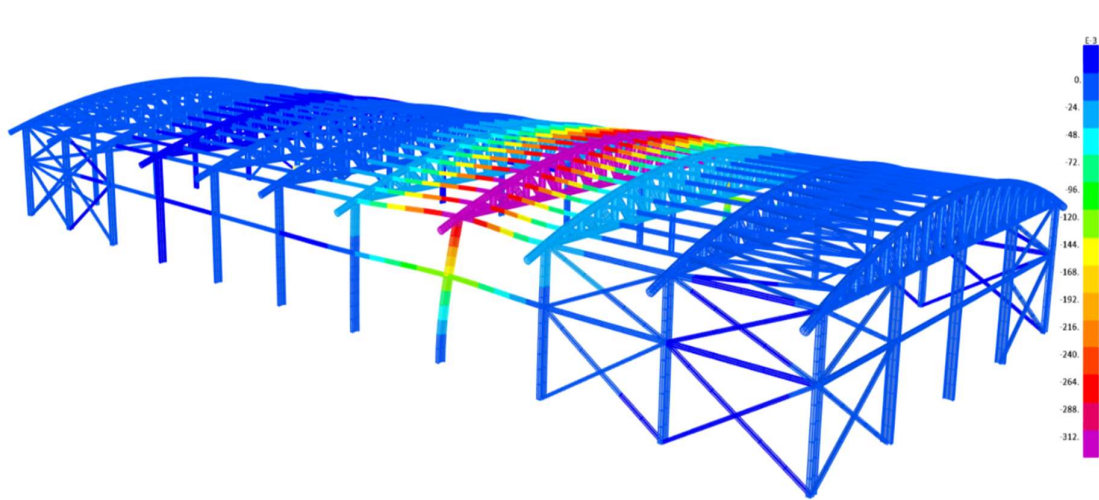


Figure 3.26. Deformation of structural elements due to the application of blast loads on column 4.

For the progressive collapse assessment, The DCR value is calculated and if it exceeds 2, we have a failure and hence a column removal. Table 3.27 shows the computation of the DCR values of two columns surrounding column 4. These results are displayed in figure 3.27 and 3.28.

Table 3.27.DCR value due to the application of blast loads of charge weight 100kg on column 4.

Members	Mpl,rd IPE 330	Moment (KNm)		DCR Values	
		Before Blast (static condition)	After Blast	Before Blast	After blast
Column 3	188.94	-33.25	-114.2	0.18	0.60
Column 4	188.94	-38.9	-1063	0.21	5.63
Column 5	188.94	-38.6	-119.9	0.20	0.64

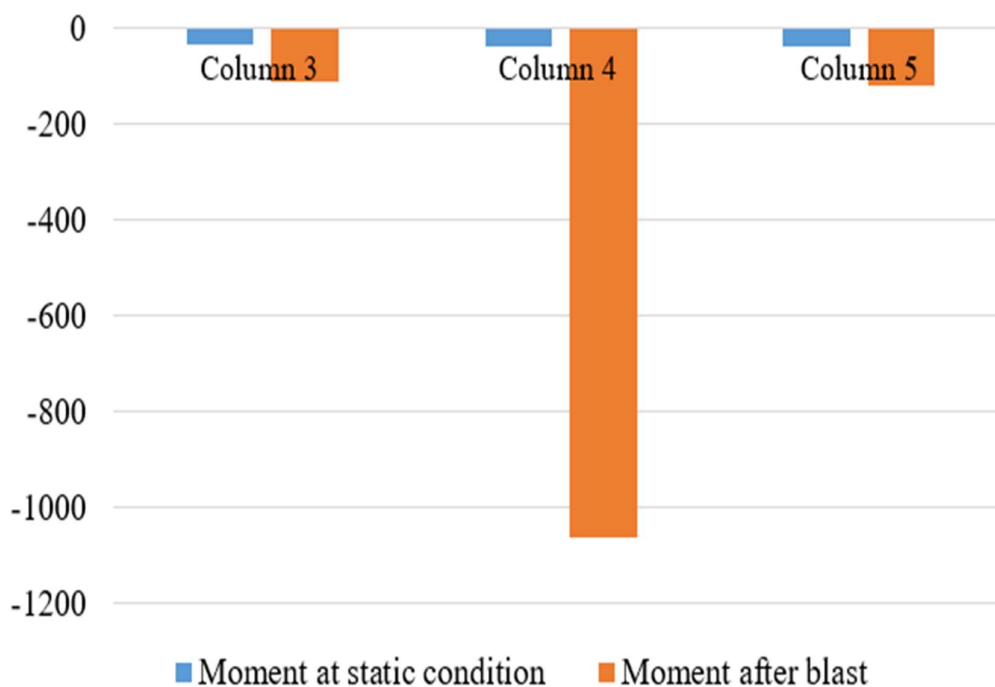


Figure 3.27.Moments results due to the application of blast loads of charge weight 100kg on column 4.

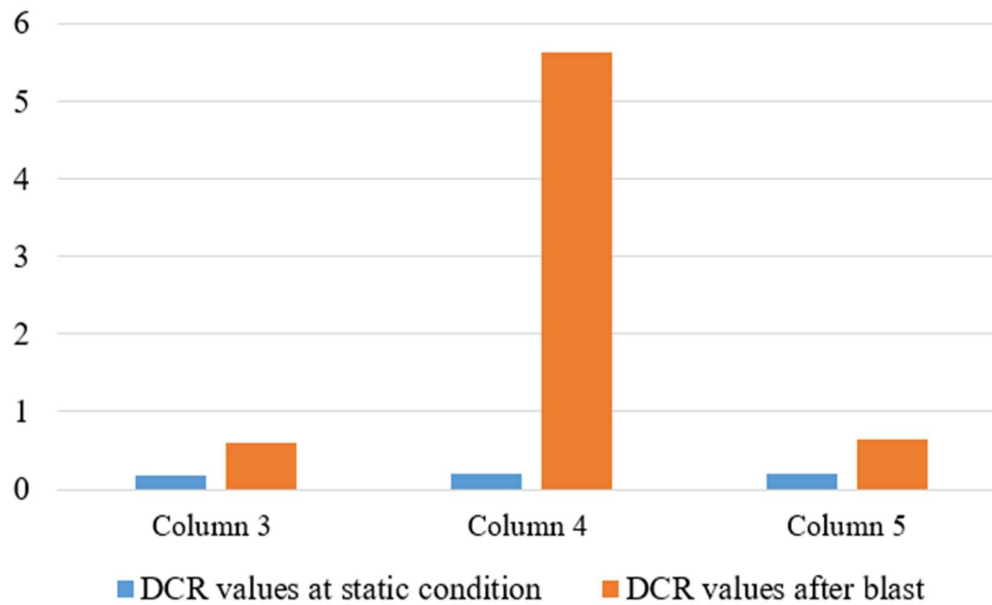


Figure 3.28.DCR values results due to the application of blast loads of charge weight 100kg on column 4.

The DCR Value of column 4 exceed 2, hence it will collapse. A second analysis is carried out in order to evaluate the impact of column 4 removal on its surrounding columns. The column removal simulation is done with the time history function rampth. Table 3.28 shows the evaluation of the DCR values. Figure 3.29 and 3.30 illustrate these results.

Table 3.28.DCR value due to the application of blast loads of charge weight 100kg after column 4 removal.

Members	Mpl,rd IPE 330	Moment (KNm)		DCR Values	
		Before removal	After removal	Before removal	After removal
Column 3	188.94	-114.2	340.2	0.60	1.8
Column 4	REMOVED				
Column 5	188.94	-119.9	385.6	0.64	2.1

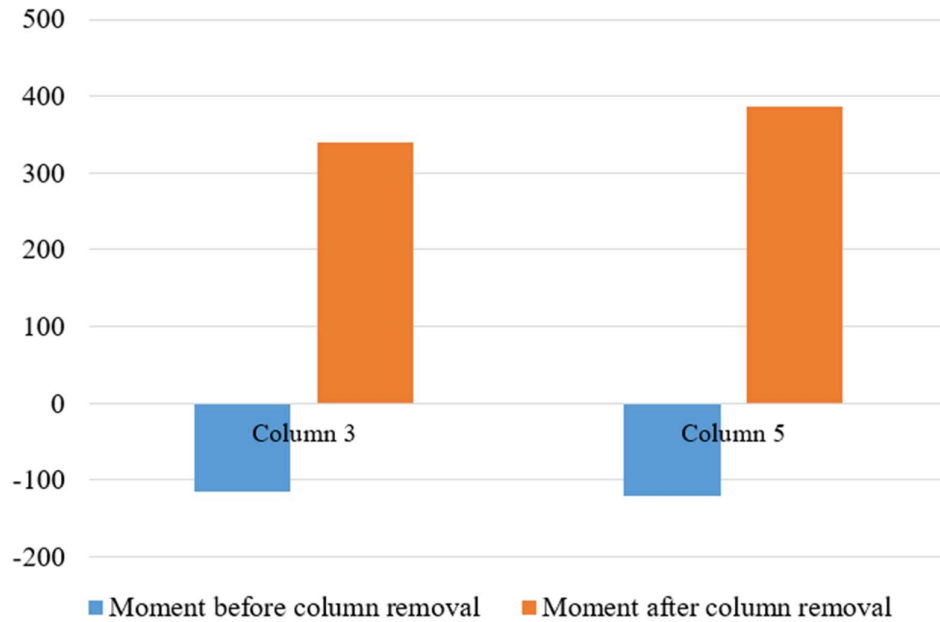


Figure 3.29. Moments results due to the application of blast loads of charge weight 100kg after column 4 removal.

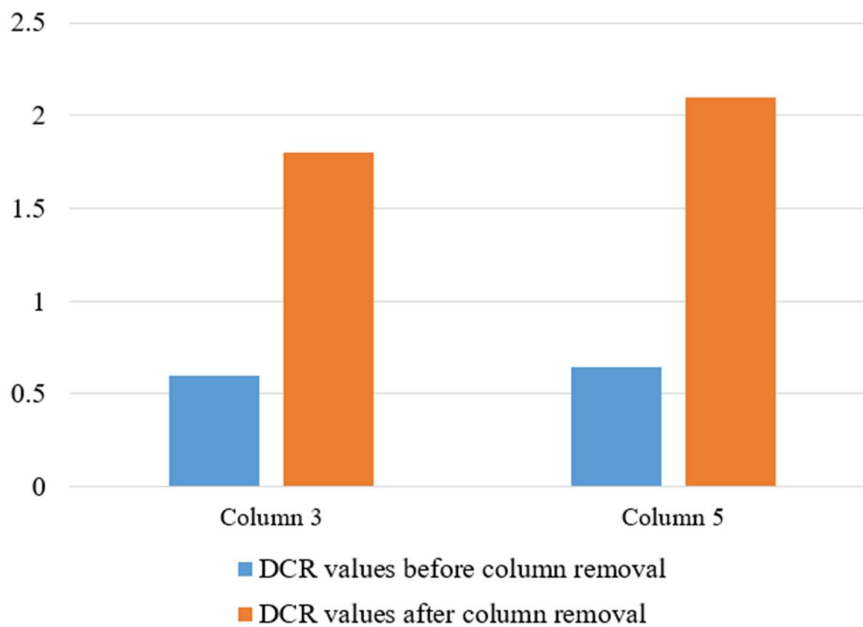


Figure 3.30. DCR values results due to the application of blast loads of charge weight 100kg after column 4 removal.

We can observe that after the column removal, the moment of column 3 and 5 increases considerably. Column 5 will collapse while column 3 will withstand. This can be due to the presence of the brace system on column 3 which reduces the solicitations transfer on this column.

A pushover analysis is again carry on in order to evaluates the state of the plastic hinge formed in the structure due to the column removal (see figure 3.31).

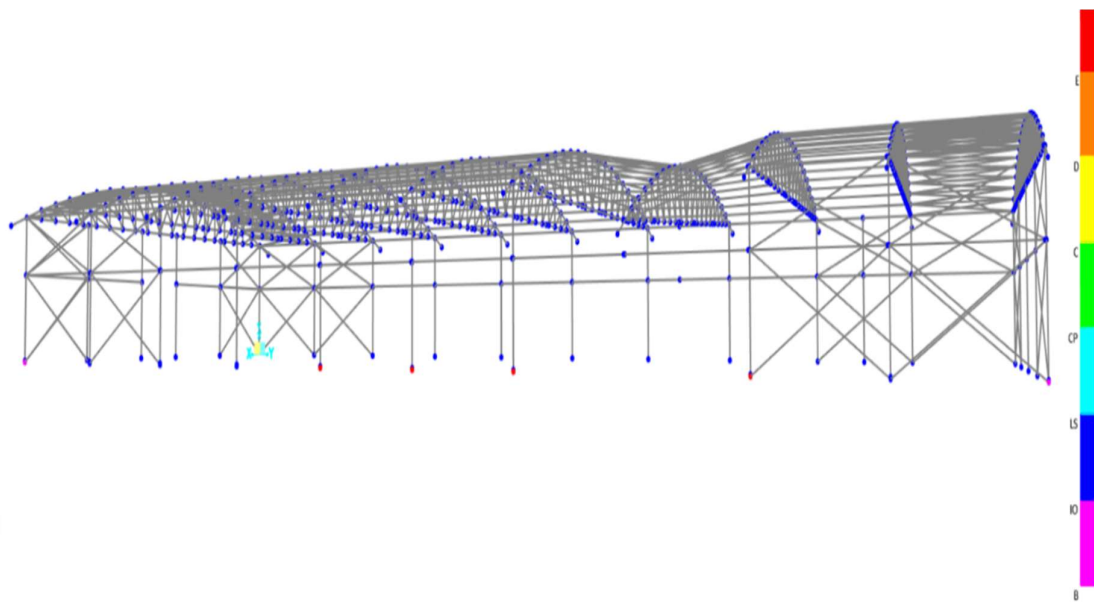


Figure 3.31.Results of the push-over analysis after column removal

On figure 3.32 which illustrates the moment-rotation curve in pushover analysis of one hinge, the one present on column 5, The first segment represent the linear elastic range from unloaded state to its effective yield. It is followed by an inelastic but linear response of reduced (ductile) stiffness. After, we have a sudden reduction in load resistance, followed by a reduced resistance and finally a total loss of resistance. From figure 3.31, we can have observed that some our hinges have reached the E-zone represent red on the legend. this implies that those hinges have collapse.

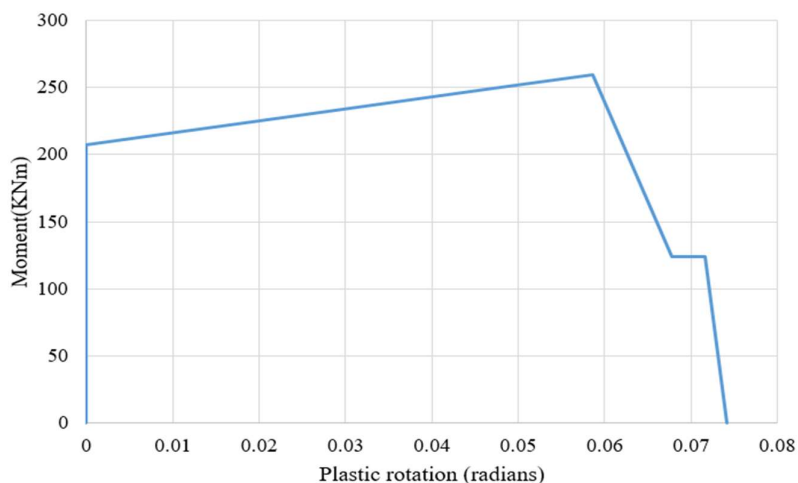


Figure 3.32.moment-rotation curve in pushover analysis of one hinge.

3.6.3.2. Blast loading on column 4 of section HE200B

Usually, HE section is recommended of the column because it withstand better under extreme load conditions and increases the robustness of the structure making it less vulnerable. We will carry on the same analysis done in section 3.6.2.1 but using an HE section of similar cross sectional area as the IPE330 section. We have chosen HE200B. its characteristics are given in Table 3.29.

Table 3.29.Properties of HE 200B.

	G	61.3	Kg/m
	h	200	mm
	b	200	mm
	d	134	mm
	h_w	170	mm
	t_w	9	mm
	t_f	15	mm
	r	18	mm
	A	78.1	cm ²
	A_{vY}	60	cm ²
I_Y	5696	cm ⁴	
W_{PL,Y}	642.5	cm ³	

For the classification,

Web in bending $\frac{d}{t_w} = 14.89 < 72$

Flange in compression $\frac{c}{t} = 5,17 < 9$

So, it is a class 1 section.

$$M_{pl,Rd} = \frac{W_{pl}f_y}{\gamma_{M0}} = 150.99 \text{ KNm}$$

The deformation obtained after the analysis is shown in figure 3.33.

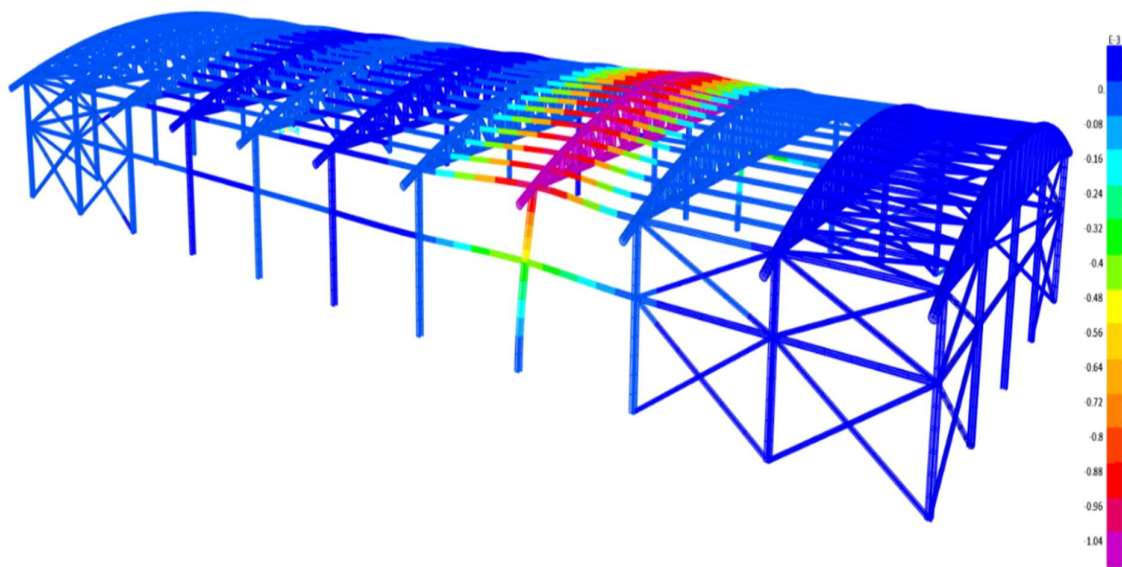


Figure 3.33. Deformation of structural elements due to the application of blast loads on column 4 of section HE 200B.

Figure 3.34 and Figure 3.35 shows the moment and displacement results with time respectively components induced by the blast loading on column 4 for the IPE 330 and HE200B sections. We can see from the figure that for the same blast load, the HE resists better than the IPE section.

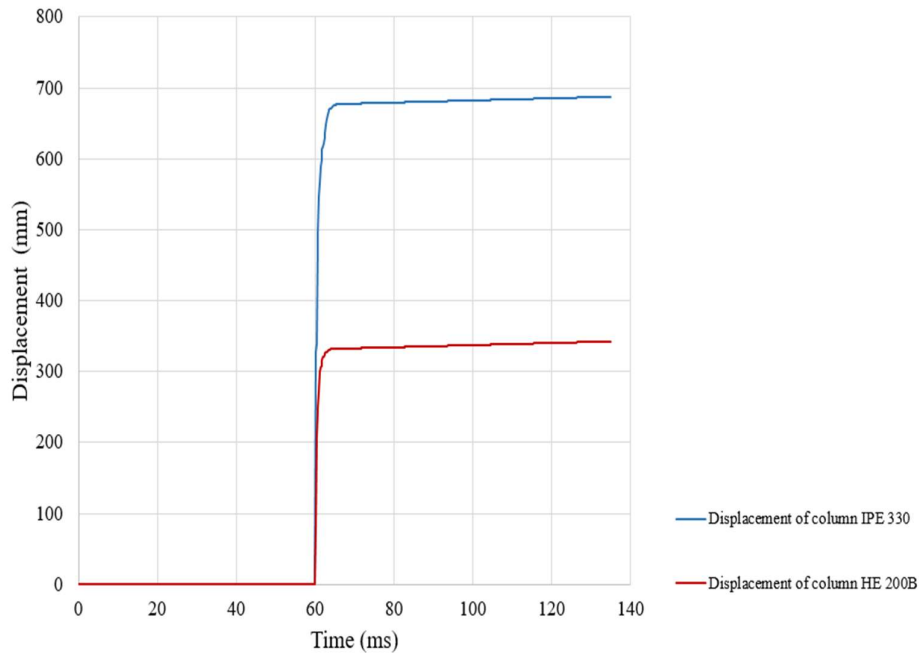
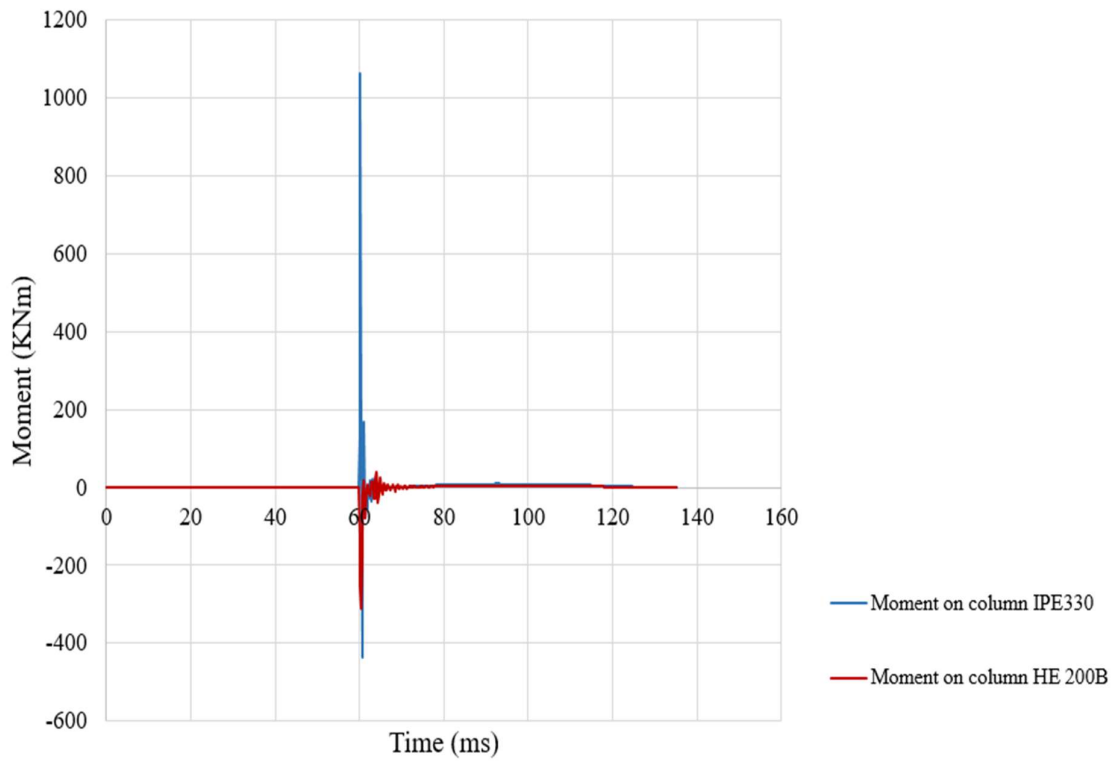
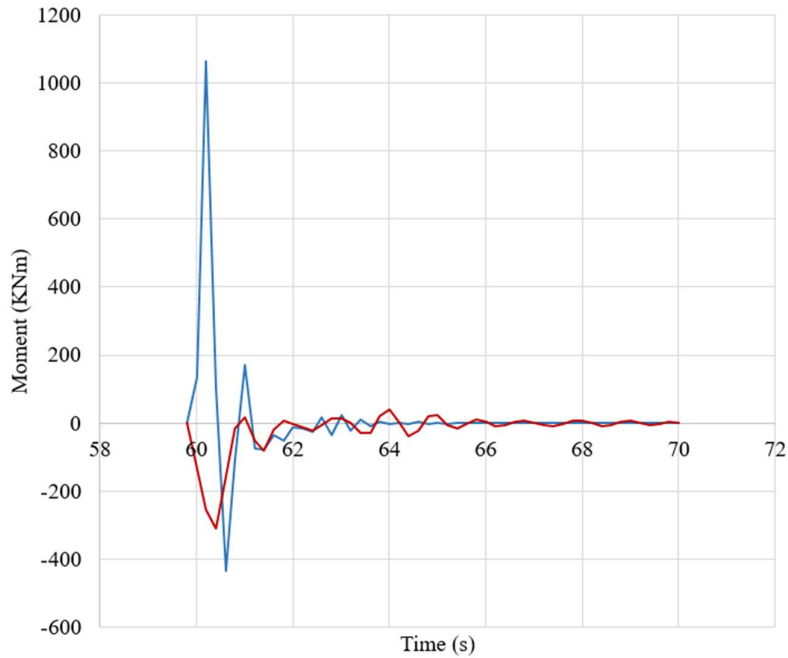


Figure 3.34. Displacement-time curve due to the application of blast loads of charge weight 100kg on column 4 for the IPE 330 and HE 200B sections.



(a)



(b)

Figure 3.35. Moment-time curve due to the application of blast loads of charge weight 100kg on column 4 for the IPE 330 and HE 200B sections.

For the evaluation of the progressive collapse of for the HE-section, the results are shown in table 3.30. These results are display in Figure 3.36 and 3.37.

Table 3.30. DCR value due to the application of blast loads of charge weight 100kg on column 4.

Members	Mpl,rd HE200B	Moment of blast (kNm)		DCR Values	
		After Blast IPE	After Blast HE	IPE	HE
Column 3	150.99	-114.2	-18.89	0.60	0.12
Column 4	150.99	-1063	-253.48	5.63	1.68
Column 5	150.99	-119.9	-19.74	0.64	0.13

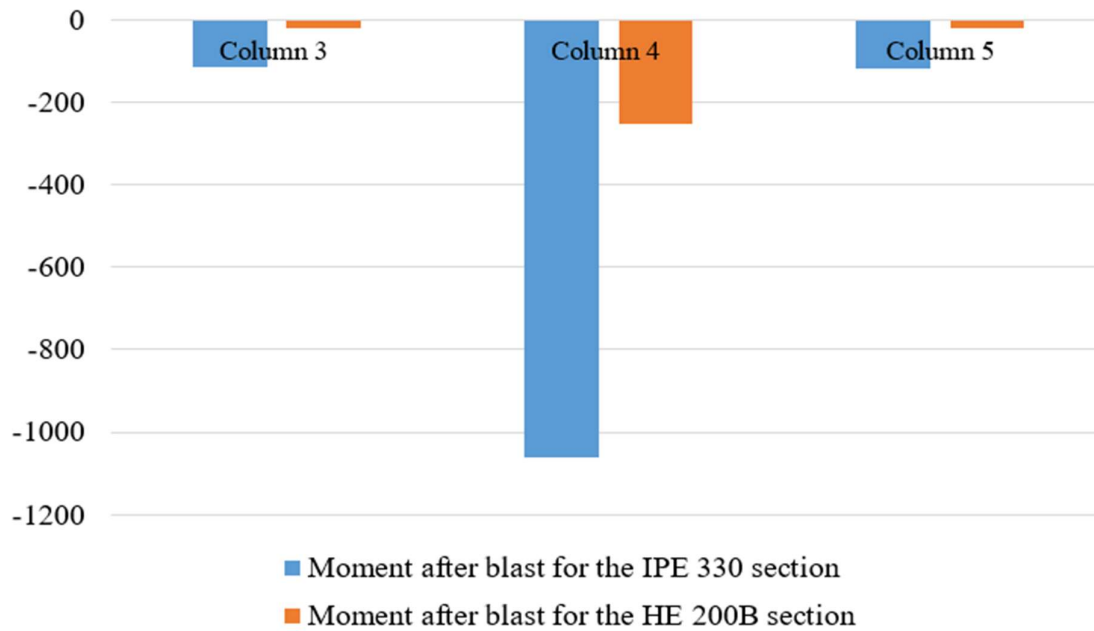


Figure 3.36. Moments results due to the application of blast loads of charge weight 100kg on column.

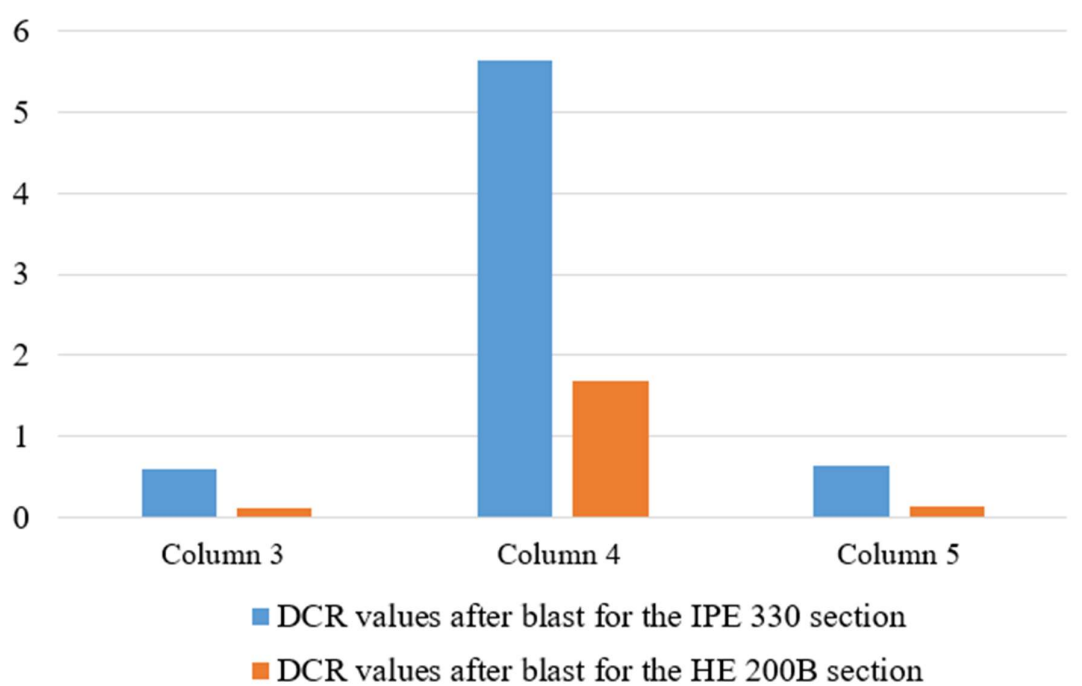


Figure 3.37. DCR values results due to the application of blast loads of charge weight 100kg on column.

The DCR Value of column 4 is less than 2 with the HE-section. With the IPE-section, we had a collapse while with the HE-section we don't. The HE section is greatly recommended for column because they withstand better accidental loads than IPE-sections.

3.7. Some possible solutions

From our analysis results presented in the previous section, we have observed that the presence of the bracing systems reduces the moment on the column. Also, we have seen that when replacing the IPE section with an HE section of similar area, there is no progressive collapse with a charge weight of 100kg as blast loads. Some possible solutions that can be taken into account by engineer when designing the structure to resist to blast loads as accidental load will be presented as follows.

3.7.1. The bracing system

The usage of more bracing is recommended. the primary function of bracing is to provide stability and ensures that lateral effects such as wind loading and collision loading are shared between all the elements. This sharing is particularly important at lines of support, where the effects of the lateral loads are often resisted at one fixed or guided bearing (depending on the chosen articulation system).

In vertical planes, there are bracing between column lines which provide load paths that are used to transfer horizontal forces to ground level. This system aims to transfer horizontal loads to the foundations and withstanding the overall sway of the structure. These are the bracings placed between two lines of columns. It can be studied in four types as shown below (Abd Samat et al., 2019).

3.7.1.1. Cross bracing

Cross-bracing (or X-bracing) uses two diagonal members crossing each other. These only need to be resistant to tension, one brace at a time acting to resist sideways forces, depending on the direction of loading. As a result, steel cables can also be used for cross-bracing.

3.7.1.2. single diagonal bracing

Unlike Cross bracing, Single diagonal bracing is designed to resist both tension forces and compression forces. In this, diagonal structural members are inserted into rectangular areas of a structural frame which is good for stabilization of the frame. For fulfilling the requirement of a comparatively efficient system, bracing elements are placed at nearly 45 degrees. This arrangement is strong and compact.

3.7.1.3. V-bracing

Two diagonal members forming a V-shape extend downwards from the top two corners of a horizontal member and meet at a center point on the lower horizontal member. Inverted V-bracing also known as chevron bracing involves the two members meeting at a center point on

the upper horizontal member. Both systems can significantly reduce the buckling capacity of the compression brace so that it is less than the tension yield capacity of the tension brace. This can mean that when the braces reach their resistance capacity, the load must instead be resisted in the bending of the horizontal member.

3.7.1.4. K-bracing

K-braces connect to the columns at mid-height. This frame has more flexibility for the provision of openings in the facade and results in the least bending in floor beams. K-bracing is generally discouraged in seismic regions because of the potential for column failure if the compression brace buckles.

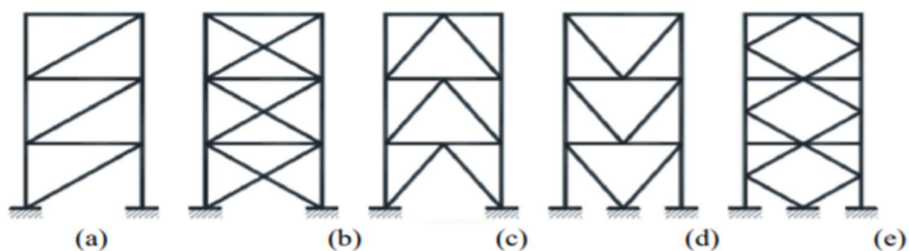


Figure 3.38.(a) Single diagonal (b) cross (c) chevron (d) V-bracing (e) K-bracing

3.7.2. The section and characteristic of the structural element

The DCR value depends strongly on the ultimate moment capacity. The plastic moment is a property of a structural section. It is defined as the moment at which the entire cross section has reached its yield stress. This is theoretically the maximum bending moment that the section can resist - when this point is reached a plastic hinge is formed and any load beyond this point will result in theoretically infinite plastic deformation. thus, using larger steel cross sections will increase the plastic moment and hence lowers the DCR value.

3.7.3. Creating obstacles on the field

We can also proceed as prevention method by creating obstacle on the field. In this way, it will reduce the standoff distance of the explosions and hence lowers the impact on the columns.as example, figure 3.39 illustrates the pressure-time history graph for a charge weight of 50kg TNT with different standoff distance. We can observe that the smaller the standoff distance the greater the impact.

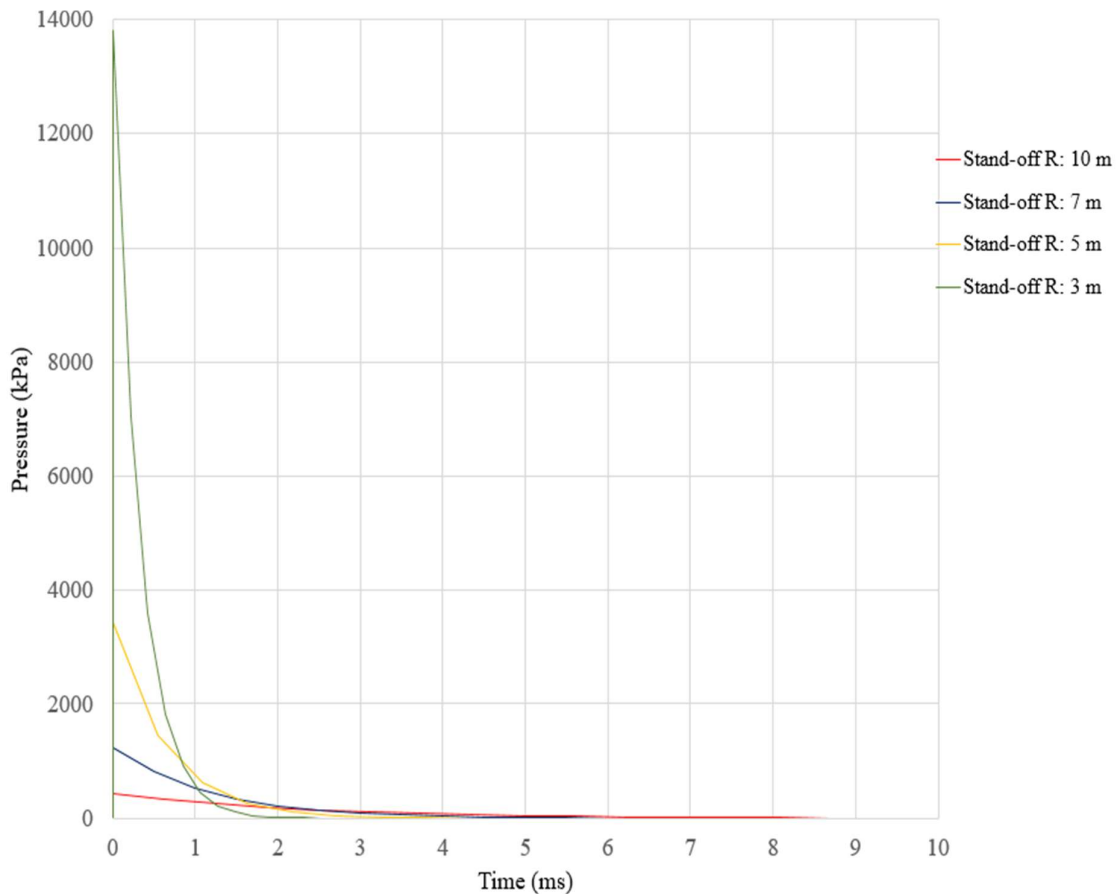


Figure 3.39. Pressure-time history graph for a charge weight of 50kg TNT with different standoff distance.

Conclusion

In conclusion, the results of the methodology of the previous chapter have been developed and applied to the study case which was a metallic hangar in Edea Cameroon. After a general presentation of the site based on its geographical location, its hydrology, its climate and its socio-economic activities, a presentation of the project was followed through its geometry and characteristics of the materials used. We modelled our structure on SAP2000 and a static analysis of the structure was done in order to ensure that our structure is stable. For the blast analysis, we did different blast load scenarios. The DCR values were used as acceptance criteria for the progressive collapse. The overall results show that the column has been highly damaged due to the different blast loads and the progressive collapse of the structure will happen depending on the intensity of the blast loads that are applied on the structure and this blast load intensity depends on several parameters such as charge weight, standoff distance and angle of incidence. Also, we saw that the bracing system plays an important role in the redistribution of lateral forces which reduces the solicitations of columns to which it is linked during the blast.

Next, we observed that the progressive collapse of the structure is equally affected by the section and its characteristic for a structural element. Some solution that could be apply have been done such that the structure can withstand better the blast loads.

GENERAL CONCLUSION

Haven come to the end of the study entitled “Progressive collapse of steel structure due to blast loads”, we recall that the aim of the work was to evaluate the progressive collapse of a structure caused by the removal of one column under blast loads with a case study of a metallic hangar located in the city of Edea in Cameroon. In order to achieve this objective, we reviewed the concept of steel, progressive collapse and blast loads in chapter 1, presented the methodology to be used in chapter 2 and the results presentation and interpretation was done in chapter 3. RC blast software was used in order to obtain the pressure-time function of the blast loads. Then structure was modelled in SAP2000 software, the solicitations were obtained and a static analysis have been done. After ensuring that our structure is stable, we moved on to the blast analysis. The goal was to find out the behaviour of the column elements under blast loads. Different blast loads scenario was done, one with a charge weight of 50kg equivalent mass of TNT applied on a column that has bracing and a column without bracing. We also did a case with a charge weight of 100kg applied on the column without bracing with the actual IPE section and with an HE section of similar area. For all these scenario, we used as acceptance criteria for the progressive collapse the DCR value and we observed the impact of column removal due to blast loads on the surrounding columns thus, we were able to find out the order of the progressive collapse.

The results obtained from the analysis revealed that, as the charge weight is increased from 50kg to 100kg equivalent mass of TNT for a fixed standoff distance, the level of damage of the column increases at an increasing rate but the progressive collapse of the surrounding column will not occur in the case of a charge weight of 50kg. In addition, the bracing system plays an important role in the redistribution of lateral forces, which reduces the solicitations of columns to which it is linked during the blast. Finally, a progressive collapse after the column removal is observed when a blast load of charge weight 100kg is subjected to a column with an IPE330 as section, whereas the same blast loads force applied on the same column with a section of HE200B which is similar to the IPE in terms of cross section area will not lead to progressive collapse. Hence, we can say that the progressive collapse of the structure is equally affected by the section and its characteristic for a structural element. Then, in order to protect steel buildings from progressive failure induced by blast loads and to reduce the vulnerability of the structural elements, design professionals may implement appropriate structural retrofits in order to increase the level of resistance of the building in case of blast events and reduce the DCR values. Some of these retrofitting measures include the usage of larger steel cross sections, the usage of more bracing and creating obstacle on the field.

The subject dealt with is very vast and it was necessary to limit the field of research for this work. However, this work cannot be without imperfections due to the failure to carry out certain analyses such as the repercussion of the blast on the substructure during the blast analysis, the impact of the column removal on the joint connection. In order to improve this work, the following suggestions can be made for further studies:

- The effect of different type of bracing system for the transfer of loads during blasts.
- The same study can be carried out with an internal blast loads.
- Local analysis on the joint connection due to the column removal.

BIBLIOGRAPHY

BOOKS AND ARTICLES:

- Abd Samat, R., Fikri Khairudin, M., Haziq Din, M., Gamal Ali, G., Bakar Fadzil, A., & Abu Bakar, S. (2019). Comparative Structural Performance of Diagrid and Bracing System in Mitigation of Lateral Displacement. *IOP Conference Series: Earth and Environmental Science*, 220(1). <https://doi.org/10.1088/1755-1315/220/1/012025>
- Activity, S. B. J. M. (2014). *Workshop on Blast Resistant Design of Structures*.
- Analysis, F. R., Date, M., Issuance, O. F., Statement, P., Flood, N., Program, I., Analysis, R. M., Map, R., Purpose, R. M. a P., Map, R., Map, R., & Map, R. (2002). Federal insurance and Mitigation Administration ,. *New York, 1*(May), 1–92.
- Army, Navy, D. of. (1990). *Department of the Army, Navy, and Air Force (1990) Structures to resist the effects of accidental explosions (with addenda). Army Technical Manual (TM 5-1300) Washington, DC*.
- Bažant, Z. P., & Zhou, Y. (2001). Why did world trade center collapse? - Simple analysis. *Archive of Applied Mechanics*, 71(12), 802–806. <https://doi.org/10.1007/s004190100189>
- Bažant, Zdeněk P., & Verdure, M. (2007). Mechanics of Progressive Collapse: Learning from World Trade Center and Building Demolitions. *Journal of Engineering Mechanics*, 133(3), 308–319. [https://doi.org/10.1061/\(asce\)0733-9399\(2007\)133:3\(308\)](https://doi.org/10.1061/(asce)0733-9399(2007)133:3(308))
- Behnam, B., Shojaei, F., & Ronagh, H. R. (2019). Seismic progressive-failure analysis of tall steel structures under beam-removal scenarios. *Frontiers of Structural and Civil Engineering*, 13(4), 904–917. <https://doi.org/10.1007/s11709-019-0525-7>
- Chopra, A. (2011). *Dynamic of Structures Chopra*.
- Cullis, I. G. (2001). Blast waves and how they interact with structures. *Journal of the Royal Army Medical Corps*, 147(1), 16–26. <https://doi.org/10.1136/jramc-147-01-02>
- Eichinger, W. E. (1985). *Mach Stem Modeling with Spherical Shock Waves*. 105.
- Ellingwood, B. R., Smilowitz, R., Dusenberry, D. O., Duthinh, D., Lew, H. S., & Carino, N. J. (2007). Best practices for reducing the potential for progressive collapse in buildings. *U.S. National Institute of Standards and Technology (NIST)*., 216.
- Gedeon, G. (2003). Building Terrorism Mitigation - Blast and CBR Measures. *FEMA 426, Reference Manual to Mitigate Potential Terrorist Attacks Against Buildings (2003), December*, 395.
- General Services Administration Alternate Path Analysis & Design Guidelines for Progressive Collapse Resistance*. (2013). 143.
- Gurley, C. (2008). Progressive Collapse and Earthquake Resistance. *Practice Periodical on Structural Design and Construction*, 13(1), 19–23. [https://doi.org/10.1061/\(asce\)1084-0680\(2008\)13:1\(19\)](https://doi.org/10.1061/(asce)1084-0680(2008)13:1(19))
- Hao, H., Hao, Y., Li, J., & Chen, W. (2016). Review of the current practices in blast-resistant analysis and design of concrete structures. *Advances in Structural Engineering*, 19(8), 1193–1223. <https://doi.org/10.1177/1369433216656430>
- Jeremić, R., & Bajić, Z. (2006). An approach to determining the TNT equivalent of high explosives. *Scientific-Technical Review, LVI*(1), 58–62.

- Jeyarajan, S., Richard Liew, J. Y., & Koh, C. G. (2015). Analysis of steel-concrete composite buildings for blast induced progressive collapse. *International Journal of Protective Structures*, 6(3), 457–485. <https://doi.org/10.1260/2041-4196.6.3.457>
- Jiang, B., Li, G. Q., & Usmani, A. (2015). Progressive collapse mechanisms investigation of planar steel moment frames under localized fire. *Journal of Constructional Steel Research*, 115, 160–168. <https://doi.org/10.1016/j.jcsr.2015.08.015>
- Jiang, J., & Li, G. Q. (2017a). Disproportionate collapse of 3D steel-framed structures exposed to various compartment fires. *Journal of Constructional Steel Research*, 138, 594–607. <https://doi.org/10.1016/j.jcsr.2017.08.007>
- Jiang, J., & Li, G. Q. (2017b). Progressive collapse analysis of 3D steel frames with concrete slabs exposed to localized fire. *Engineering Structures*, 149, 21–34. <https://doi.org/10.1016/j.engstruct.2016.07.041>
- Jiang, J., Li, G. Q., & Usmani, A. (2015). Effect of Bracing Systems on Fire-Induced Progressive Collapse of Steel Structures Using OpenSees. *Fire Technology*, 51(5), 1249–1273. <https://doi.org/10.1007/s10694-014-0451-0>
- Jr, J. R. H., Asce, M., Woodson, S. C., Asce, M., Pekelnicky, R. G., Asce, M., Poland, C. D., Asce, M., Corley, W. G., Asce, H. M., Sozen, M., & Asce, H. M. (2005). *Can Strengthening for Earthquake Improve Blast and Progressive Collapse Resistance? August*, 1157–1177.
- Kang, H., Shin, J., & Kim, J. (2013). Analysis of Steel Moment Frames subjected to Vehicle Impact. *Apcom & Iscm*, 1–8.
- Karim, M. R., & Fatt, M. S. (2005). Impact of the Boeing 767 Aircraft into the World Trade Center. *Journal of Engineering Mechanics*, 131(10), 1066–1072. [https://doi.org/10.1061/\(asce\)0733-9399\(2005\)131:10\(1066\)](https://doi.org/10.1061/(asce)0733-9399(2005)131:10(1066))
- Karlos, V., & Solomos, G. (2013). *Calculation of blast loads for application to structural components, JRC Technical report, EUR 26456 EN*. <https://doi.org/10.2788/61866>
- Karzova, M. M., Khokhlova, V. A., Salze, E., Ollivier, S., & Blanc-Benon, P. (2015). Mach stem formation in reflection and focusing of weak shock acoustic pulses. *The Journal of the Acoustical Society of America*, 137(6), EL436–EL442. <https://doi.org/10.1121/1.4921681>
- Kiakojouri, F., Biagi, V. De, Chiaia, B., & Reza, M. (2020). Progressive collapse of framed building structures: Current knowledge and future prospects. *Engineering Structures*, 206(January), 110061. <https://doi.org/10.1016/j.engstruct.2019.110061>
- Kim, J., & Kim, T. (2009). Assessment of progressive collapse-resisting capacity of steel moment frames. *Journal of Constructional Steel Research*, 65(1), 169–179. <https://doi.org/10.1016/j.jcsr.2008.03.020>
- Lane, B. (2003). A suggested cause of the fire-induced collapse of the World Trade Towers. *Fire Safety Journal*, 38(6), 589–591. [https://doi.org/10.1016/S0379-7112\(03\)00058-4](https://doi.org/10.1016/S0379-7112(03)00058-4)
- Löfqvist, C. (2016). *Response of buildings exposed to blast load: Method Evaluation*. 100. <http://www.byggmek.lth.se/fileadmin/byggnadsmekanik/publications/tvsm5000/web5216.pdf>
- Lu, X., Li, Y., Guan, H., & Ying, M. (2017). Progressive Collapse Analysis of a Typical Super-Tall Reinforced Concrete Frame-Core Tube Building Exposed to Extreme Fires. *Fire Technology*, 53(1), 107–133. <https://doi.org/10.1007/s10694-016-0566-6>

- Neff, M., & Fiume, E. (1999). A visual model for blast waves and fracture. *Proceedings of Graphics Interface 2009*, 193–202.
- Ngo, T., Mendis, P., Gupta, A., & Ramsay, J. (2007). Blast loading and blast effects on structures - An overview. *Electronic Journal of Structural Engineering*, 7(January), 76–91.
- Nöldgen, M., Fehling, E., Riedel, W., & Thoma, K. (2012). Vulnerability and Robustness of a Security Skyscraper Subjected to Aircraft Impact. *Computer-Aided Civil and Infrastructure Engineering*, 27(5), 358–368. <https://doi.org/10.1111/j.1467-8667.2011.00748.x>
- Oswald, C. J., & Zehrt, W. (2010). Update to UFC 3-340-02 for blast resistant design of masonry components. *Proceedings of the 34th Department of Defense Explosives Safety Board Seminar*, July.
- Qian, Y., Li, Y., Jungwirth, S., Seely, N., Fang, Y., & Shi, X. (2015). The Application of Anti-Corrosion Coating for Preserving the Value of Equipment Asset in Chloride-Laden Environments: A. *Int. J. Electrochem. Sci*, 10(November 2017), 10756–10780.
- Rigby, S., Fay, S., Tyas, A., Warren, J., & Clarke, S. (2015). Angle of incidence effects on far-field positive and negative phase blast parameters. *International Journal of Protective Structures*, 6(1), 23–42. <https://doi.org/10.1260/2041-4196.6.1.23>
- Ronagh, M. and. (2011). Plastic Hinge Length of RC Columns Subjected to Both Far-Fault and Near-Fault Ground Motions Having Forward Directivity. *The Structural Design of Tall and Special Buildings*, 24(July 2014), 421–439. <https://doi.org/10.1002/tal>
- Social. (1998). No Title. *ペインクリニック学会治療指針 2*, 43(March), 1–9. <https://doi.org/10.1037/0033-2909.126.1.78>
- Song, D., Tang, R., Yang, F., Qiao, Y., Sun, J., Jiang, J., & Ma, A. (2018). Development of high-performance enamel coating on grey iron by low-temperature sintering. *Materials*, 11(11), 1–14. <https://doi.org/10.3390/ma11112183>
- Starossek, U. (2007). Progressive Collapse of Structures World Trade Center — September 11 , 2001. *Engineering Structures*, 29(December), 2302–2307. <https://doi.org/10.1016/j.engstruct.2006.11.025.1>
- Strom, R. W., & Ebeling, R. M. (2002). Methods Used in Tieback Wall Design and Construction to Prevent Local Anchor Failure, Progressive Anchorage Failure, and Ground Mass Stability Failure. *Work*, 14. vulcanhammer.net
- TM5-1300, 1990, “Structures to Resist Effects of Accidental Explosions,” Technical Manual 5-1300, Department of the Army, Navy and Air Force, Washington DC, 1990.
- UFC 3-340-02, 2008., “Structures to Resist the Effects of Accidental Explosions”, United States of America Department of Defense, Washington, D.C.
- Ullah, A., Ahmad, F., Jang, H. W., Kim, S. W., & Hong, J. W. (2017). Review of analytical and empirical estimations for incident blast pressure. *KSCE Journal of Civil Engineering*, 21(6), 2211–2225. <https://doi.org/10.1007/s12205-016-1386-4>
- Verma, S., Choudhury, M., & Saha, P. (2015). *Blast resistant design of structure*. 64–69.
- Vlassis, A. G., Izzuddin, B. A., Elghazouli, A. Y., & Nethercot, D. A. (2009). Progressive

collapse of multi-storey buildings due to failed floor impact. *Engineering Structures*, 31(7), 1522–1534. <https://doi.org/10.1016/j.engstruct.2009.02.009>

Yankelevsky, D. Z., Karinski, Y. S., & Feldgun, V. R. (2020). Dynamic punching shear failure of a RC flat slab-column connection under a collapsing slab impact. *International Journal of Impact Engineering*, 135(September 2019), 103401. <https://doi.org/10.1016/j.ijimpeng.2019.103401>

Yandzio E., and Gough M., 1999, Protection of Buildings against Explosions, Steel Construction Institute

WEBOGRAPHY

https://en.wikipedia.org/wiki/Blast_wave

<https://link.springer.com/article/10.1007/s11831-020-09436-y>

<https://www.hindawi.com/journals/sv/2017/6708341/>

<http://sedigest.in/article/overview-progressive-collapse/>

<https://www.nbmw.com/articles-reports/others/others-article/blast-loading-and-its-effects-on-structures.html>

https://fr.slideshare.net/SoumyabrataSaha1/blast-load-and-its-analysis?next_slideshow=1

<https://www.theworldmaterial.com/different-types-of-steel-classification/>

<http://www.sabelsteel.com/news/the-bessemer-process-and-modern-steelmaking/>

<https://link.springer.com/article/10.1007/s11069-013-0835-3>

ANNEXES

Annex 1. Load distribution according to building category

Categories of loaded areas	q_k [kN/m ²]	Q_k [kN]
Category A		
- Floors	1,5 to <u>2,0</u>	<u>2,0</u> to 3,0
- Stairs	<u>2,0</u> to 4,0	<u>2,0</u> to 4,0
- Balconies	<u>2,5</u> to 4,0	<u>2,0</u> to 3,0
Category B	2,0 to <u>3,0</u>	1,5 to <u>4,5</u>
Category C		
- C1	2,0 to <u>3,0</u>	3,0 to <u>4,0</u>
- C2	3,0 to <u>4,0</u>	2,5 to 7,0 (<u>4,0</u>)
- C3	3,0 to <u>5,0</u>	<u>4,0</u> to 7,0
- C4	4,5 to <u>5,0</u>	3,5 to <u>7,0</u>
- C5	<u>5,0</u> to 7,5	3,5 to <u>4,5</u>
category D		
- D1	<u>4,0</u> to 5,0	3,5 to 7,0 (<u>4,0</u>)
- D2	4,0 to <u>5,0</u>	3,5 to <u>7,0</u>

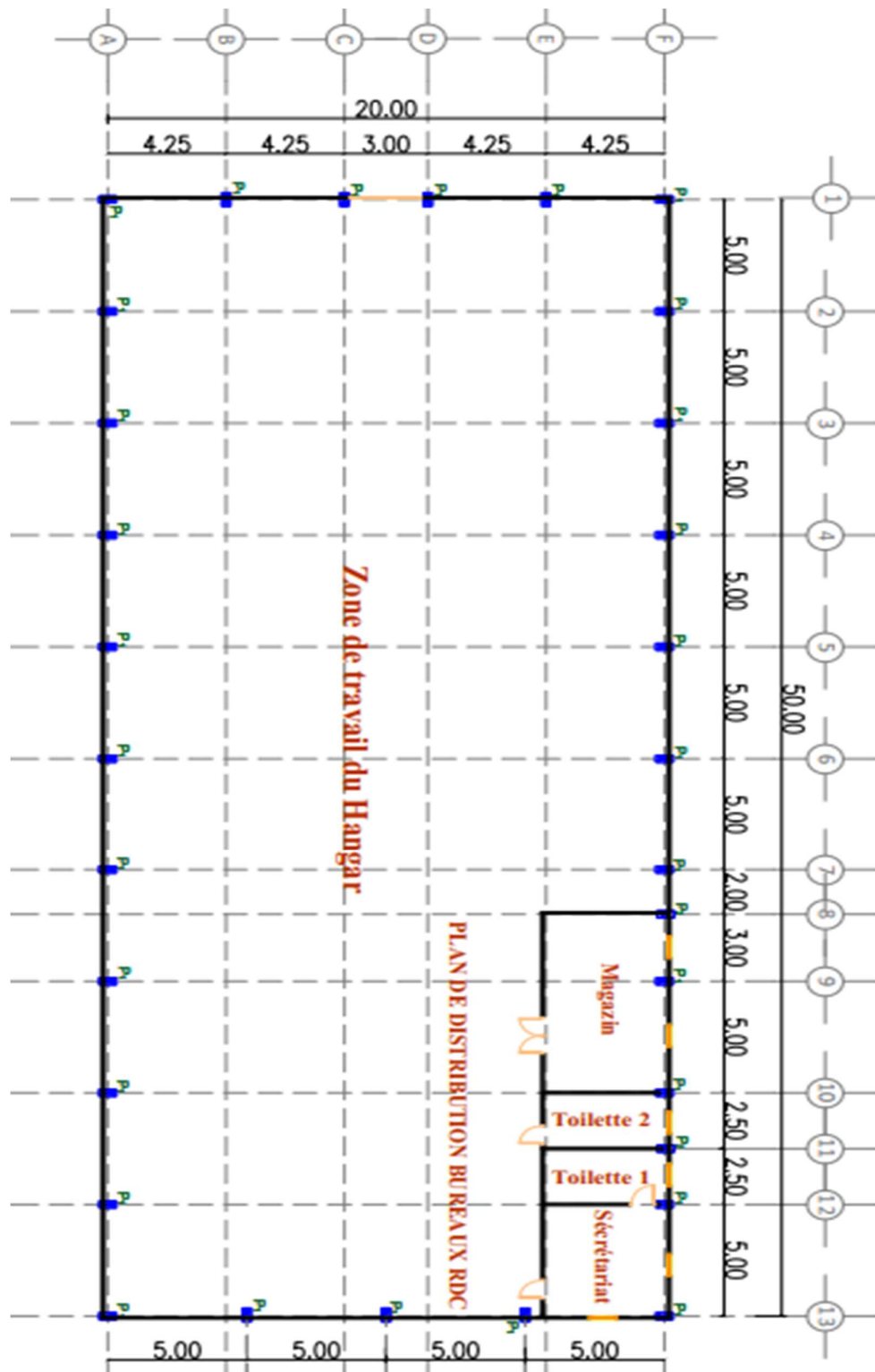
Annex 2. Values for ψ factor

Action	ψ_0	ψ_1	ψ_2
Imposed loads in buildings, category (see EN 1991-1-1)			
Category A : domestic, residential areas	0,7	0,5	0,3
Category B : office areas	0,7	0,5	0,3
Category C : congregation areas	0,7	0,7	0,6
Category D : shopping areas	0,7	0,7	0,6
Category E : storage areas	1,0	0,9	0,8
Category F : traffic area, vehicle weight $\leq 30\text{kN}$	0,7	0,7	0,6
Category G : traffic area, $30\text{kN} < \text{vehicle weight} \leq 160\text{kN}$	0,7	0,5	0,3
Category H : roofs	0	0	0
Snow loads on buildings (see EN 1991-1-3)*			
Finland, Iceland, Norway, Sweden	0,70	0,50	0,20
Remainder of CEN Member States, for sites located at altitude $H > 1000$ m a.s.l.	0,70	0,50	0,20
Remainder of CEN Member States, for sites located at altitude $H \leq 1000$ m a.s.l.	0,50	0,20	0
Wind loads on buildings (see EN 1991-1-4)	0,6	0,2	0
Temperature (non-fire) in buildings (see EN 1991-1-5)	0,6	0,5	0
NOTE The ψ values may be set by the National annex. * For countries not mentioned below, see relevant local conditions.			

Annex 3. Building category

Category	Specific Use	Example
A	Areas for domestic and residential activities	Rooms in residential buildings and houses; bedrooms and wards in hospitals; bedrooms in hotels and hostels kitchens and toilets.
B	Office areas	
C	Areas where people may congregate (with the exception of areas defined under category A, B, and D ¹⁾)	<p>C1: Areas with tables, etc. e.g. areas in schools, cafés, restaurants, dining halls, reading rooms, receptions.</p> <p>C2: Areas with fixed seats, e.g. areas in churches, theatres or cinemas, conference rooms, lecture halls, assembly halls, waiting rooms, railway waiting rooms.</p> <p>C3: Areas without obstacles for moving people, e.g. areas in museums, exhibition rooms, etc. and access areas in public and administration buildings, hotels, hospitals, railway station forecourts.</p> <p>C4: Areas with possible physical activities, e.g. dance halls, gymnastic rooms, stages.</p> <p>C5: Areas susceptible to large crowds, e.g. in buildings for public events like concert halls, sports halls including stands, terraces and access areas and railway platforms.</p>
D	Shopping areas	<p>D1: Areas in general retail shops</p> <p>D2: Areas in department stores</p>
<p>¹⁾ Attention is drawn to 6.3.1.1(2), in particular for C4 and C5. See EN 1990 when dynamic effects need to be considered. For Category E, see Table 6.3</p> <p>NOTE 1 Depending on their anticipated uses, areas likely to be categorised as C2, C3, C4 may be categorised as C5 by decision of the client and/or National annex.</p> <p>NOTE 2 The National annex may provide sub categories to A, B, C1 to C5, D1 and D2</p> <p>NOTE 3 See 6.3.2 for storage or industrial activity</p>		

Annex 4. Distribution plan



Annex 5. Structural plan

